Alma Mater Studiorum – Università di Bologna

DOTTORATO DI RICERCA IN

Scienze Farmaceutiche

Ciclo XXIV

Settore Concorsuale di afferenza: 03/D1

Settore Scientifico disciplinare: CHIM/08

Design, synthesis and biological evaluation of substituted naphthalene diimides as anticancer agents

Presentata da: Marialuisa Micco

Coordinatore Dottorato — **Prof. Maurizio Recanatini**

Relatore — **Prof. Vincenzo Tumiatti**

Esame finale anno 2012

Contents

Preface

This PhD thesis has been carried out at the Department of Pharmaceutical Sciences *Alma Mater Studiorum*-University of Bologna (Italy), under the supervision of Prof. Vincenzo Tumiatti, and at the UCL School of Pharmacy (UK) in the Biomolecular Structure Group, under the supervision of Prof. Stephen Neidle.

The whole PhD thesis is devoted to the study of new molecules for the treatment of cancer.

This thesis is organized in different chapters: the first chapter is a briefly introduction of the physiopathological aspects and the current approaches for the treatment of cancer. The second chapter explanes the importance of DNA as antincancer target. Chapter three, four and five deal with different important targets considered in the drug design process of this work. Chapter six and seven contain the two parts related to the drug design of the two series of compounds reported in the present thesis together with the synthetic methods, biological evaluations, result and discussions, conclusions and experimental procedures.

Finally, I would like to thanks the National Cancer Institute for the biological evaluation of several derivatives, and other researchers involved in the present investigation:

- Dr. Guendalina Zuccari, Department of Pharmaceutical Science, University of Bologna;
- Prof. Vito Pistoia and Dr. Lizzia Raffaghello, Laboratory of Oncology, G. Gaslini Institute, Genova;
- Dr. Claudia Sissi, Department of Pharmaceutical Science, University of Padova;
- Prof. Stefano Alcaro, University of Catanzaro;
- Prof. Claudio Stefanelli and Dr. Maddalena Zini, Department of Biochemistry, University of Bologna;
- Dr. Maria Luisa Di Paolo, Department of Biological Chemistry, University of Padova;
- Prof. Stephen Neidle, Dr. Stephan Ohnmacht, Dr. Gavin Collie, Dr. Mekala Gunaratnam, Vanessa Petrucci, Biomolecular Structure Group, UCL School of Pharmacy, London.

I would also thank MIUR (Rome), University of Bologna and Polo Scientifico-Didattico di Rimini for their financial support.

Abstract

It has been proved that naphthalene diimide (NDI) derivatives display anticancer properties as intercalators and G-quadruplex-binding ligands, leading to DNA damage, senescence and down-regulation of oncogene expression**.**

This thesis deals with the design and synthesis of disubstituted and tetrasubstituted NDI derivatives endowed with anticancer activity, interacting with DNA together with other targets implicated in cancer development.

Disubstituted NDI compounds have been designed with the aim to provide potential multitarget directed ligands (MTDLs), in order to create molecules able to simultaneously interact with some of the different targets involved in this pathology. The most active compound, displayed antiproliferative activity in submicromolar range, especially against colon and prostate cancer cell lines, the ability to bind duplex and quadruplex DNA, to inhibit Taq polymerase and telomerase, to trigger caspase activation by a possible oxidative mechanism, to downregulate ERK 2 protein and to inhibit ERKs phosphorylation, without acting directly on microtubules and tubuline.

Tetrasubstituted NDI compounds have been designed as G-quadruplex-binding ligands endowed with anticancer activity. In order to improve the cellular uptake of the lead compound, the N-methylpiperazine moiety have been replaced with different aromatic systems and methoxypropyl groups. The most interesting compound was **1d,** which was able to interact with the G-quadruplexes both telomeric and in HSP90 promoter region, and it has been co-crystallized with the human telomeric G-quadruplex, to directly verify its ability to bind this kind of structure, and also to investigate its binding mode. All the morpholino substituted compounds show antiproliferative activity in submicromolar values mainly in pancreatic and lung cancer cell lines, and they show an improved biological profile in comparison with that of the lead compound.

In conclusion, both these studies, may represent a promising starting point for the development of new interesting molecules useful for the treatment of cancer, underlining the versatility of the NDI scaffold.

CHAPTER 1
INTRODUCTION

1.1 CANCER

Cancer is a term used for diseases in which abnormal cells divide without control and are able to invade other tissues. Cancer cells can spread to other parts of the body through the blood and lymph systems.

Cancer should be considered just not one disease but a pathology comprising many different diseases, in fact there are more than 100 different types of cancer. The name of most cancers derives directly from the organ or type of cell in which they grow. For example, cancer that begins in the colon is called colon cancer; cancer that begins in basal cells of the skin is called basal cell carcinoma.

Cancer types can be grouped into broader categories. The main categories of cancer include:

- Carcinoma: cancer that begins in the skin or in tissues that line or cover internal organs.
- Sarcoma: cancer that begins in bone, cartilage, fat, muscle, blood vessels, or other connective or supportive tissue.
- Leukemia: cancer that starts in blood-forming tissue such as the bone marrow and causes large numbers of abnormal blood cells to be produced and enter the blood.
- Lymphoma and myeloma: cancers that begin in the cells of the immune system.
- Central nervous system cancers: cancers that begin in the tissues of the brain and spinal cord.

All cancers begin in cells, the body's basic unit of life. The body is composed by many types of cells. These cells grow and divide in a controlled way to produce other cells as they are needed to keep the body healthy. When cells become old or damaged, they die and they are replaced by new cells. However, sometimes this orderly process goes wrong. The genetic material (DNA) of a cell can become damaged or changed, producing mutations which affect normal cell growth and division. These abnormal extra cells may form a mass of tissue called tumor (Figure 1.1).

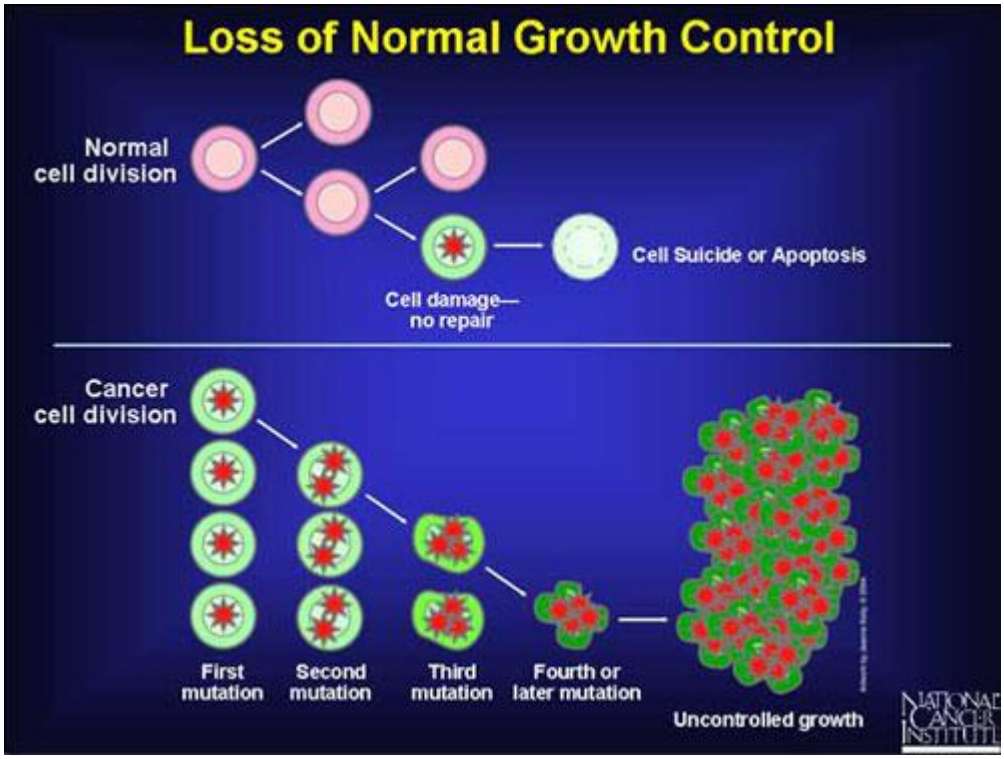

Figure 1.1: Cancer progression[2]

Not all tumors are cancerous; tumors can be benign or malignant.

- Benign tumors are not cancerous. They can often be removed, and, in most cases, they do not come back. Cells in benign tumors do not spread to other parts of the body.
- Malignant tumors are cancerous. Cells in these tumors can invade nearby tissues and spread to other parts of the body. The spread of cancer from one part of the body to another is called metastasis.

Some cancers do not form tumors. For example, leukemia is a cancer of the bone marrow and blood.[1]

Cancer is predicted to be an increasingly important cause of morbidity and mortality in all regions of the world. The forecasted changes in population demographics in the next two decades mean that even if current global cancer rates remain unchanged, the estimated incidence of 12.7 million new cancer cases in 2008 will rise to 21.4 million by 2030, with nearly two thirds of all cancer diagnoses occurring in low- and middle-income countries. In Italy, in 2008 cancer killed approximately 248,000 people and it represents the second most common cause of death after cardiovascular diseases (Figure 1.2).[2]

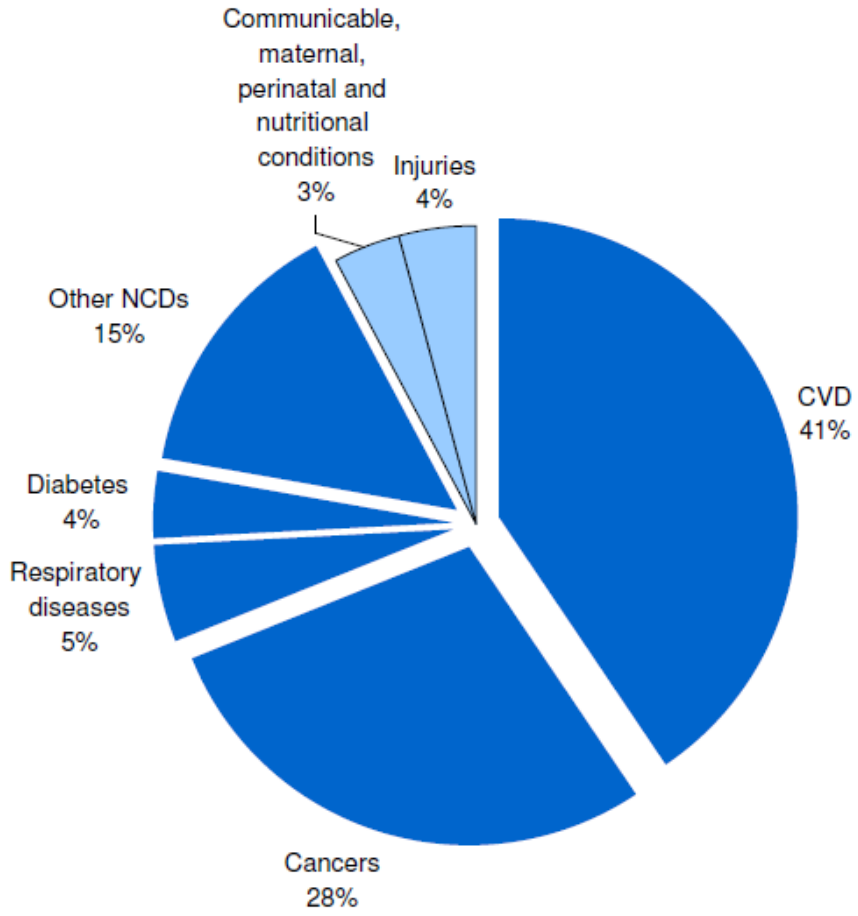

Figure 1.2: Proportional mortality in Italy in 2008 (% of total deaths, all ages)[2]

1.1.1 Cancer therapy

Cancer therapy generally includes psychosocial support, surgery, radiotherapy, chemotherapy that is aimed at curing the disease or considerably prolonging life while improving the patient's quality of life.

1.1.2 Chemotherapy

Chemotherapeutic drugs should eradicate malignant tumor cells by inhibiting some of the mechanism involved in cellular division. Accordingly, the antitumor compounds developed through this approach are cytostatic or cytotoxic. These kind of drugs are characterized by severe therapeutic problems. One of them is related to their low selectivity, so they are not able to eliminate all cancer cells in the body and they can hit healthy cells. Furthermore, they are endowed with non-specific toxicity due to their biodistribution

throughout the body, which requires the administration of a large total dose to achieve high local concentrations in a tumor.[3] Another problem related to chemotherapy is the drug resistance. Cancer cells are able to become simultaneously resistant to different drugs (multidrug resistance) by several mechanisms. This may represent a significant impediment to a successful chemotherapy.[4]

1.1.3 Molecular targeted therapy

The discovery of specific molecular characteristics of malignant cells prompted the development of a new class of drugs known as targeted therapeutics.[5] These compounds act on particular tumorigenic molecules and directly inhibit cellular growth and survival machinery to eradicate tumor cells.[6] Molecular targeted therapeutic agents can be small molecular substances of defined molecular weight and structure, or macromolecules such as antibodies. They have greater selectivity and produce fewer side effects.[7] One of the first molecular targets to be discovered was the estrogen receptor, which stimulates proliferation of mammary cells when activated by estrogen. Tamoxifen is an estrogen inhibitor now used for the treatment of estrogen receptor positive tumors. [8]

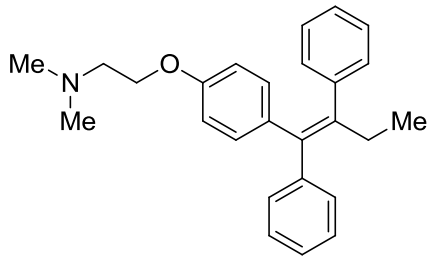

Tamoxifen

Another example of targeted therapy is the monoclonal antibody Trastuzumab, that targets gene amplified HER2 in select breast cancers to produce disease control not previously thought possible.[9]

MOLECULAR TARGETS

Some cancers depend on one or a few genes for the maintenance of the malignant phenotype. This concept is known as "oncogene addiction". Cancer cells contain multiple genetic and epigenetic abnormalities, and the reversal of only one or few of these abnormalities can inhibit the growth of these cells.[10]

Examples of possible targets are:

- k-ras: the oncogene shares a potent ability to transform cells.[11] The mutated form promotes DNA transformation[12] and it is found at high frequency in a variety of human tumors.[11]

- c-myc: this proto-oncogene encodes a multifunctional transcription factor that plays a critical role in a broad range of cellular processes, including cell growth, differentiation and transformation. Elevated expression of c-myc promote tumorigenesis, whereas reduction of its expression has been associated with the induction of apoptosis.[13]
- kit: it is a proto-oncogene encodes a receptor tyrosine kinase. The activation of this receptor is associated with cell proliferation and survival.[14]
- Hsp90: it regulates the conformation, activation, function and stability of so-called "client proteins". In particular has been shown to support malignant transformation and it is overexpressed in cancer cells.[15]

1.1.4 Multi-Target-Directed Ligand approach

Multi-Target-Directed Ligand approach is particularly relevant to multifactorial diseases, and it has been reported for pathologies like schizophrenia and neurodegenerative conditions such as Alzheimer's disease.[16,17,18] Multi-Target-Directed Ligands (MTDLs) have multiple biological profile and they are able to hit or modulate different targets thought to be responsible for the disease pathogenesis. This strategy may not be easy, because the drug could also bind targets that are not involved with the disease and could be responsible for side effects (Figure 1.3)[18]

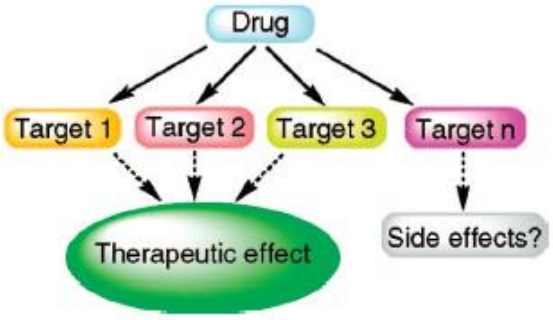

Figure 1.3: MTDLs approach to drug discovery[16]

Cancer is a highly complex disease involving multiple biochemical pathways and, therefore, it is interesting design new MTDLs to increase the success of cancer therapeutics. There are several examples about anticancer agents designed using this approach. [16] Among them, there are compounds **I** and Lapatinib. **I** was discovered from a screening of 160,000

commercialy available compounds and it is a Hsp90/tubulin inhibitor.[20] Lapatinib was rationally designed as ligand for the epidermal growth factor receptor (EGFR) and ErbB2 kinases[21] and showed a good selectively for these two kinases from a panel of 317 kinases.[22] Lapatinib has been approved for patient use in more than 90 countries worldwide for treatment of ErbB2 positive breast cancer.[23]

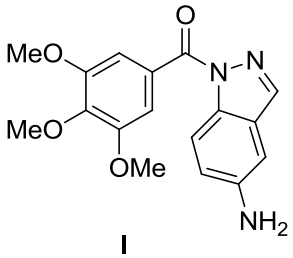

I

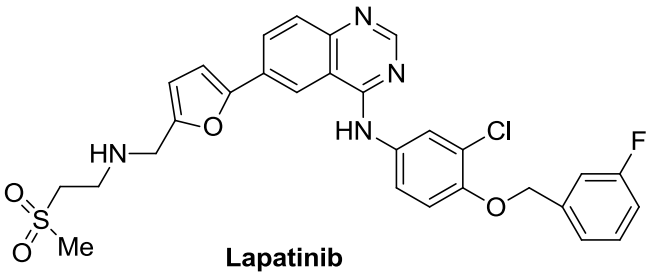

Lapatinib

CHAPTER 2
DNA AS ANTICANCER DRUGS TARGET

DNA is involved in cell proliferation and cancerogenetic processes and, for this reason, it is the molecular target for many drugs used in cancer therapeutics.[24]

Based on their possible interaction with DNA, such molecules have been classified in four wide groups:

- Alkylating agents, which are able to covalently bound DNA;
- Agents able to truncate DNA double helix;
- Agents that reversibly interact with double helix of DNA;
- Agents that intercalate between the DNA bases.

Among these, the intercalating agents are the most important and many anticancer drugs in clinical use interact with DNA through intercalation.[3]

Drugs can interact with DNA also through stabilization of particular four-stranded DNA structures termed G-quadruplexes.[25] For better understanding, a detailed explanation of this argument will be covered in chapter 3.

2.1 DNA INTERCALATION

Intercalating agents are usually molecules with aromatic or heteroaromatic ring systems. They are inserted between adjacent base pairs perpendicularly to the axis of the DNA helix. The created complex is stabilized by non-covalent interactions like Van der Waals, hydrophobic and hydrogen bonding. This insertion cause conformational changes in the DNA, like separation between the base pairs and, as result of the intercalation process, DNA results unwound (Figure 2.1).

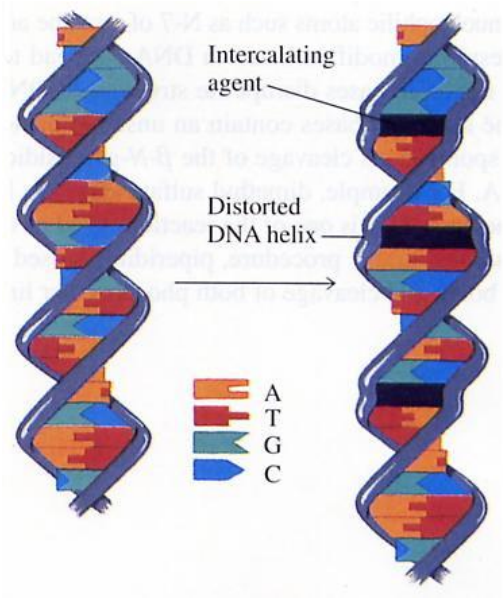

Figure 2.1: Deformation of DNA by an intercalating agent[26]

These structural changes can interfere with the ability of the DNA to recognize its associated proteins like polymerases, transcription factors and topoisomerases, leading to problems in replication processes and cellular death.[3]

In particular, the poison of the topoisomerase is the most important interaction of a DNA-intercalator. An intercalating agent is able to stabilize the ternary complex DNA-intercalator-topoisomerase and the enzymatic process cannot continue. This complex is detected by the cell as a damaged portion, so it starts a series of events, such as activation of p53 protein, which induces cell apoptosis (Figure 2.2).[27]

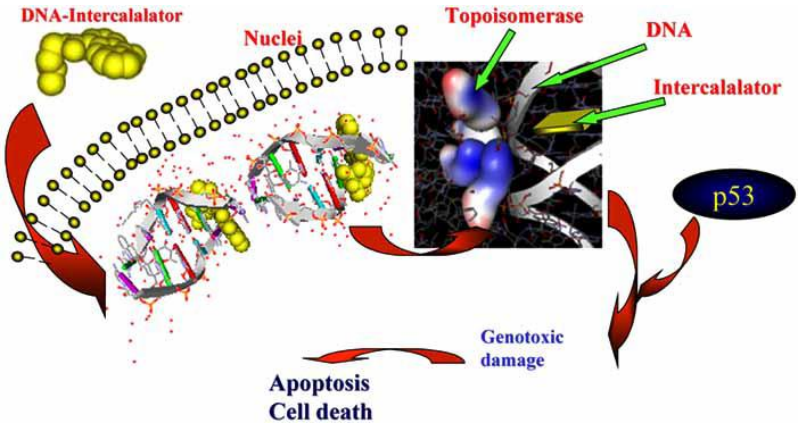

Figure 2.2: Schematic representation of the mechanism of cytotoxicity of a DNA-itercalator.[21]

2.2 INTERCALATING AGENTS

Intercalators represent a wide group of compounds that could be classified in two main groups: classical and non-classical intercalators.

Classical intercalators (Figure 2.3) display their cytotoxicity by inhibiting Topoisomerase II. They can be further divided in subfamily, based on the nature of their chromophore unit:

- Naphtalimide and related compounds, such as Mitonafide, Amonafide, Azonafide and Elinafide;
- Intercalators based on the pyridocarbazole system, such as Ellipticine and 9-methoxyellipticine;
- Anthracycline, such as Doxorubicine, Daunomicine and Mitoxantrone;
- Antibiotics of the Echinomycin family, such as Echinominine and Triostina;
- Acridine and related compounds, such as Amsacrine;
- Actinomycin;
- Analogues of Benzimidazo-[1,2,c]quinazoline.

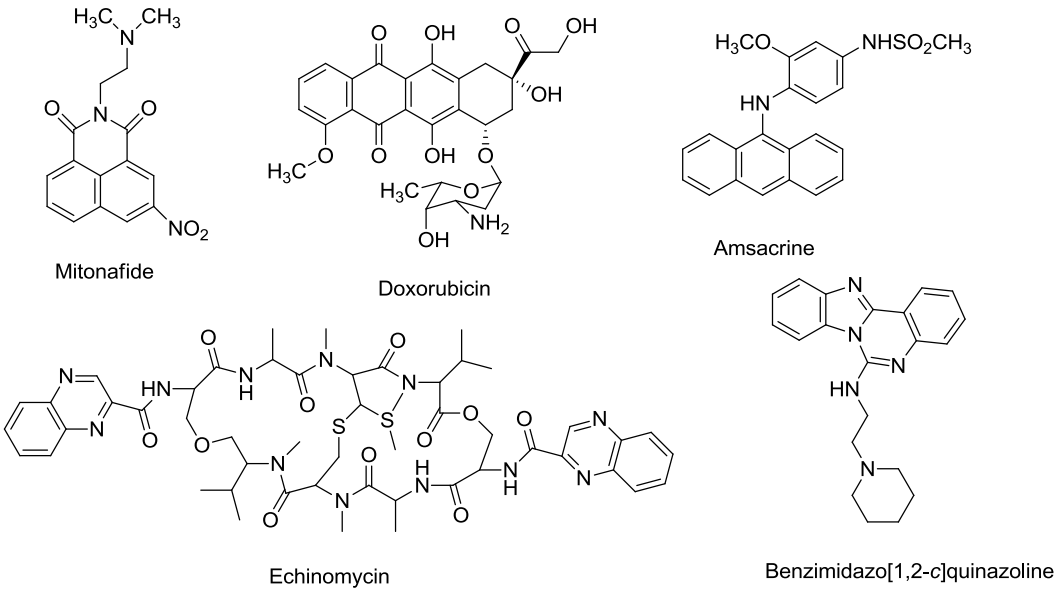

Figure 2.3: Structures of classical intercalators

These compounds present different chemical structures and they exert their anticancer activity also using other mechanisms of action. For instance, Anthracyclin has oxidoreductive properties and, for this reason, it is able to induce DNA-damage through ROS-formation.

Non-classical intercalators (Figure 2.4) are characterized by the presence of a huge aromatic planar system. They are able to stabilize triple-helix DNA structures more strongly than duplex-helix. They can be classified in two groups:

- Threading Intercalators;
- Tris-intercalators.[28]

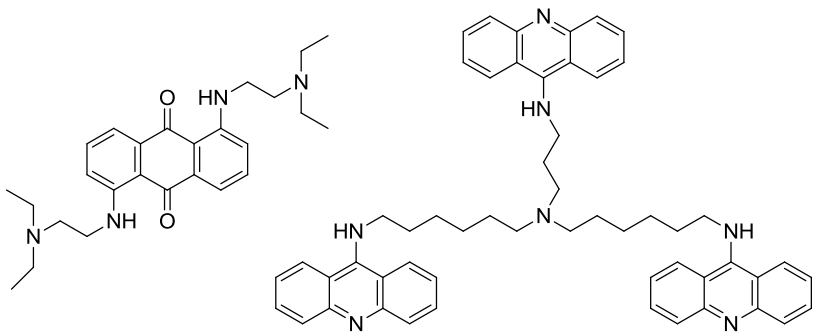

Figure 2.4: Structures of non classical intercalators

Among all the intercalators developed, Braña et al. in 1970s published a series of Naphthalimides as anticancer agents.[29] Structure Activity Relationships (SAR) analysis in this series showed that:

- a basic terminal group in the side chain is important for the cytotoxic activity;
- when the nitrogen atom in the basic side chain is separated from the ring nitrogen by two methylene units, the growth inhibition is maximal;
- the best substitution at the basic side chain is constituted by a dimethylamine or a pyrrolidine residue;
- substitution at position 5 in the naphthalic ring gives optimal results.

The most active compounds in this series were Amonafide and Mitonafide (Figure 2.5).

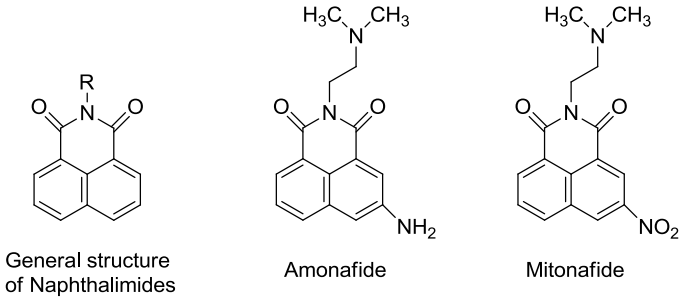

Figure 2.5: Naphthalimides developed by Braña et al.

Both Amonafide and Mitonafide have been tested in clinical trials. They are able to intercalate the double-stranded DNA, confirmed by NMR techniques.[30] Amonafide is active against P388 and L1210 leukemia models. Mitonafide has *in vivo* activity against KB and HeLa cells, as well as *in vivo* activity against murine and human tumor cell lines.[31,32] Both the compounds induce a topoisomerase II-mediated DNA cleavage at nucleotide N. 1830 on Pbr322 DNA. This cleavage is not observed in related naphthalimides, lacking the basic side chain.[33]

Amonafide can be metabolized in two different pathways (Figure 2.6):

- the first one by cytochrome CYP1A2 leading to an oxidized product;
- the second one by *N*-acetyltransferase 2 (NAT2) leading to a *N*-acetyl-amonafide metabolite still metabolically active. NAT2 enzymes catalyze the acetylation of a

wide variety of amines, include arylamine and heterlocyclic aromatic amines, Amonafide, hydralazine, isoniazid, procainamide, and sulfonamides.

Recently, it has been demonstrated that the most important side effects of Amonafide arise from its acetylated metabolites.[34]

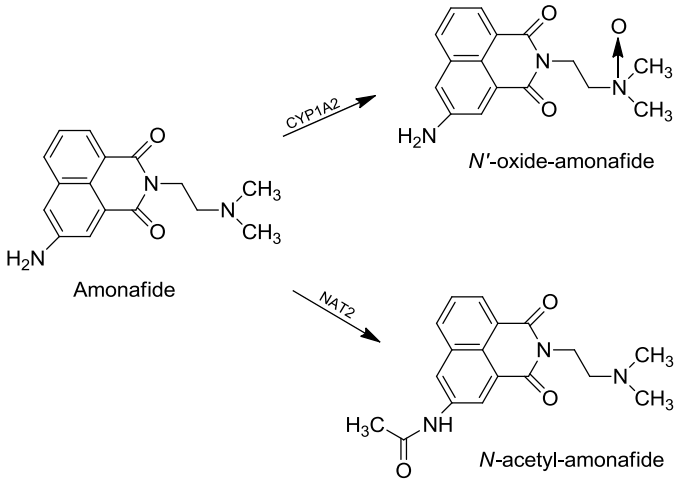

Figure 2.6: Metabolism of amonafide

Amonafide and Mitonafide present similar chemical structures. They differ just for the substituent on the aromatic ring: Mitonafide has an electron-donating amino group, while Amonafide presents an electron-withdrawing nitro group. It has been suggested that the nitro group promotes the formation of a charge transfer complex with DNA bases, while the amino group allow the stabilization of DNA-drug complex through hydrogen bonds with the phosphate group of the DNA backbone.

Several studies have been carried out on Amonafide and Mitonafide, and an initial assessment of the SAR of these molecules led to the synthesis of compounds having a 5-amino-8-nitronaphthalimide nucleus. This new series of compounds was more active than Amonafide and Mitonafide on human colon carcinoma cell line CX-1 and human hepatic stellate cell line LX-1.[35] Following this study, Zee-Cheng and Cheng published a series of *bis*-nitro and *bis*-amino derivatives. The most active compounds were **II** and **III** having, both *in vitro* and *in vivo*, prominent antileukemia and antimelanoma activity.[36]

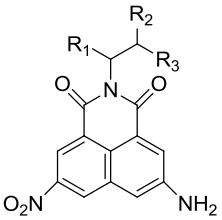

General formula
of 5-amino-8-nitro-naphthalimides

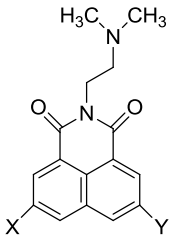

II: X = Y = NH_2
III: X = Y = NO_2

The activity of mononaphthalimides has been improved by the insertion of the anthracene rather than the naphthalene nucleus. The most interesting compound was Azonafide. It is more active than Amonafide against UACC375 (human melanoma), OVCAR3 (ovarian cancer) and L1210 (leukemia) cell lines.[37]

In order to study the relevance of the nucleus linearity, phenanthrene and azaphenanthrene analogues were synthesized. These agents are less able than Azonafide to inhibit tumor cells growth, indicating the importance of the anthracene chromophore.[38]

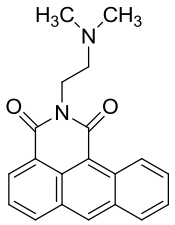

Azonafide

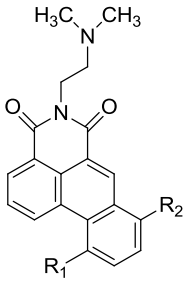

IV: Phenanthrene derivative

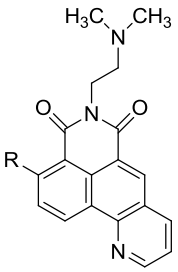

V: Azaphenanthrene derivative

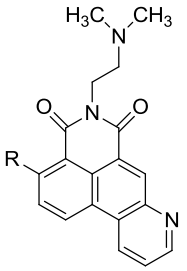

VI: Azaphenanthrene derivative

Other mononaphthalimides analogues were obtained by replacing the imidazolic ring with a π-deficient pyrazine ring. This new series of compounds, known as pyrazinonaphthalimides, showed a stronger intercalating activity. These compounds have been tested against HT-29 (human colon carcinoma), HeLa (human cervical carcinoma) and PC-3 (human prostate carcinoma) cell lines showing IC_{50} values in micromolar range. Compounds containing a trifluoromethyl group presented a lower activity. This result could be the explained by the steric hindrance of the trifluoromethyl group, that could prevent its intercalation [39]

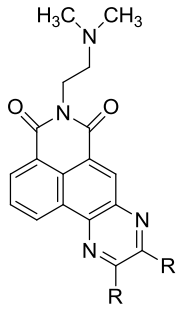

VII: R = H
VIII: R = CF_3

The introduction of a pyrazine ring gave promising results. The next step was the synthesis of compounds bearing π-deficient rings, like furane or thiophene, conjugated with the aromatic system of Amonafide. The heterocycles have been introduced in two possible orientation and all the compounds synthesized have been screened against HT-29, HeLa and PC-3 cell lines. All the assayed compounds were more potent than Amonafide. In particular, among the different molecules, the compound bearing a furan ring oriented toward the outside of the molecule **IX** was the most active.

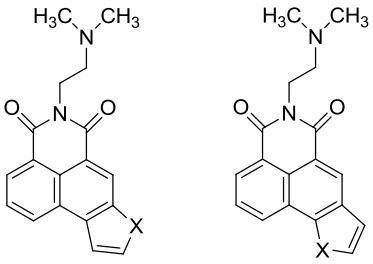

IX: R = O
X: R = S

XI: R = O
XII: R = S

IX was 10-fold more active against HT-29, 20-fold against HeLa, and 40-fold against PC-3 than the lead compound Amonafide. In order to explain the activity of **IX**, Braña et al. carried out molecular modeling investigations. They constructed four different model complexes depending on four different orientations of **IX** into DNA (Figure 2.7).

- orientation with the side chain in the major groove and the furan ring stacking between the bases T and G;

- orientation with the side chain in the major groove and the furan ring stacking between A and C:
- orientation with the side chain in the minor groove and the furan stacking between T and G;
- orientation with the side chain in the minor groove and the furan ring stacking between A and C.

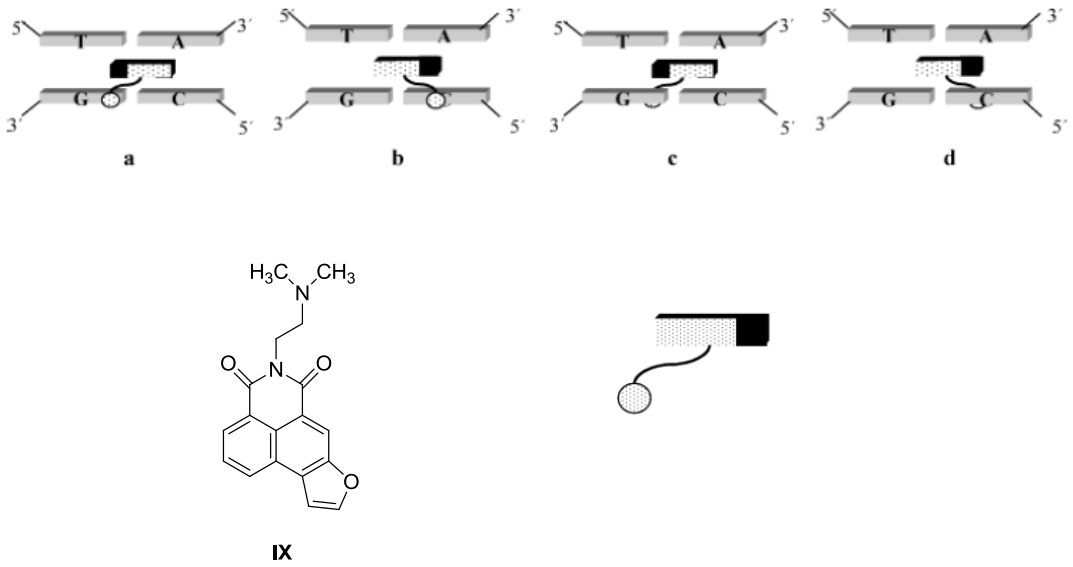

Figure 2.7: Possible interaction model of **IX** DNA; the black square represents the orientation of the furan ring, and the sphere represents the protonated dimethylamino group of the side chain.[40]

The more stable orientation was that where the side chain remained in the major groove of the DNA dinucleotide and the furan ring was stacked between A and C.[40]

A series of novel thiazonaphthalimides inspired by the interesting antitumor activity showed by this scaffold characterized by a fused aromatic ring with the naphthalimide skeleton, was synthesized by Li *et al*.

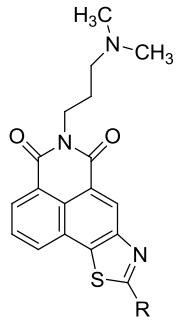

XIII: R = H
XIV: R = CH_3
XV: R = CF_3

These derivatives showed a strong DNA intercalation. Also in this series, the aminoalkyl side chain is important to the DNA binding, especially in placing the protonated side-chain nitrogen atom in a way suitable for hydrogen bonding formation with the DNA double helix. In this case the intercalating abilities of thiazonaphthalimides is enhanced by a three methylene units spacer between the two nitrogen atoms. The affinity for the DNA led to greater cytotoxic potency, so all these compounds were more active than Amonafide against A549 (human lung cancer) and P388 (murine leukemia) cell lines. In particular, **XIV** was more active against P388 and **XV** more active against A549 cell lines.[41]

In order to improve the activity of naphthalimides by increasing the binding capacity to DNA, a series of bis-naphthalimides agents was designed. These new molecules had structural features of Amonafide and Mitonafide. They were characterized by two naphthalimide units linked by a chain bearing at least one nitrogen atom. They are also characterized by different substituents on the aromatic rings.[28] These compounds were more potent than Amonafide and Mitonafide against HT-29 cell lines and the antiproliferative activity was sensibly influenced by the nature of the substituent on the aromatic rings. However, the most active compound was the unsubstituted one on the aromatic rings. This compound, called Elinafide, showed an excellent antiproliferative activity against HT-29 cell line. Moreover, *in vivo* studies showed that Elinafide not only inhibited tumor growth, but also induced tumor regression. Furthermore, the absence of the nitro group on the aromatic ring seemed to reduce the neurotoxicity associate with Mitonafide.[42,43]

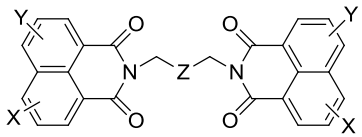

Y = H, 6-NO_2, 6-NH_2
X = H, 3-NO_2, 3-NH_2, 3-$NHCOCH_3$,
3-Br, 2-OH, 3-OH, 4-OH
Z = aminoalkylic chain

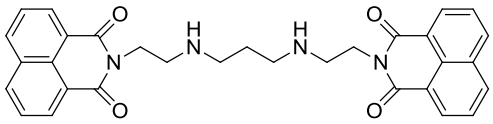

Elinafide

Structural studies showed that Elinafide form a sequence-specific complex with an exanucleotide d(ATGCAT)$_2$ portion where two naphthalimide units bisintercalate at TpG and CpA steps of the DNA, stacking with G and A. The *N*,*N*-bis(ethylene)-1,3-propylenediamine chain lies in the major groove and one of the protonated amino groups interacts via hydrogen bond with O6 of guanine in the major groove, while the other one could form and hydrogen bond to guanine O6 of the opposite strand or establishes a weaker hydrogen bond with N7 of the same base (Figure 2.8)[44]

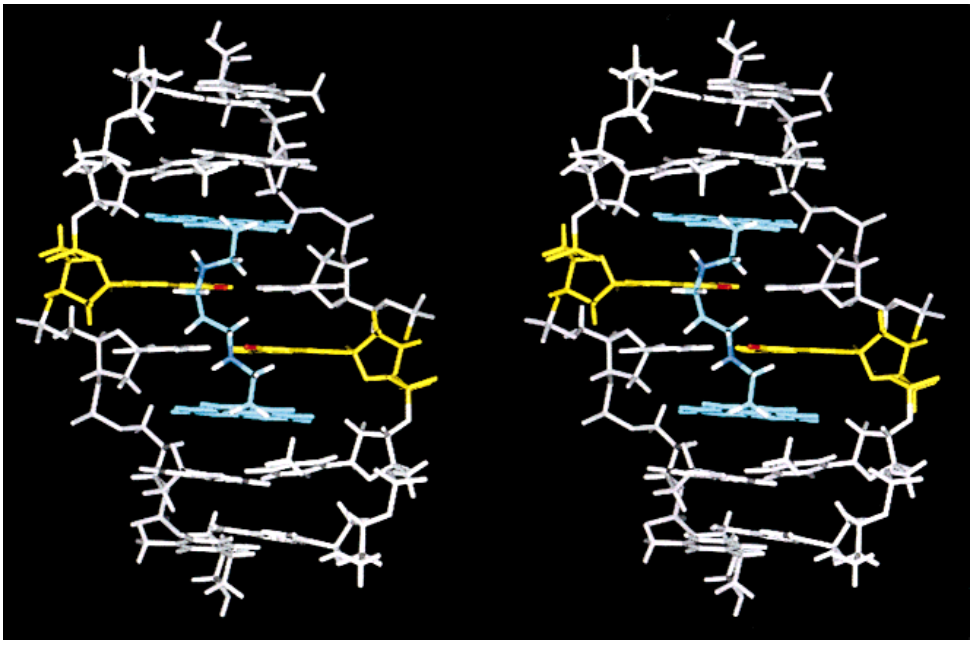

Figure 2.8: Stereoview of the complex elinafide-d(ATGCAT)2; Elinafide is in blue, guanine is in yellow and the oxygen atom is in red[39]

Later, a series of symmetric and non-symmetric analogues of Elinafide has been reported. In these molecules the naphthalene scaffold was replaced by an acenaphthene system. Among the derivatives, the non-symmetric compounds are less cytotoxic than the symmetric ones.[45,43]

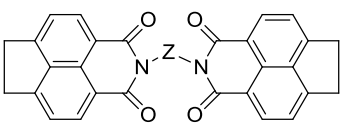

Symmetrical bis-derivatives of Elinafide

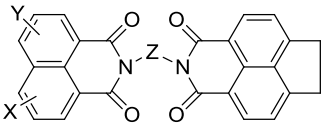

Asymmetrical bis-derivatives of Elinafide

In order to improve the activity of Elinafide, compound DMP-840 has been developed. It is a *bis*nitro-*bis*naphthalimide that binds DNA with high affinity and it was active against many tumor cell lines. Its mechanism of action has been studied by Nitiss *et al*.in particularthe molecule forms a stable ternary complex with DNA and TOPOII but did not poison TOPOII.[46]

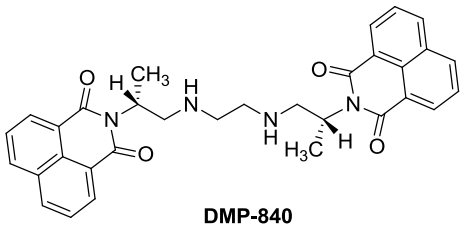

DMP-840

A further development was represented by the replacement of the naphtalenediimide structure with the 1,4,5,8-tetracarboxylic-naphthalendiimide (NDI) moiety to obtain more active intercalator agents. Both these features have a big aromatic system and two co-planar carbonyl groups. The new intercalators designed (N-BDMPrNDI, DMe-NDI, Phen-NDI) were able to intercalate into DNA and, in addition they could stabilize the triple helix DNA. Instability of triple-helix DNA was due to the repulsion between the nucleotides of these triple helix. Such structures are strictly implicated in the genes regulation. Several studies pointed out that an increase in the stability of these structure could be useful in anti-genes and antisense therapy.[47]

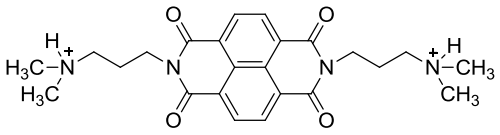

N-BDMPrNDI

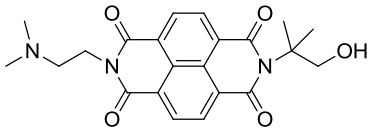

DMe-NDI

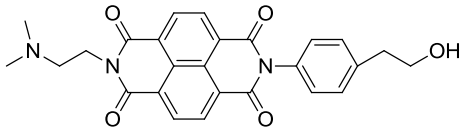

Phen-NDI

CHAPTER 3
G-QUADRUPLEX STRUCTURES

3.1 TELOMERES AND TELOMERASE

The natural ends of chromosomes resemble DNA breaks and should be protected from the DNA damage response machinery, avoiding chromosome fusions.

Telomeres are special heterochromatic structures, that protect the ends of eukaryotic chromosomes from degradation and, for this reason, they are essential for ensuring chromosome stability. Mammalian telomeres are formed by tracts of double-stranded TTAGGG repeats, which extend for 2-100 kb in humans (Figure 3.1). In particular, the end of the telomere is characterized by the presence of a 50-500-nucleotide protrusion of single-stranded repeats from the 3' end (this part is called G-tail or G-overhang).[48] Chromosome ends display high stability and are, in contrast to chromosome fragments, protected from end-to-end fusions and rearrangements.[49,50] This is possible because telomeres are associated by a specialized six-protein complex, known as Shelterin complex (also known as telosome), which binds to the telomere in a T-loop configuration.[51] These specific configuration provides a protective cap that defines the natural end of the chromosome and masks the telomere from the DNA damage response machinery.[52]

Proteins that compose Shelterin complex are:

- TRF1 also known as TERF1 (telomeric repeat-binding factor 1)
- TRF2 also known as TERF2
- RAP1 also known as TERF2IP (repressor and activator protein 1)
- TIN2 also known as TINF2 (TRF1-interacting nuclear protein 2)
- TPP1 also known as ACD (POT1-and TIN2-interacting protein)
- POT1 (protection of telomeres 1)

TRF1, TRF2 are directly bound to the double-stranded telomeric repeats, whereas POT1 attaches to the single-stranded G-overhang. These three proteins are interconnected by TIN2 and TPP1, forming a complex that allows cells to distinguish telomeres from sites of DNA damage. About RAP1, it does not bind TTAGGG repeats and its telomeric localization depend on interaction with TRF2. All these proteins have a complex role in

telomere length regulation, protection from enzymatic attack, and in the control of signaling cascades from the natural chromosome ends.[52,53]

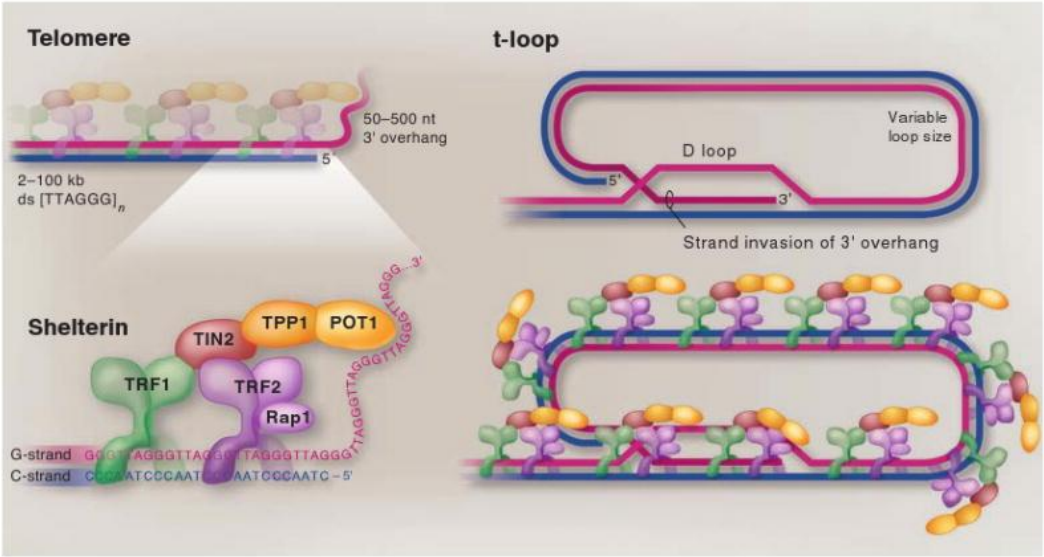

Figure 3.1: Mammalian telomeres.[54]

During each cell division cycle, telomeres shorten as a result of the incomplete replication of linear DNA molecules by conventional DNA polymerases, which is known as "end-replication problem". DNA polymerase cannot fully replicate DNA molecules which contain 3'-overhangs and the consequence is the continuous loss of telomeric sequences.[55] When telomeres become critically short, they lose their protective properties and send cells into a terminal arrest (terminative senescence) or cause cell death.[52] This implies that there is a limited number of divisions of a cell, known as the Hayflick limit.[56]

To overcome this problem, an enzyme, called telomerase, is capable of *de novo* synthesis of telomeric DNA.[55] Telomerase is an RNA-dependent DNA polymerase that adds multiple copies of the TTAGGG motif to the 3' ends of linear chromosomes. Telomerase is a large enzymatic complex of over 30 proteins,[57] but the active complex consists of (Figure 3.2):

- a telomerase RNA component (TERC or hTR), which provides the template for the synthesis of telomeric DNA;
- a reverse transcriptase catalytic subunit (TERT of hTERT);
- a pseudouridine synthase called dyskerin (DKC1).[57]

This complex is assembled in Cajal bodies in the nucleus and is shuttled to telomeres by the telomerase Cajal body protein 1 (TCAB1).[58]

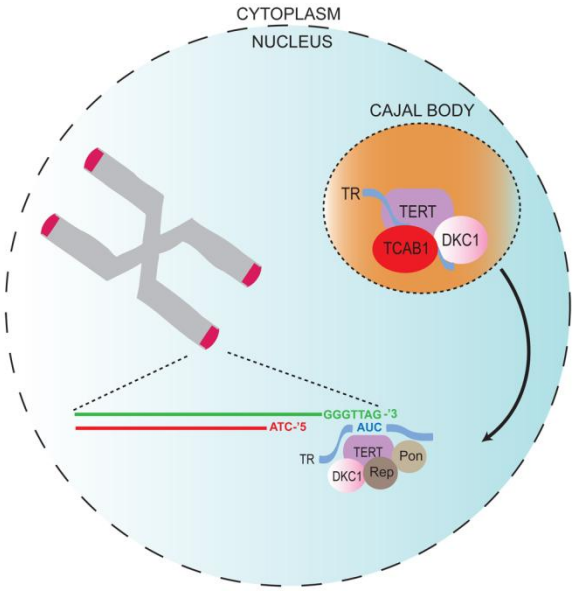

Figure 3.2: The telomerase complex[52]

The ATPases pontin (also known as RUVBL1) and reptin (also known as RUVBL2) sequester this immature complex into an active conformation, that associates with the terminal exposed 3' hydroxyl group and initiates nucleotide addition at the chromosome ends.[59] The activity of telomerase is negatively regulated by the Shelterin proteins TRF1 and POT1 to maintain telomeres at a constant length.[60]

This process is essential for highly proliferative cells like embryonic and adult stem cells. However, although telomerase is expressed in these compartments, this is not sufficient to maintain the telomeres length that is associated with cell division. So, telomeres became shorter with age in most tissues,[61] and this progressive telomeres shortening has been proposed to be one of the molecular mechanisms underlying ageing.[51,62] Telomeres length generally decreases to 50% from newborn to middle aged individuals.[63]

Human tumors (more than 85%) regain the ability to activate telomerase, and telomeres shortening is counterbalanced by the synthesis of telomeric sequences. As result cancer cells became immortal.[64]

Almost 15% of tumors do not express telomerase. This finding led to the discovery that there are alternative lengthening of telomeres pathways (ALT).[65] This process involved

the helicases (BLM and WRN), which are also implicated in DNA replication, recombination, and repair.[66,67] BLM and WRN are bound to and stimulated by TRF2, but their specific function in telomere maintenance is not known.[68] Recently has been shown that topoisomerase IIIα is essential in the ALT pathway.[69]

3.2 G-QUADRUPLEX

G-rich oligonucleotide sequences, can associate together in physiological ionic conditions to form four-stranded structures termed G-quadruplexes.[70] The fundamental unit of G-quadruplex is called G-quartet (also known as G-tetrad). G-quartets are planar alignments composed by four guanine bases interacting via Hoogsteen hydrogen bonds (an alternative to the classic Watson and Crick base pairing) to form a cyclic hydrogen-bonded square arrangement.[71] The resulting structure presents an aromatic surface with the negatively charged phosphate groups in the peripheral region of the square. The center of the tetrad is characterized by the presence of four carbonyl groups that are always coordinated by mono- or divalent cations, most commonly K^{+}[72] and Na^{+},[73] but also NH^{4+},[74] Pb^{2+},[75] or Sr^{2+}.[76]

Several G-quartets are held together by π-π interactions to form a G-quadruplex.[72,77] The presence of the coordinating cation is essential for G-quadruplex stability. In the absence of it, the negative electrostatic potential generated by the carbonyl groups would destabilize the structure.[78]

G-tetrads (Figure 3.3) were first discovered in 1962, and G-quadruplex structures were fully characterised in 1989.[79,80]

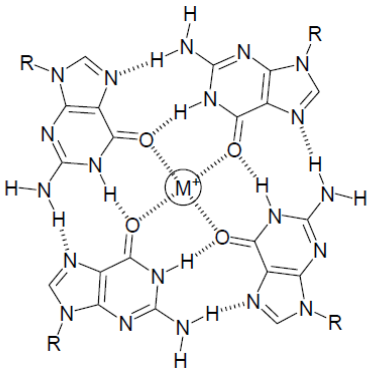

Figure 3.3: G-tetrad

G-quadruplexes are made up of one, two, or four DNA strands, which can run parallel or antiparallel, and the DNA sections which are involved in the quadruplex, but not part of the G-tetrads, form loops.[71] Due to steric constraints, the quartets cannot stack directly on top of each other, but are slightly twisted, with the result that the G-quadruplex exists as a quadruple helix. This helix is characterized by a central hydrophobic core and four lateral negatively charged grooves, which are the cavities formed by the phosphodiester backbone. The center of the hydrophobic core constitutes a tunnel of positively charged ions, which coordinate the four carbonyl groups of each G-quartet.[81]

G-quadruplexes have different topologies, depending on different features. They can be formed by guanines from the same strand (intramolecular G-quadruplex) or by interactions among guanines from different strands (intermolecular G-quadruplex) (Figure 3.4).

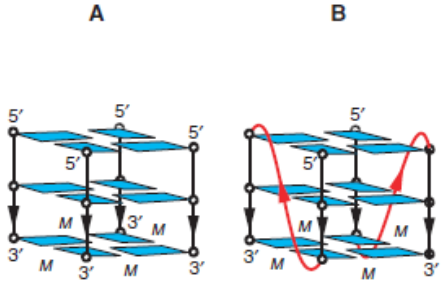

Figure 3.4: Schematic structure of human telomeric G-quadruplexes. A: intramolecular G-quadruplex B: intermolecular G-quadruplex[71]

Depending on the strand polarity and on the sequence, two strands can be interconnected in different ways (Figure 3.5): lateral loops generally connect two antiparallel adjacent strands, diagonal loops connect two antiparallel opposite strands, and propeller or double chain reversal loops bond two adjacent parallel strands.[82]

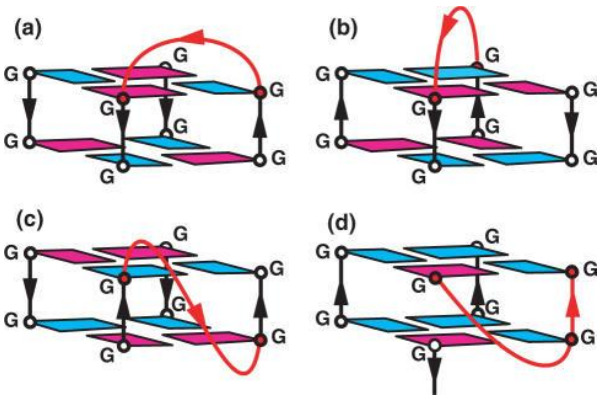

Figure 3.5: Possible loop types. (a) lateral edgewise loop (b) diagonal loop (c) propeller loop (d) V-shaped loop.[83]

The glycosidic conformations of guanines (*syn* or *anti*) within a G-tetrad are geometrically associated with the relative strand orientations. For example, in parallel strand structures only the *anti* conformation has been observed, while in antiparallel G-quadruplexes exists both *syn* and *anti* conformations.[81]

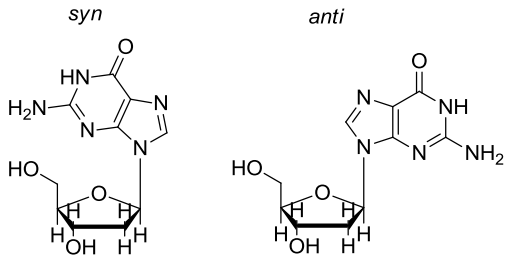

The type of cation involved in the coordination of G-quadruplex is also important. The same sequence can assume different G-quadruplex topologies, depending on the cation. For example, telomeric DNA is parallel in K^+ containing crystals,[72] and mostly antiparallel in Na^+ solution[84] and NH_4^+.[85]

3.3 G-QUADRUPLEX IN CANCER DISEASE

Biological interest in G-quadruplex structures was little until the early 1990s, when it was discovered that the end of chromosomes were G-rich sequences that could fold into G-quadruplex structures *in vitro*, under conditions very similar to the physiological environment.[86] Telomerase plays an important role in cancer, maintaining cellular

immortalization by catalyzing telomere extention, consequently it can be considered a valuable target for cancer research. Moreover, G-rich telomeric single-stranded overhang are able to form G-quadruplex structure. Thus, molecules able to stabilize telomeric G-quadruplexes, could inhibit telomerase and be useful in anticancer therapy.

In 2000, Hanahan and Weinberg proposed six hallmarks involved in cancer process. They were: self-sufficiency in growth signals, insensivity to anti-growth signals, evasion of apoptosis, sustained angiogenesis, limitless replicative potential, and tissue invasion and metastasis.[87] G-quadruplex were found in the promoter regions of oncogenes implicated in all these six events, particularly in transcription factors like c-myc, or in the small GTPase k-ras and in the receptor tyrosine kinase kit. This latter is a clinically validated drug target for treating gastrointestinal stromal tumors.[88] Telomeric G-quadruplexes are available from single-stranded DNA template, while G-quadruplexes in gene promoters are formed from duplex DNA, and consequently are more difficult to obtain. However, during DNA replication, transcription and recombination process, these double-stranded regions become transiently single-stranded, and at this point it is possible to obtain G-quadruplex.[89]

As a consequence of the above studies the G-quadruplexes of these proto-oncogenes become potential targets to take into account as a novel anticancer strategy.[25]

3.3.1 Telomeric G-quadruplex

The human single-stranded telomeric overhang, can fold up into a number of G-quadruplex structures. All these structures have different features depending on the coordinating cation used and its concentration.[72,84,90] The first crystal structure of the sequence d[AGGG(TTAGGG)$_3$] with K^+ ions was obtained from Parkinson *et al.* in 2002. The crystal structure showed a monomeric G-quadruplex with all four strand in a parallel arrangement. The linking trinucleotide loops located on the exterior of the quadruplex core, were in a propeller-like rearrangement and all the guanine glycosidic bonds had an *anti* conformation (Figure 3.6).

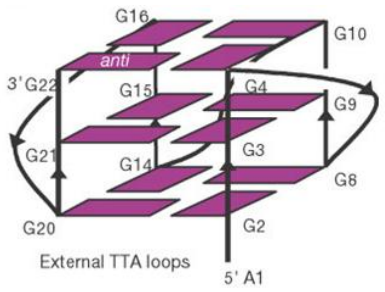

Figure 3.6: Schematic representation of the telomeric G-quadruplex[72]

The loops were composed of TTA bases, and the adenine was intercalated between the two thymines (Figure 3.7). Also, since they were formed by three bases, the loops were quite extended and, for this reason, they conferred to the grooves a characteristic v-shape form. The potassium ions were located between two tetrads, coordinating the carbonyl groups from both.[72]

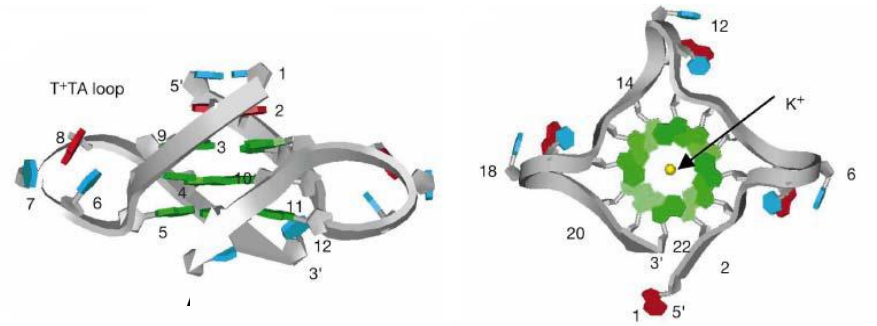

Figure 3.7: A: Side view of the telomeric quadruplex. It is possible to see the intercalation of the adenine (red) between the two thymines (light blue) in the propeller loops. B: Top view of the structure. The potassium ion is indicated by an arrow. Guanines are coloured in green.[72]

Several studies have been done to investigate the telomeric sequence in K^+ solutions, using circular dicroism (CD)[91] and NMR techniques.[73] These studies showed that the sequence was able to form a number of different structure at equilibrium. Anyway, further studies that imitated cell environment conditions, demonstrated that the preferred conformation is the parallel one.[91,92] For this reason, the structure of biological relevance could be represented by the one obtained by crystallographic methods.[72]

The presence of G-quadruplex structures *in vivo* has been demonstrated in ciliates,[93,94,89] but the exact biological role of these induced G-quadruplexes is still under investigation. Studies with G-quadruplex specific antibodies, demonstrated that G-quadruplex structures were cleaved during replication process,[93] and further investigation indicated an implication of G-quadruplexes in telomerase recruitment.[94]

3.3.2 G-quadruplex formed from *c-kit* sequence

The human proto-oncogene *c-kit* encodes for a family of growth factor receptors with tyrosine-kinase activity, so it is responsible for cellular proliferation, differentiation and survival.[95] *c-kit* mutations are associated with uncontrolled cell proliferation in tumors like prostate, gastrointestinal and adenocarcinoma lung cancers.[96] Since there are only a small number of tumors correlated with *c-kit* overexpression, this proto-oncogene could be considered a target for these specific types of cancer. *C-kit* promoter region presents two G-rich sequences:

- *ckit87up* (Ckit-1) at -87 to -109 bp
- *Ckit-2* at -140 to -160 bp

It has been demonstrated that these two sequences could form G-quadruplex structures *in vitro*.[96,97]

The G-quadruplex structure of *Ckit-1* has been characterized by NMR in K^+ solution and it is shown in Figure 3.8.

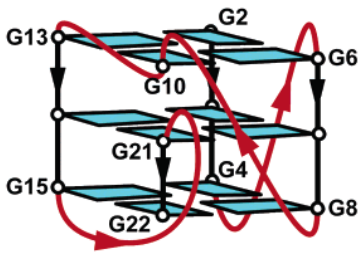

Figure 3.8: Schematic representation of *Ckit-1* structure.[98]

This structure showed an unusual topology. It was an intramolecular parallel G-quadruplex, formed by three G-tetrads with all the glycosidic bonds arranged in *anti* conformation but, a guanine not belonging to a G-tract (G_{10} in Figure 3.8) was involved in

the formation of the G-quartet and, for this reason, there were four loops in the structure. Moreover, it has been observed an additional Watson-Crick base pairing between A_1 and T_{12}. This bond was very important for the stability of the structure.[98]

Recently, the first crystal structure of *ckit-1* has been published.[99] The X-ray structure is in accord with the earlier NMR topology assignment. However, it revealed a highly significant difference in the dimension of the large cleft in the structure.

The first NMR indications about the structure of *ckit-2* has been obtained in 2009.[100] The paper reported that *ckit-2* presented at least two different topologies in equilibrium. However, after long exposure (weeks) of the sample at temperature between 25°C and 28°C the conformation showed in Figure 3.9 A, (with a parallel arrangement, glycosidic bonds in *anti* conformation and three propeller loops) was the predominant.

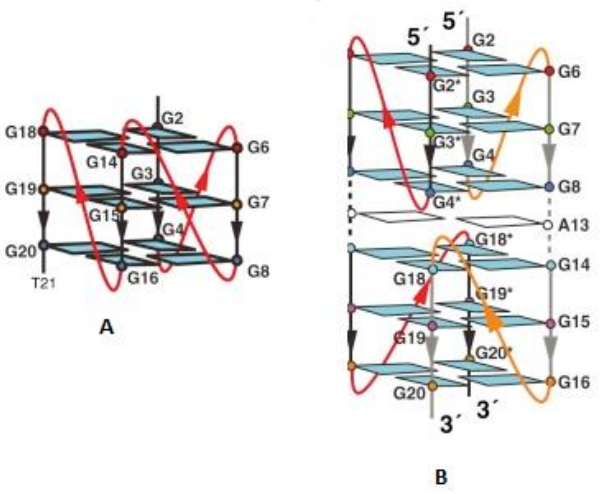

Figure 3.9: Schematic representation of the two conformation of *ckit-2* G-quadruplex. A: monomeric G-quadruplex. B: the dimeric G-quadruplex topology.[101]

Few months later, Patel et al. also proposed the NMR structure of *ckit-2*.[101] Their studies showed the presence of two forms in equilibrium: the one indicated by the precedent study (Figure 3.9 A) obtained at 20 mM KCl concentration, and the second one characterized by a dimeric parallel topology (Figure 3.9 B) obtained at 100 mM KCl concentration. The authors indicated the dimeric structure as the thermodynamically stable conformation, since the monomeric form was converted into the dimeric after a few months.

The dimeric conformation was composed of six G-tetrads, which form a 5’ monomer and a 3’ monomer, with parallel strands and all the glycosilic bonds in *anti* conformation.[101]

3.4 G-QUADRUPLEX-BINDING LIGANDS

G-quadruplex structures can be stabilized by small molecule ligands. The ligands can interact with G-quadruplex trough different binding mode: external stacking, intercalation, or groove binding. (Figure 3.10) However, intercalator binding between G-tetrads inside the quadruplex is very difficult, since the G-quadruplex is an extremely stable and rigid structure, so the distortion of quadruplex integrity requires a very high energy cost. Consequently, the most probably binding mode for ligands is the stacking on the outer planes.[102]

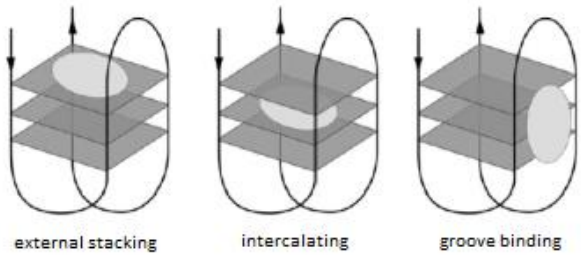

Figure 3.10: Representations of ligand-G-quadruplex complex.[102]

G-quadruplex ligands are usually characterized by an aromatic system, which is able to perform π-π stacking interactions with the terminal G-tetrads of the G-quadruplex. Some compounds showed terminal amino groups in the side chains, which can be protonated *in situ* and are assumed to interact with negatively charged phosphates in the grooves at the sides of the G-quadruplex. Positive charge generally increases the affinity for negatively charged nucleic acids, and confer more hydrophilic property to the molecule.[103]

There are several classes of G-quadruplex binding ligands. Here it will be reported only those related to the most important ligands .

Antraquinones and related compounds

The first quadruplex-interactive ligand as a telomerase inhibitor was discovered in 1997. It was a symmetric molecule, the 2-6-disubstituted aminoalkylamido anthraquinone BSU-1051.[104]

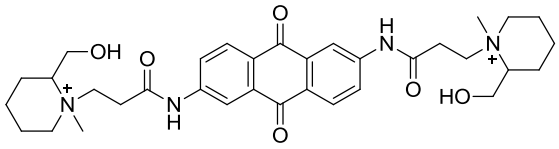

BSU-1051

The compound showed a telomerase inhibitory value ($^{tel}IC_{50}$) of 23 μM and it bound the G-quadruplex formed by the telomeric 7-mer d(TTAGGGT). Subsequently, many derivatives have been synthesized to investigate different substitution patterns and side chains. In particular, 1,4-, 1,5-, 1,8-, 2,6-, and 2,7-regioisomers with various substituent on the chromophore have been investigated.[105,106]

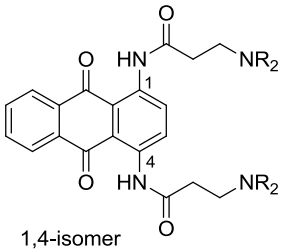

1,4-isomer

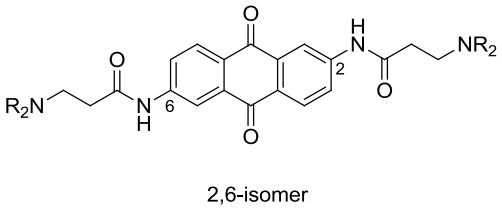

2,6-isomer

All these compounds showed high levels of cytotoxicity, possibly due to redox cycling.[107]

Consequently, a series of 2,7-fluorenone analogues have been synthesized to decrease cytotoxicity by prevention of redox cycling through removal of one of the quinone carbonyl moieties.[108]

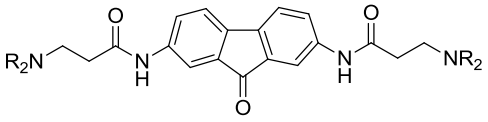

2,7-fluorenone

This series showed a decrease of about 10 fold in cytoxicity against a panel of human-tumor-derived cell lines. However they were less active against telomerase, probably caused by a decrease in electron deficiency of the 2,7-fluorenone chromophore. This fact, disfavoured π-stacking interactions with the G-quadruplex binding site.

Acridine derivatives

To improve the affinity and binding for G-quadruplex structures, a series of acridine based ligands was designed. The acridine core was chosen because it was similar with the anthraquinone in terms of interaction with G-quadruplex DNA, but it also presented a single nitrogen in the core, which is protonated at physiological pH. This feature represented an extra source of interaction with the G-quadruplex, since the positively charged ring is likely to be complementary to the channel of negative electrostatic potential of G-quadruplexes. Based on these studies, a library of 3,6-disubstituted acridines was synthesized.[109]

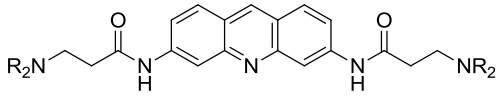

3,6-disubstituted acridines

These molecules showed improved telomerase inhibitor activity and lower cytotoxicity. This result encouraged the development of other classes of acridine based compounds. Two of them were the more interesting and reported below.

The first class of acridine derivatives was published by Stevens and co-workers, and presented an extension of the acridine aromatic core. The pentacyclic acridine RHPS4 was able to inhibit telomerase activity *in vitro* ($^{tel}IC_{50}$ = 0.33 μM)[110] and *in vivo*.[111,112,113]

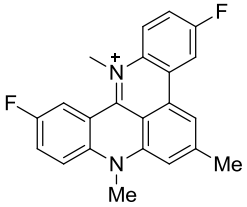

RHPS4

Moreover, the compound formed 2:1 complexes with the telomeric sequence $d(TTAGGGT)_4$.[114] RHPS4 inhibited melanoma cell growth in a dose dependent manner, generating cell cycle alteration and apoptosis. This drug caused a telomere damage resulting in telomeres uncapping,[111] which is correlated with the loss of POT1,[113] while TRF2 remains localized at the telomeres. Also, the ligand caused the formation of telomere dysfunction-induced focus (TIF), where phosphorylated γ-H2AX and other damage response factors are recruited to the telomeres, along with the immediate loss of POT1.[113] Moreover, other studied revealed a decrease of telomerase expression, probably due to a c-myc down-regulation.[111] Recently, it has been shown that in combination with taxol, RHSP4 caused tumor regression in uterine carcinoma UXF1138L xenograft.[115]

The second important class of acridine derivatives, designed by Neidle and co-workers, is represented by a series of 3, 6, 9-trisubstituted acridines.[116] The lead compound was BRACO-19 and to date, is one of the most investigated G-quadruplex binding ligands.

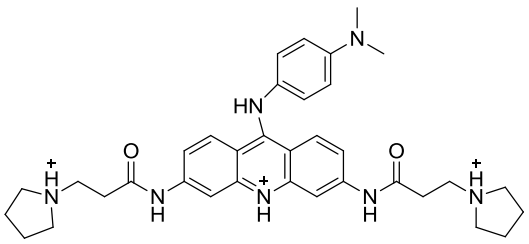

BRACO-19

BRACO-19 showed significant telomerase inhibitory activity, with a $^{tel}IC_{50}$ value of 6.3 μM.[117] *In vitro* it was able to inhibit cell growth at sub-cytotoxic concentrations in a number of cancer cell lines, to induce senescence,[118] telomere shortening,[119] telomere end-to-end fusion,[120] and displacement of the protein POT1[121] from telomeres of treated cells. *In vivo*, BRACO-19 has been evaluated in xenograft models of the vulval carcinoma cell line A431 in combination with paclitaxel, showing a major antitumor effect than paclitaxel alone.[118] As single agent, BRACO-19 was tested in uterine carcinoma xenograft UXF1138L, showing high activity against early-stage tumors.[119] The compound was found to enter the nuclei, and cancer cells exposed to the ligand *in vitro* and *in vivo*, showed complete loss of hTERT expression and very rapid telomere shortening. The antitumor effects were apparent within a very few days after the start of treatment and this fact

suggested that BRACO-19 does not act as a simple telomerase inhibitor, but the more rapid damage response could be consequence of G-quadruplex stabilization at the telomere ends.

A complex between BRACO-19 and the bimolecular telomeric quadruplex d(TAGGGTTAGGGT) has been crystallized by Campbell *et al.*[122] The core of the molecule is packed in a sandwich-type manner between two monomers; the positively charged side chains in position 3 and 6 each extend into a wide groove, while the side chain in position 9 inserts into a narrow hydrophobic pocket (Figure 3.11)

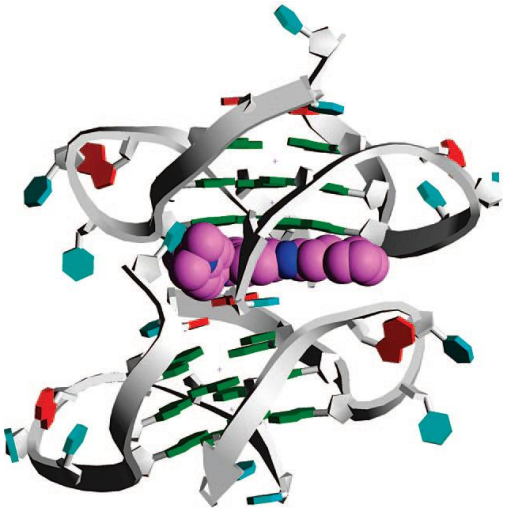

Figure 3.11: Crystal structure of a BRACO-19 complex. The ligand (mauve) is shown at the interface of the two quadruplexes[122]

Telomestatin

Telomestatin is a macrocyclic natural product consisting of seven oxazole rings and one thiazoline ring. It was isolated from the actinomycete *Streptomyces anulatus*. It is currently the most efficient *in vitro* telomerase inhibitor, with a $^{tel}IC_{50}$ value of 5 nM.[123,124]

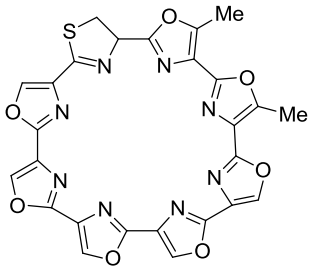

Telomestatin

Telomestatin is able to induce the formation of intramolecular G-quadruplexes with telomeric sequences *in vitro*.[124] The compound caused growth inhibition in a wide range of cancer cells, with the development of senescence, as well POT1 displacement from telomeres.[125,126,127] Telomestatin caused telomere end-to-end fusion in a series of leukemic cells, which led to apoptosis.[128] An analogue effect was observed after U937 xenograft treatment with increased doses of the drug,[129] where histological examination of treated tumor showed a large number of apoptotic cells. Recently, it was demonstrated that initiation of G-quadruplexes by telomestatin leads to the dissociation of topoisomerase IIIα, which is essential for the ALT pathway, from telomeres in ALT cells.[69,130] The main problem with this ligand is that its synthesis is very challenging[123,124,131] and the analogues designed to date do not reproduce the same efficacy.[132]

Perylene derivatives

The first perylene derivative, named PIPER, was designed as specific quadruplex ligand.[133] The compound displayed G-quadruplex stabilization and telomerase inhibition in the micromolar range. Furthermore, PIPER was able to form G-quadruplex structure in the c-myc promoter sequence when in duplex conformation, and it showed the same property towards ciliate telomeric sequence, but not for the human one.[134]

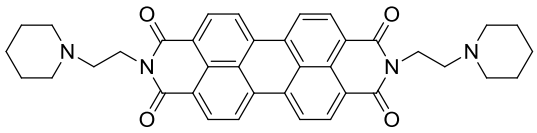

PIPER

Based on this scaffold, a series of analogues has been synthesized. The modifications to the original structure were focused mainly on the type of terminal amine,[135] the nature of the side chain,[136] the number of the side chains,[137] and the extention of the aromatic core.[138] In particular, the disubstituted perylene derivatives with polyamine side chain showed good G-quadruplex binding efficacy in FRET assay. Also, in electrophoresis and CD experiments they showed particular affinity for the parallel G-quadruplex conformation.[139] Among all the derivatives synthesized, compounds POL-3 and POL-8 showed improved telomerase inhibitor activity with respect to PIPER.

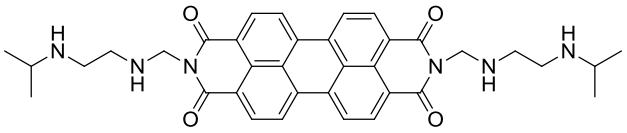

POL-8

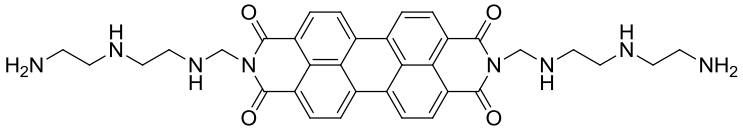

POL-3

Naphthalene diimide (NDI) derivatives

Tetrasubstituted NDIs are excellent motifs for the molecular recognition of G-quadruplexes, since they present a π-acidic core that is ideal for performing π-π stacking interactions with G-tetrads. Also, the four side chains bearing amino group at the end could interact with the grooves at the sides of the G-quadruplex.[140-142]

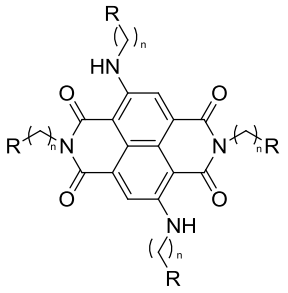

NDIs derivatives

A series of NDI compounds with different terminal amine functions and side chain length have been reported by Cuenca *et al*. These compounds showed exceptional affinity for telomeric G-quadruplex DNA in FRET assays with ΔT_m values between 14 and 35 °C at 0.5 μM. Molecules with very high affinity for G-quadruplex displayed very high toxicity against MCF7 and A549 cancer cell lines, with IC_{50} values of 10-200 nM, and up to 10-fold selectivity over a normal fibroblast cell line. However, competition FRET experiments, demonstrated that the most potent G-quadruplex binding agents, did not displayed a high selectivity for G-quadruplex DNA over duplex DNA.

In the same publication,[140] trisubstituted NDIs were also reported. These derivatives, generally had lower affinity for G-quadruplex than tetrasubstituted, maybe because the lack of a side chain reduced the interactions with the grooves at the sides of the G-quadruplex.

To better understand the binding mode of NDIs, a tetrasubstituted derivative of this series (**XVI**) has been co-crystallized with a an intramolecular human telomeric 23-mer G-quadruplex DNA (Figure 3.12).[141]

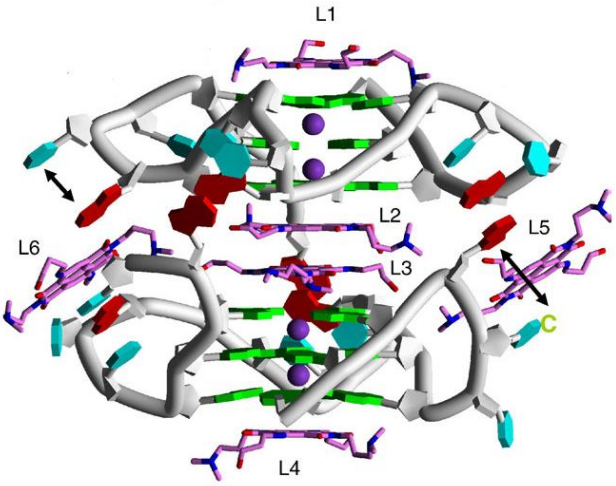

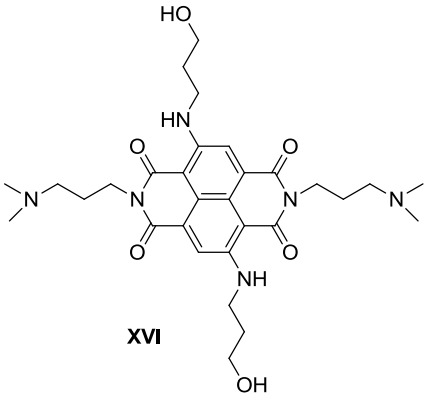

XVI

Figure 3.12: The 23-mer crystal structure of the intramolecular quadruplex of the sequence d[TAGGG(TTAGGG)$_3$] complexed with ligand **XVI** [141]

As shown in Figure 3.12, the terminal G-tetrads are coordinated by one NDI core each. Four NDI molecules coordinate the G-tetrads of two G-quadruplexes, and two NDI molecules display external interactions with bases in the loops at the sides of the G-quadruplexes.

Among the derivatives synthesized by Cuenca *et al.* compound **XVII** resulted particularly interesting.

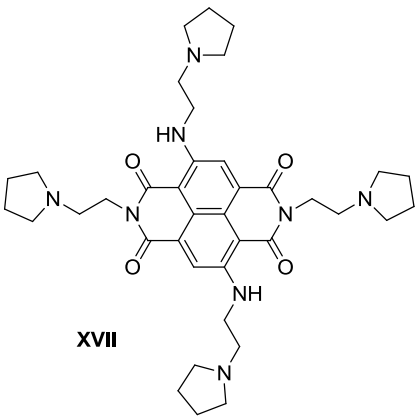

XVII

It showed high affinity for the G-quadruplex in the promoter region of the oncogene *c-kit*, and it was evaluated for the treatment of gastrointestinal stromal tumors (GIST),[142] since over 80% of GIST cells present a mutation in the *c-kit* gene. Treatment of GIST882 cells with **XVII** resulted in suppression of *c-kit* mRNA and *c-kit* protein expression, together with a decrease in telomerase activity. These results suggested a dual mechanism of action of this compound, as it stabilized both a *c-kit* promoter G-quadruplex and the telomeric G-quadruplex. However, this compound showed toxicity against normal fibroblast cell line WI38 (IC_{50} = 0.06 μM)[140] 26 times higher than towards GIST882 (IC_{50} = 1.6 μM).[142] Unfortunately, this fact was not a promising starting point for *in vivo* evaluation.

To improve the interaction with the grooves at the sides of the G-quadruplex and also to obtain a better selectivity for cancer cell lines, computer modeling studies led to a series of NDIs derivatives synthesized by Hampel *et al*.[143] All the compounds in this series presented an *N*-methylpiperazine as end group and different length of the side chains, to determine how deeply end groups could reach into the grooves.

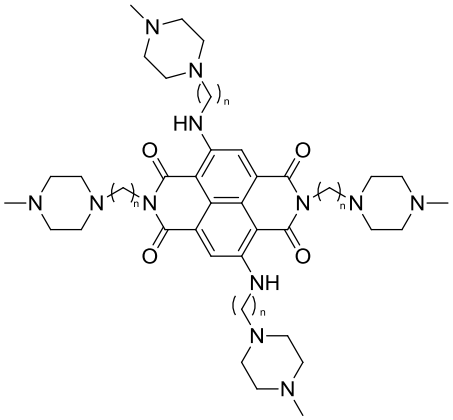

n = 3 **BMSG-SH-3**
n = 4 **BMSG-SH-4**
n = 5 **BMSG-SH-5**

The molecules showed high affinity for the telomeric G-quadruplex sequence F21T in FRET experiments with ΔT_m values between 24 and 28 °C, stabilizing quadruplex with a parallel-type topology. The affinity for the *ckit-2* was moderate, and for *ckit-1* and T-loop DNA was really low (ΔT_m 1-5 °C). Moreover, it was able to stabilize the G-quadruplex in the HSP90 promoter region. Also they were selective for G-quadruplex DNA in competition FRET assay: the 10:1 duplex:quadruplex ratio did not interfere with the stabilization of G-

quadruplex. *In vitro*, BMSG-SH-3 and BMSG-SH-5 inhibit the binding of hPOT1 and Topo IIIα to telomeric G-quadruplex. All the compounds were tested in a panel of tumor cell lines, including pancreatic cancer cell lines Mia-Pa-Ca-2, PANC-1 and HPAC, where they showed IC_{50} values of 0.1-0.2 μM and they were less toxic in the normal human fibroblast cell line WI38, which does not express telomerase. *In vivo* studies on BMSG-SH-3 using Mia-Paca-2 xenograft models, confirmed the activity against pancreatic cancer and the compound was found to be selectively localized in the treated tumor. Furthermore, BMSG-SH-3 was able to reduce telomerase activity and the expression of the chaperone protein HSP90, a regulator of telomerase.

Recently, the crystal structures of the complexes between BMSG-SH-3 and BMSG-SH-4 and the 22-mer d(AGGG[TTAGGG]$_3$) human telomeric intramolecular quadruplex have been published (Figure 3.13).[144] Both the compounds promoted parallel-stranded quadruplex topology, binding exclusively to the 3' surface of each quadruplex with extensive π-π contacts.

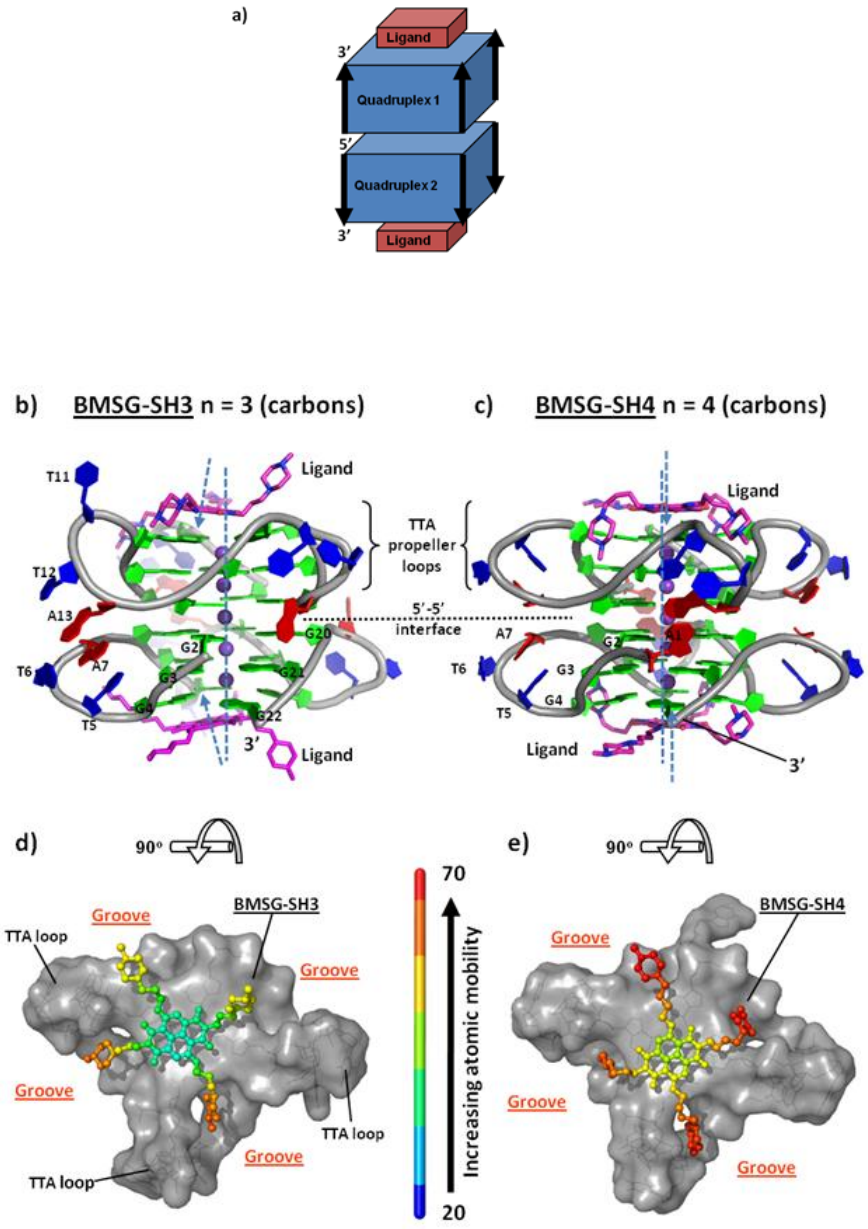

Figure 3.13: (a) Schematic showing quadruplex associations with 5′–5′ packing interactions and 3′ ligand binding. (b, c) Cartoon representations of the BMSG-SH-3/Gtel22 and BMSG-SH-4/Gtel22 complex structures. (d, e) Representations, projected onto the plane of the terminal G-quartets, of the Gtel22 quadruplex solvent-accessible binding surfaces with the bound ligands BMSG-SH-3 and BMSG-SH-4 shown colored by crystallographic temperature factors (or B-factors). Temperature factors provide a measure of atomic mobility in the crystal lattice.[144]

In both structures, the side chains are positioned within the G-quadruplex groove regions, interacting through hydrogen bonds, water bridges, and electrostatic contacts with the negatively charged phosphate groups. Atomic mobility has been measured by the crystallographic temperature factors (B factors), and they showed that the four *N*-methylpiperazine end groups of BMSG-SH-3 are significantly less mobile that those of BMSG-SH-4 (Figure 3.13 d and e). Consequently, BMSG-SH-4 binding to the G-quadruplex is slightly destabilized. This result is in accord with FRET data.

CHAPTER 4
POLYAMINES AND CANCER

Natural polyamines are ubiquitous, characterized by a low molecular weight, and play multifunctional roles in cell growth, differentiation, and survival. The only polyamines synthesized in mammalian cells are Putrescine (Put), Spermidine (Spd) and Spermine (Spm). They are protonated at physiological pH, and this polycationic nature allows them to bind electrostatically negatively charged molecules like nucleic acids, proteins and membranes.[145]

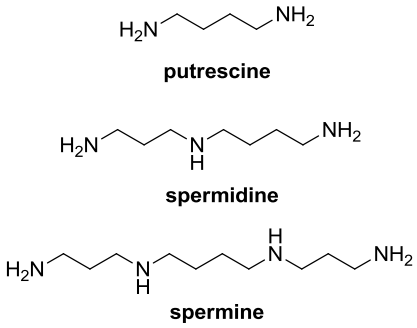

Polyamines can also be obtained from the diet (cheese and meat)[146] and from other sources, such as intestinal bacteria [147, 148]

Studies on patients with leukemias, melanomas, adenocarcinomas and lymphomas showed high amounts of polyamines in serum and urine. Consequently polyamines were proposed as biochemical markers of neoplasia. In addition, high levels of polyamines can be found in other conditions like cystic fibrosis, psoriasis and pregnancy. This fact can underline that polyamines are implicated in many physiological or pathological situation related to cell growth or cell death.[149]

The link between polyamines and cancer was elucidated. Genetic alterations, expression levels and activities of polyamine-metabolizing enzymes changes rapidly during tumorigenesis resulting in high levels of polyamines in many type of tumors.[145]Furthermore, polyamines participate in the apoptotic pathway and are able to interact with DNA modulating DNA-protein interaction.[150] All these features and the pathways correlated with

them can be considered potential targets for anticancer therapy. Further explanation will be provided in the following sections.

4.1 POLYAMINES SYNTHESIS, DEGRADATION AND ROLE IN CELL CYCLE

Polyamines are formed in the cytoplasm by enzymatic decarboxylation of ornithine, an amino acid produced as part of the urea cycle, which involves both cytosolic and mitochondrial enzymes (Figure 4.1).[151] In the first stage of the polyamines synthesis, ornithine is converted in Putrescine (Put) by the action of ornithine decarboxylase (ODC). Decarboxylation of S-adenosylmethionine (SAM), by S-adenosylmethionine decarboxylase (AMD) yields decarboxylated SAM (dcSAM), which donates its propyl amine moiety for the formation of Sperimidine (Spd) and Spermine (Spm) by spermidine synthase (SRM) and spermine synthase (SMS), respectively.

Polyamines are degradated by spermidine/spermine N^1-acetyltransferase (SSAT), a propylamine acetyltransferase. SSAT monoacetylates Spd and can either mono- or di-acetylate Spm. Diamines and acetylated polyamines are substrates for the diamine transporter (DAX), and they are eliminated in urine. Acetylated Spd and Spm are also substrates for a flavin-dependent polyamine oxidase (PAO) which catalyses their back conversion to Put. Also, a spermine oxidase (SMO), which can oxidize non-acetylated spermine, has been characterized.[152]

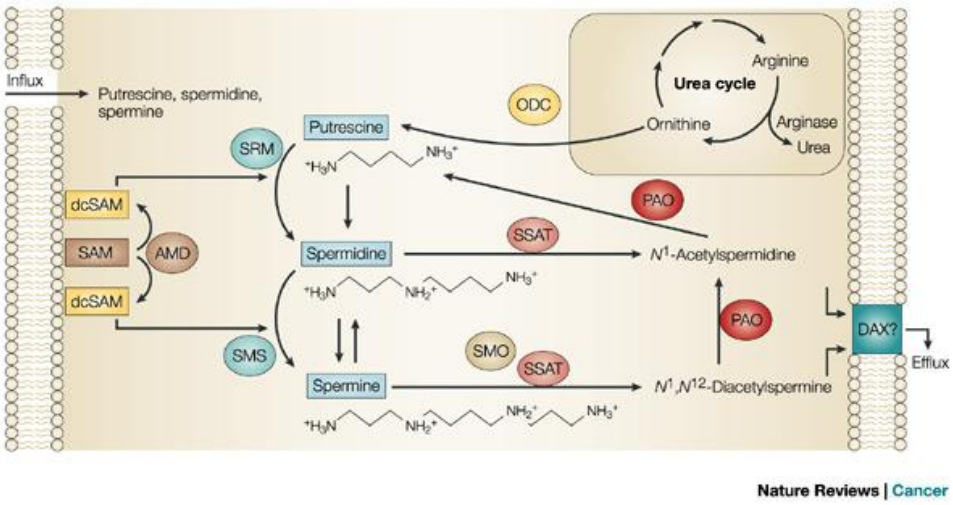

Figure 4.1: Polyamine metabolism in mammals[151]

ODC is an essential metabolic effector required for normal development in mammals.[153] It is frequently described as the rate-limiting step in polyamine synthesis but this is inaccurate: the supply of the aminopropyl donor dcSAM, by the action of AMD also influences the conversion of Put into the higher polyamines.[154]

ODC is an homodimer with two active sites formed at the dimer interface between the *N*-terminal domain of one subunit and the C-terminal domain of the other.[155] It has very short half-life (10-30 minutes in mammalian systems), and it is destroyed by the 26S proteosome.[156]

ODC protein levels in cells are regulated by two proteins termed antizyme (AZ) and antizyme inhibitor (AZIN).[154] AZ binds to the ODC monomer thus inactivating the protein and targeting it for degradation by the 26S proteosome. AZIN binds to AZ more tightly than ODC and can displace it, preventing the degradation. Induction of AZ also blocks polyamine transporter (Figure 4.2).[157]

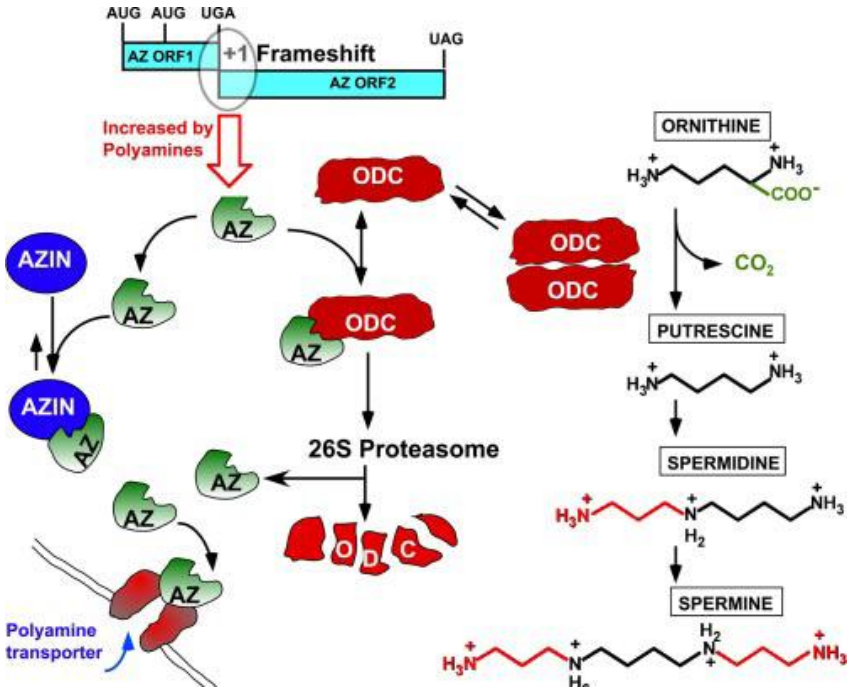

Figure 4.2: Role of antizyme and ODC in polyamine metabolism[157]

ODC plays an important role in neoplastic transformation. The *Odc* gene promoter region contains sequences that allow response to hormones, growth factors and tumor promoters. In particular, ODC mRNA synthesis is increased by the *c-Myc* oncogene[158], a transcription factor required for the proliferation of normal cells. Its over-expression can lead to uncontrolled growth and cancer.[159] ODC is also target of the *Ras* oncogene: mutant *k-Ras* oncogene increases cellular polyamine levels by increasing ODC enzyme activity.[160]

ODC can react quickly with nitric oxide resulting in inactivation of the enzyme. Therefore nitric oxide is considered an inhibitor of polyamine synthesis.[161]

An important enzyme of polyamine catabolism is SSAT, an highly inducible enzyme whose primary function is to maintain polyamine homeostasis. A rise in polyamines content causes induction of SSAT resulting in acetylation of Spd and Spm (by the transfer of the acetyl group from acetyl-coenzyme A to the N^1 position of both Spd and Spm), and consequent degradation via the SSAT/PAO pathway.[162] Cancer can develop mechanisms to prevent the induction of SSAT in order to maintain high polyamine levels. It has been shown that activated *K-Ras* suppressed SSAT expression by a mechanism involving the

PPARγ, a member of the nuclear hormone receptor family and an important regulator of cell proliferation and differentiation.[163,164]

Mammalian cells are endowed with a Polyamines Transporter System (PAT) which has yet to be molecularly defined. This system contributes to the intracellular polyamines amount and it could be a valid strategy to introduce drugs with polyamine scaffold into the cell.[156]

Polyamines are important mediators in the cell regulation process. Depending on environmental signals, they can promote cell growth or cell death.

Normal cell growth is regulated by proteins known as cyclins and cyclin-dependent kinases (cdks). Increasing and decreasing of cyclins A, B, D and E and their respective cdk, are key steps for the cell cycle progression.[165] In particular, in the G_1 phase, cyclins D1, D2 and D3, and cyclin E can activate the appropriate cdks. Once activated, cdks can phosphorylate specific substrates leading to cell cycle progression.[166] Cdks are inhibited by molecules called cdk inhibitors (cdkIs). They block the activity of cyclin-cdk complexes, resulting in break of cell cycle progression.[167,166] How polyamines affect the cyclin/cdk system is still not clear. It seems that polyamines are able to regulate cyclins degradation but the exact mechanism is not yet defined.[168]

It has been shown that polyamine and ODC levels change during the cell cycle. They display two peaks: one in conjunction with the G_1/S transition and the second in the G_2 phase (Figure 4.3).[169]

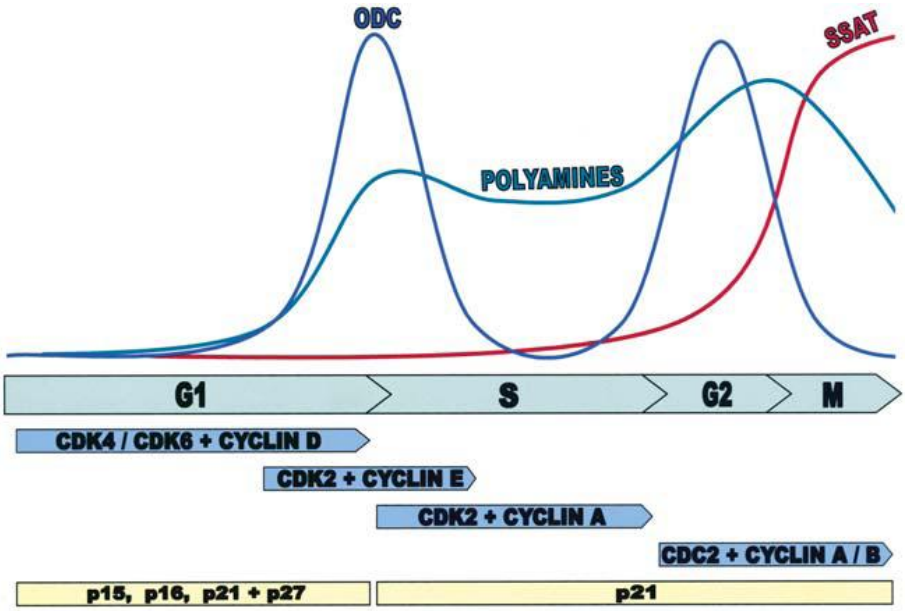

Figure 4.3: Polyamines metabolism and cell-cycle-regulatory proteins[165]

There are several examples showing the implication of polyamines in cell cycle. Thomas *et al*. founded that in MCF-7 breast cancer cells, estradiol, which stimulates proliferation of these cells, increased intracellular polyamine levels in G_1 phase.[170] Other studies showed the implication of cyclin D1 as major mediator of cell cycle progression in MCF-7 cells in G_1 phase.[166,171,172] It has been suggested that Put and Spd could regulate cyclin D1 and E, respectively.[150]

4.2 POLYAMINES AND APOPTOSIS

Beside the activity of polyamine in cell growth, they are also implicated in cell death process, in particular in the programmed cell death (apoptosis).[173,174]

Apoptosis is a physiological cell death regulated by genetic mechanisms, and morphological and biochemical changes in cell nuclei, including chromatin condensation and internucleosomal DNA fragmentation [175]

Mitochondria plays an important role during the apoptotic process: membrane permeabilization and the resulted cell death, depend on the balance between pro-apoptotic and pro-survival molecules acting at mitochondria level (Figure 4.4).

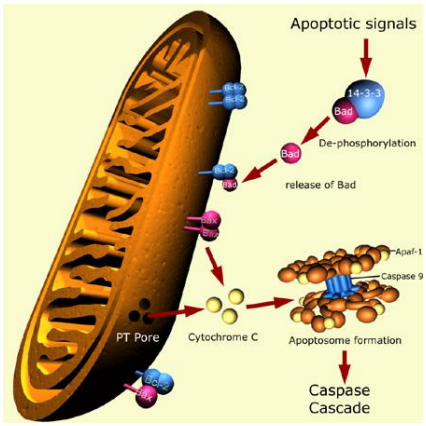

Figure 4.4: Mithocondria in apoptosis process[176]

Mitochondrial and post-mitochondrial phases of apoptosis, terminate with a proteolytic cascade which involves proteins known as caspases. They have a key role in the cell death program.[177] Caspases are aspartate-specific cysteinyl proteases whose act as initiators and executioners of apoptosis.[178] They are produced in cells as inactive proenzymes containing three domains: an NH_2-terminal domain, a large subunit (~20 KDa) and a small subunit (~10 KDa). Caspases can be divided in two groups. In the group I there are caspases-1, -4 and -5 which are involved in the immune response. In the group II, there are caspases involved in the apoptosis and they can be also divided in two classes:

- Initiator caspases (apical): caspase-2, -8, -9, -10
- Effector caspases (executioner): caspase-3, -6, -7

Initiator caspases can be stimulated by different apoptotic signals like the death-inducing signaling complex (DISC), the apoptosome, and the p53-induced protein with a death domain PIDDosome. When recruited, initiator caspases activate the executioner. Once effector caspases are activated, they interact with a broad spectrum of proteins, leading to cell death.[179] Effector caspases, could also be activated by catepsin and calpains, two non-caspases proteases.[180] The activity of caspase-9 and -3 can be inhibited by inhibitor of apoptosis proteins (IAPs).[181]

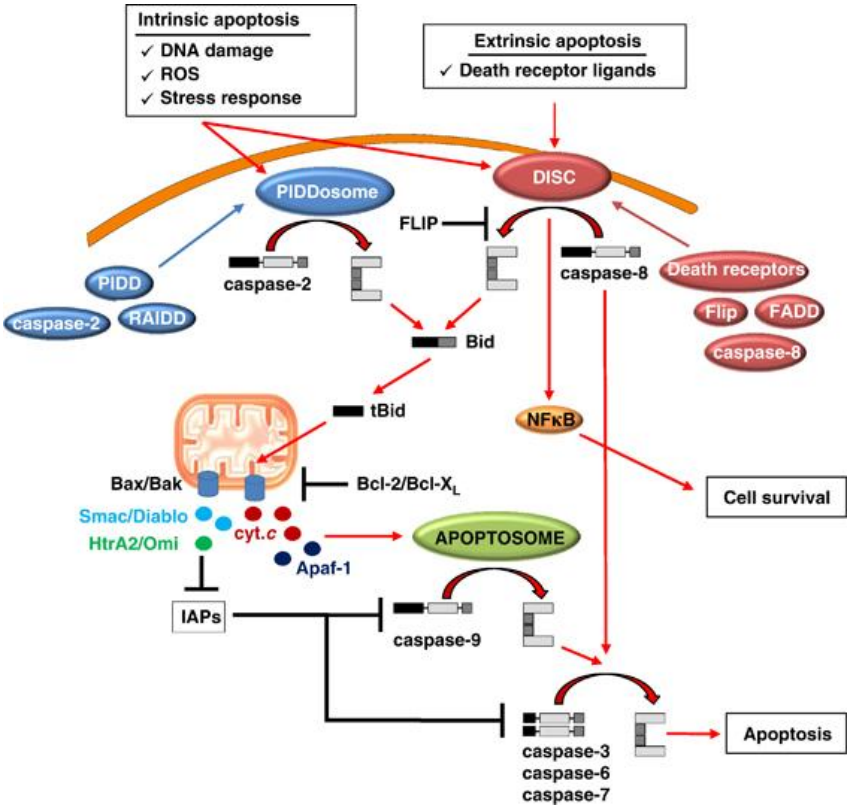

Figure 4.5: Overview of caspase cascades and their inhibitors[181]

Apoptosis could be triggered by two pathways (Figure 4.5):

- Extrinsic pathway: is receptor-depending. Extracellular ligands (like TNFα) stimulate DISC assembly leading to activation of procaspase-8. The active caspase-8 can activate caspase-3 triggering the apoptosis pathway.
- Intrinsic pathway: it is mediated by mitochondria. Release of cytochrome C from mitochondria leads to apoptosome formation which mediates activation of caspase-9. This pathway is controlled by proteins from Bcl-2 family.

Intrinsic and extrinsic pathways can crosstalk: caspase 8 can cleave Bid forming the active, truncated *t*-Bid, which can bind Bcl-2 and inactivate it, resulting in apoptosis. Anyway, both pathways converge at level of caspase-3.[182,181]

Polyamines are strictly involved in the apoptosis process, although the wide number of investigations have not yet completely elucidate their roles and revealed contradictory results.[150] Thomas *et al*. showed that Spm can prevent apoptosis induced by ionomycin, a Ca^{2+} mobilitation agent. This effect could be correlated with the role of polyamines in

calcium mobilitation in T cells.[183] Apoptosis protective effects due to the action of polyamines, have been published also by Desiderio *et al*. They showed that addition of polyamines can inhibit dexamethasone-induced apoptosis in thymocytes.[184]

On the other hand, there are evidences about a protective role of polyamines in apoptosis. Packham *et al*. showed that *Odc* gene is involved in apoptosis induced by overexpression of *c-myc*, an oncogene correlated either in cell proliferation and apoptosis. In this context ODC expression induced cell death *c-myc* mediated in a dose-dependent manner.[185,186]

The presence of acetylpolyamines in cancer cells is an important link between polyamines and carcinogenesis.[187,188] Usually, they are not found into the cell, because they are the main product exported from the cell.[165] The oxidation of acetylated polyamines by PAO and serum amine oxidase produce H_2O_2 andaldehydes , strong inducers of apoptosis.[189,190] Moreover, H_2O_2 produced during the oxidation induce SSAT activity and cause oxidative stress (Figure 4.6).[191]

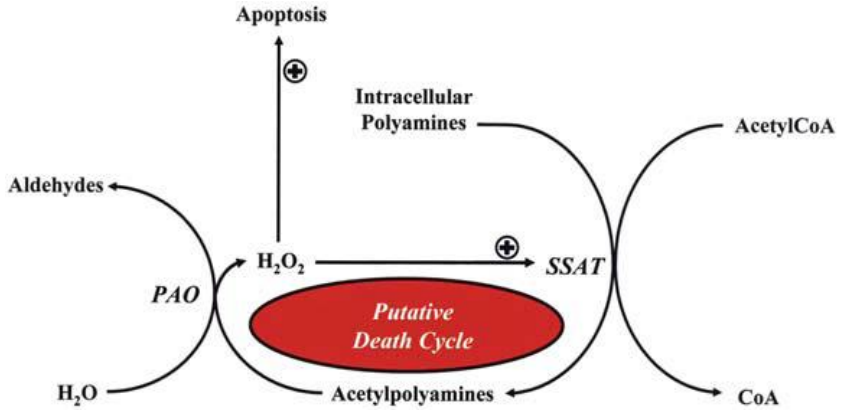

Figure 4.6: polyamine metabolism and the potential for cell death[165]

Anyway, further studies, some using MDL 72527, a specific PAO inihibitor,[192,193] and other using transgenic mouse that over-express SSAT,[194] indicated that apoptosis is not directly correlated with polyamine oxidation. In some cell types, they do not need to be oxidized to induce cell death. The excessive accumulation or depletion of polyamines can interfere with DNA-protein interaction,[195] protein-protein interaction,[196] and mitochondrial integrity[197] leading to apoptosis.

Polyamines can interact with caspases. Stefanelli *et al*. carried on several studies to understand their cellular roles. Results showed that polyamines (especially Spm) could directly induce the release of cytochrome C from mithocondria leading to programmed cell death. In particular, Spm could activate caspase-3 more efficiently than Spd, while Put is inactive.[198,199,197]

Apoptosis is also correlated with p53 tumor suppressor. p53 is a transcription factor that targets many genes and microRNAs in response to cellular stress. As tumor suppressor it blocks cell cycle progression and/or induce apoptosis, in response to DNA damage.[200] Studies showed that wild-type p53 could regulate transcription of *bax* gene, a member of Bcl-2 family, strictly connected with apoptosis.[201,202] The interaction between polyamines and p53 has been investigated by Li *et al*. They founded that in intestinal mucosal epithelial cells, polyamines negatively regulated post-transcription of p53. Moreover, accumulation of p53 activated the transcription of cell cycle arrest genes, leading to growth-inhibition (Figure 4.7).[82]

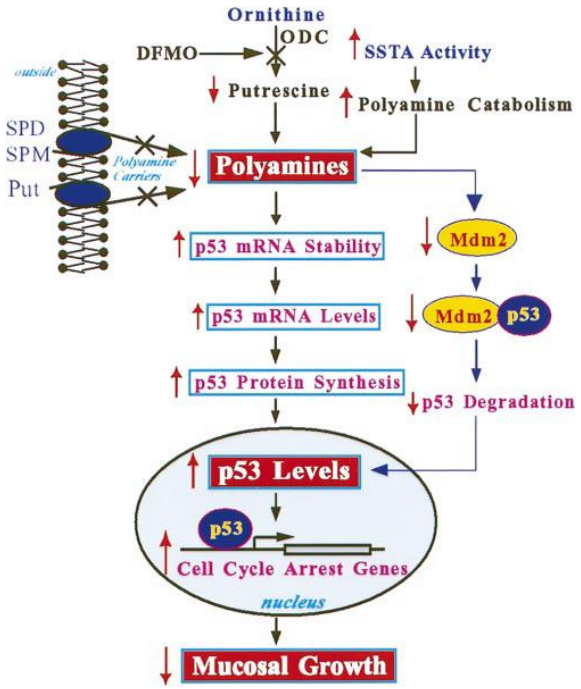

Figure 4.7: regulation of expression of the p53 gene by cellular polyamines[182]

Another factor implicated in apoptosis and cell growth is the nuclear transcription factor NF-κB.[203,204] This factor has both apoptotic and antiapoptotic functions, depending on cell type and death stimulus.[205,206] Once activated, NF-κB can interact with genes implicated in apoptosis, like *Fas ligand*, *p53* and *c-myc*.[207] Li *et al.* investigated about the implication of polyamines in NF-κB regulation and they showed that in normal intestinal epithelial cells, polyamines negatively regulate the NF-κB activation.[208] Consequently, depletion of polyamine from these cells, resulted in increased activity of NF-κB, due to degradation of the inhibitor protein-κB, necessary for NF-κB inactivation.[209] On the other hand, Shah *et al.* indicated that polyamines, in particular Spm, up-regulated genes involved in cancer cell proliferation in MCF-7 breast cancer cells.[195,210]

4.3 POLYAMINES AND DNA

Polyamines can interact with duplex and triplex B-DNA (the main DNA conformation in functional organisms) structures.[211] DNA is a polyelectrolyte with negative charges on the phosphate groups, so the driving force in polyamine-DNA interaction is electrostatic[212] and a minor contribution is due to hydrophobic interactions.[150] Several crystallographic studies have been carried out on different DNA conformation (including A- and Z-DNA) to understand the binding between polyamines and DNA. Polyamines have been found in a variety of locations, but more frequently near the phosphate backbone.[213,214] Other methods placed spermine either in the major groove[215,216] or the minor groove of the DNA.[217]

There is abundant evidence that Spm can alter the structure of DNA, for example micromolar concentrations of Spm can convert some B-DNA sequences to the A- or Z-conformation.[215] Z- and B-DNA have different features (for example in the Z-DNA the phosphate groups are more exposed) and, Z-DNA seems to be implicated in transcriptional control.[218] The binding mode between Spm and Z-DNA has been proved by X-ray crystallographic studies.[219]

The interaction between polyamines and DNA promotes DNA bending (Figure 4.8). Polyamines neutralize the negative charges on DNA phosphate resulting in reduction of the energy required for bending and, consequently, attraction between two DNA segments.[220,221]

However, Maruyama *et al.* proposed that this kind of interaction could screen the electrostatic repulsion among phosphate anions in DNA molecules and improve the stability of the second structures of DNA.[222]

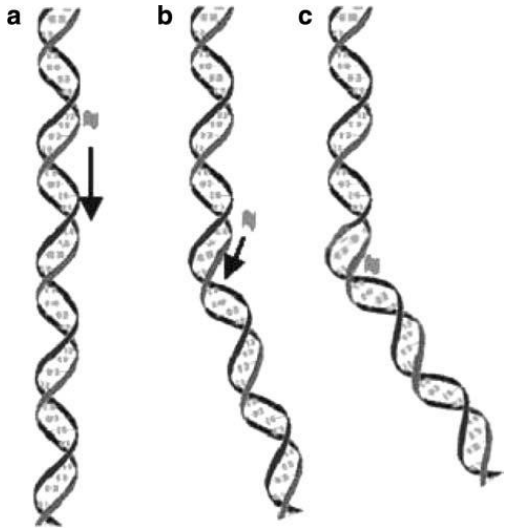

Figure 4.8: Schematic representation of the dynamical bending mechanism by polyamine. a A free polyamine ion diffuses along the DNA chain. b Starting of small bending which then allows the polyamine localization in the major groove. c The bending angle is increased and stabilized by the polyamine ion[223]

DNA conformational changes induced by polyamines and DNA bending, can modulate the interaction of transition factors with DNA and thus control the expression of a network of genes, and maybe cancerogenesis.[150]

Another important interaction with nucleic acid is represented by polyamines and G-quadruplex structures. NMR studies carried out by Keniry *et al.* showed for the first time that Spm can bind DNA quadruplexes. Spm also discriminated between folded antiparallel quadruplexes and linear parallel quadruplexes.[224] A more recent study showed stabilizing and denaturating effects of polyamines on G-quadruplex. Concentrations of polyamines lower than 1 mM cause stabilization of G-quadruplex due to electrostatic and hydrophobic interactions and, maybe contribute also to the DNA condensing effect. On the other hand, concentration higher than 1 mM denaturated G-quadruplex, presumably by hydrogen-bonding interactions between guanines and the amino or imino groups of polyamines.[225]

4.4 POLYAMINES IN MEDICINAL CHEMISTRY

Polyamine have been widely investigated in medicinal chemistry. They may be considered a "universal template" able to recognize different receptor systems, since both affinity and selectivity may be fine-tuned by inserting different substituents or by modifying the chain length between the nitrogen atoms of a polyamine scaffold. Its flexibility allows it to assume a suitable conformation for the interaction between protonated amine functions and receptor anionic sites.[226,227,228,229]

Polyamines have numerous cellular effectors sites that are frequently dysregulated in cancer and, for this reason, several studies have been carried out to find molecules able to interfere with the biochemical pathway of polyamines and, of course, became potential anticancer agents.

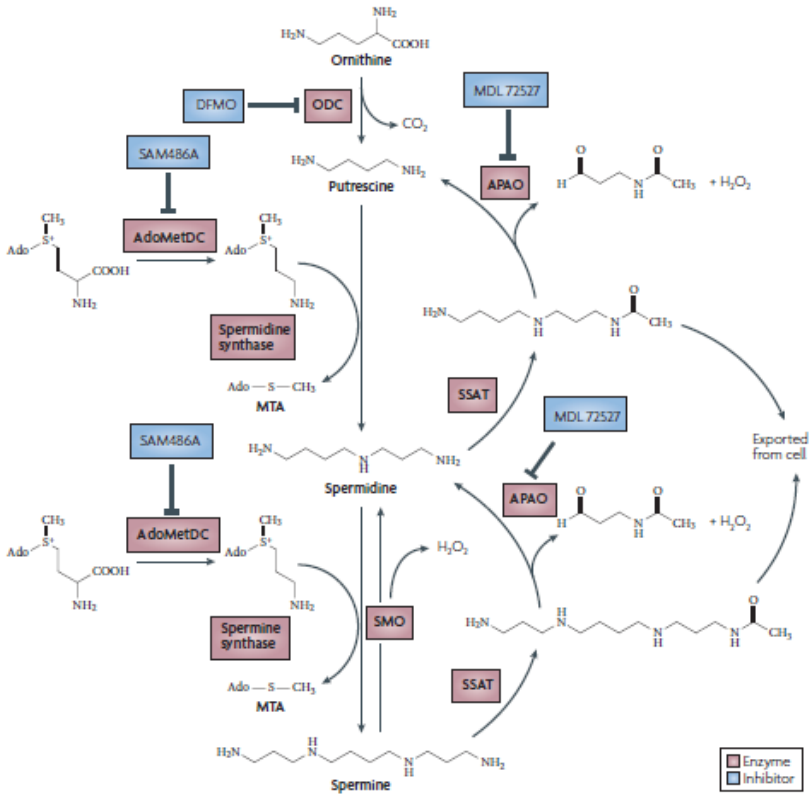

Figure 4.9: Targets in the polyamine metabolic pathway[156]

As shown in Figure 4.9, several steps of the polyamines biosynthesis pathway have been targeted.

One of the most important molecule designed was 2-difluoromethylornithine (DFMO), that was the prototypical inhibitor of ODC. DMFO was designed in early 1980s and it is an enzyme-activated irreversible inhibitor. Initially it competes with ornithine for binding to the active site of ODC, thus it is decarboxylated by ODC to create a highly reactive intermediate that inactivates ODC by covalent bond with Cys360 or Lys69. DMFO has been evaluated in phase I and II trials[230,231,232,233], but these trials had no success. The poor results were probably related to pharmacokinetic and pharmacodynamic factors, like reduced transport in the cells and activation of compensatory mechanisms to replace polyamines depletion.[156] Recently, it has been shown a possible role of DMFO as cancer chemopreventive in combination with nonsteroidal anti-inflammatory agents.[234,235]

In addition to ODC, AMD is another important enzyme in the polyamine biosynthesis and, one of the first AMD inhibitors discovered was methylglyoxalbis(guanylhydrazone) (MGBG). This molecule was in study as antileukaemic agent when it was discovered its role as competitive inhibitor of AMD.[236,237] The antiproliferative activity of MGBG could be a consequence of two factors: inhibition of AMD and interference in mitochondrial structure and functions. However, studies on L1210 cells showed that its antineoplastic properties are related to the antimitochondrial effects, which happens before the destabilization on polyamines system.[238] Since MGBG showed systematic toxicity, it has not been subjected to clinical development, but it could be considered a lead structure.[239] Among MGBG analogues developed, SAM486A was a potent competitive AMD inhibitor with low mitochondrial activity.[240] SAM486A has been tested in phase I and II trials, as single agent or in combination with 5-fluorouracil and leucovorin for the treatment of metastatic colon cancer. Its therapeutical activity is still under investigation.[241,242,243]

Furthermore, specific inhibitor of aminopropyl transferases SRM and SMS have been developed. Among all the inhibitor designed, the “transition-state analogues” were the most interesting. In particular, compound AdoDATO was a specific inhibitor of SRM.[244] Treatment of different types of mammalian cells with AdoDATO showed reduction of Spd levels, but increment of Put and Spm levels, resulting in not interesting growing inhibitory

effects.[245] Also, since AdoDATO is endowed with primary amine functions in its structure, it could be a possible substrate of SSAT and various amine oxidase, limiting its therapeutic utility.[156]

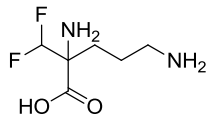

DFMO

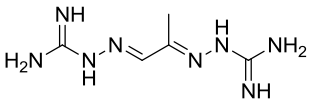

MGBG

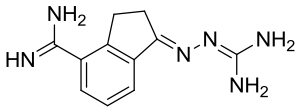

SAM486A

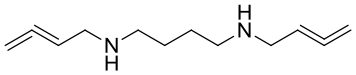

MDL 72527

Another approach to design molecules able to inhibit the activity of polyamines, was to create compounds structurally similar to the natural polyamines, but with different chain lenght.[246] Compounds **XVIII-XX** and MDL 27695 showed interesting antitumor activity. **XVIII** and MDL 27695 were tested on HeLa cell lines exhibiting IC_{50} values of 5 and 50 µM, respectively, but they did not show any correlation between DNA binding properties and antitumor activity.[247,248]

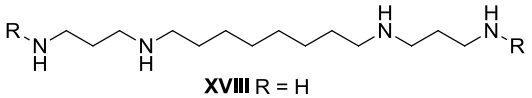

XVIII R = H
XIX R = Me
XX R = Et

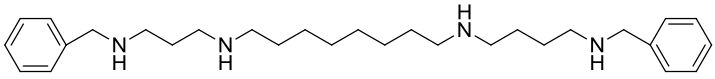

MDL 27695

Another series of symmetrically substituted polyamines (**XXI-XVI**) have been synthesized to improve the antitumor activity. These compounds, called bis(ethyl)polyamines, were active on polyamine system down-regulating ODC and ADM. Moreover, they have been transported into the cells by PAT.[249,250,251]

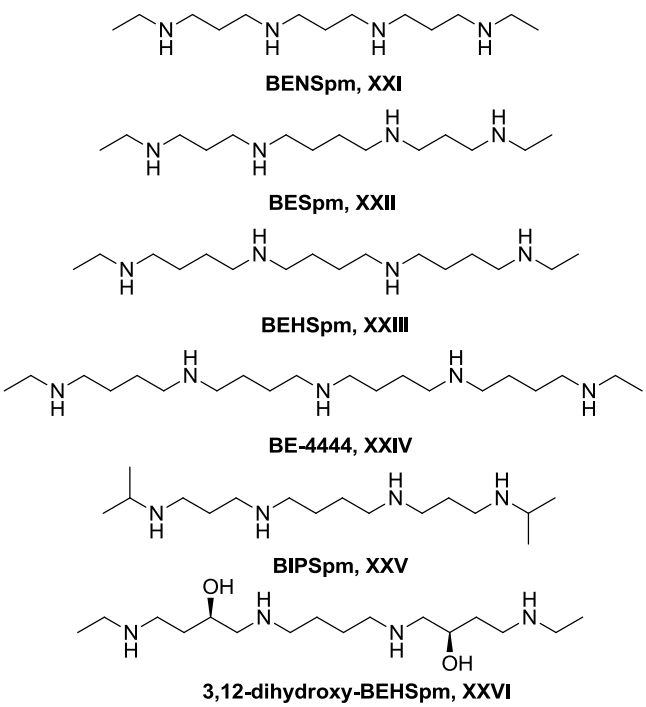

Among these derivatives, the most interesting compounds were **XXI**, which has a 3-3-3 backbone, **XXIII** (4-4-4) and **XXIV** (4-4-4-4). Compound **XXIV** has been tested in human brain tumor cell lines U-251 MG and SF-767. In these cell lines it showed several effects: inhibition of cell growth, cytotoxic activity, induction of variable G1/S block, and intracellular polyamines depletion.[252] Phase I and II clinical trials of compound **XXI**, showed that the drug is safe but did not show any interesting clinical effects in patients with breast or lung cancer,[253,254,255] so a treatment of **XXI** in combination with other chemotherapeutic agents has been proposed.[256] Phase I studies of **XXIII**, revealed neuro- and hepatotoxicity issues. However, this side effects could be reduced by the introduction of hydroxyl groups into the intermediate chain (compound **XXVI**). This fact is probably due to a more rapidly phase 2 metabolism.[257,258]

In order to study the correlation between the polyamines mobile chain and antitumor activity, the so called "second generation" of bis(ethyl)polyamines has been synthesized. These compounds presented a spatial constraint in the central region of the polyamine chain in **XXIII**. The *n*-butane fragment has been replaced with less mobile chains, like *cis*- and

trans-cyclopropyl (**XXVII**), triple bond (**XXVIII**) or 1,2-disubstituted aromatic ring (**XXIX**). These compounds showed interesting antitumor activities in different cell lines.[259]

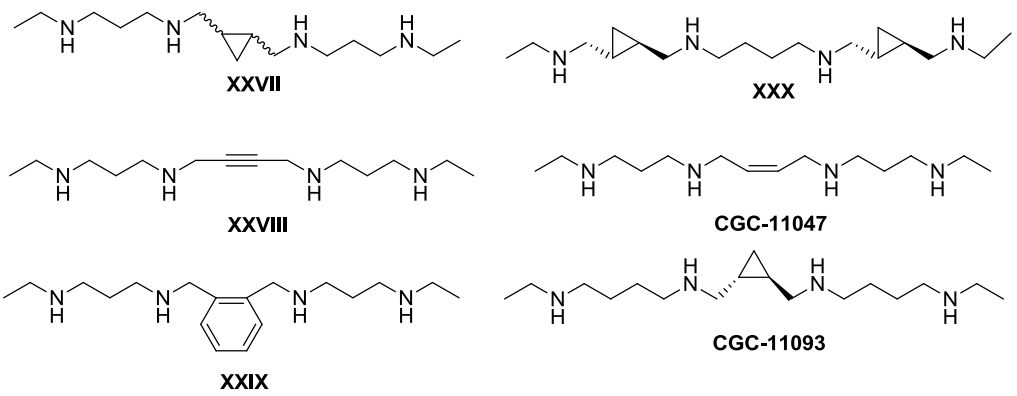

The most interesting compounds were CGC-11093 and CGC-11047. The first one, characterized by a *trans*-cyclopropyl moiety in its central part, was active as antitumor agent *in vitro* and *in vivo* against DU-145 nude mouse xenografts.[260] Moreover, CGC-11093 increases the *in vitro* and *in vivo* anti-myeloma activity of the proteasome inhibitor bortezomib. The combination of these two agents compromised multiple myeloma viability and clonogenic survival, and increased drug-induced apoptosis over that achieved by either single agent.[261] The second one, characterized by a *cis* double bond, was able to inhibit the growth of both small cell and non-small cell lung cancer cells *in vitro*. In non-small cells it down-regulated ODC activity, increased polyamines catabolism leading to a greater polyamines depletion and accumulation of CGC-11047. It also delayed the progression of the tumor in an *in vivo* model of human non-small cell lung cancer.[262]

Also, compounds with a 4-4-4 or 4-4-4-4 backbone with *trans*-cyclopropyl or *trans*-cyclobutyl moieties in noncentral regions (**XXX**) were active *in vitro* against prostate tumor cell lines like DU-145, LnCap and PC-3. The improved activity could be attributed to an enhanced DNA binding.[263,264] This latter property is very important, because the interaction of polyamines with DNA could enhance their antitumor activity. For this reason, several efforts have been made to find polyamines analogues able to interact with DNA.

Compounds **XXXI** and **XXXII** are oligoamines that were active against a panel of a prostate tumor cells in vitro (LnCap, DU-145 and PC-3) showing IC_{50} values an order of magnitude lower than that of analogues previously studied. Their cytotoxicities were

correlated with their ability to alter DNA/chromatin condensation during cell division, causing DNA aggregation.[265] In particular, compound **XXXI** was active against human breast cancer cells *in vitro* and *in vivo*, and its cytotoxic effects were associated with multiple apoptotic mechanisms in specific breast cancer cell lines.[266] In addition, compound **XXXI** was able to specifically suppress the expression of estrogen receptor α and estrogen receptor target genes in the estrogen-receptor-positive MCF-7 and T47D human breast cancer cell lines.[267]

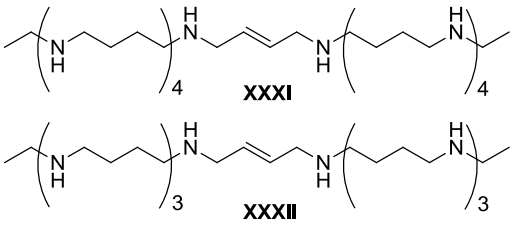

XXXI

XXXII

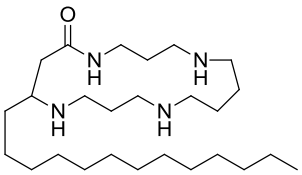

XXXIII

Other approaches to the design of polyamines analogues, were to synthesized compounds similar to a series of compounds called budmunchiamines, which are macrocyclic polyamines displaying a potent antitumor activity and able to deplete ATP.[268] In particular **XXXIII** showed the best anticancer profile. It was readily imported by cells and caused a huge depletion of cellular polyamines, and its cytotoxicity is strictly correlated to its ability to deplete ATP.[269]

Further studies to better understand the role of the terminal substituents on the polyamine chain, and to explore the chemical space surrounding the terminal alkyl groups, led to the synthesis of a series of monoalkilated polyamines, like compounds **XXXIV-XXXVI**.[270] These molecules produced cytotoxicity in NCI H157 non-small-cell lung carcinoma cells, and in prostate cell lines DU145, PC-3 and LnCap with different mechanisms, all of them leading to apoptosis.[190,271,272] They also presented different effects on the cell cycle. **XXXVI** produced a significant G_2/M block and a concurrent decrease in the G_1 fraction, while **XXXIV** had no effects on the cell cycle.[273]

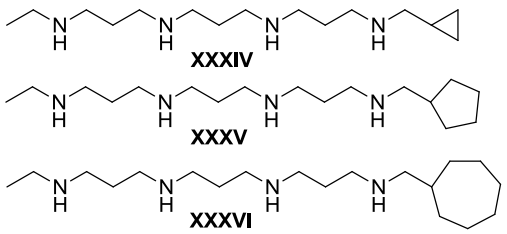

With the aim to develop a SAR model for alkylpolyamine analogues, several molecules have been synthesized. These derivatives incorporated chemical diversity into the terminal alkyl substituent and they had different polyamine backbone structure (like 3-4, 3-3-3, 3-3-3-3). They showed similar biological profiles to the polyamines described above: cytotoxicity, apoptosis, induction of SSAT and SMO and alteration of cellular polyamine levels. Also, most of them were taken up into tumor cells by the PAT.

Among all the alkylpolyamine analogues synthesized, compounds **XXXVII, XXXVIII** and **XXXIX** were selected for further trials.[246]

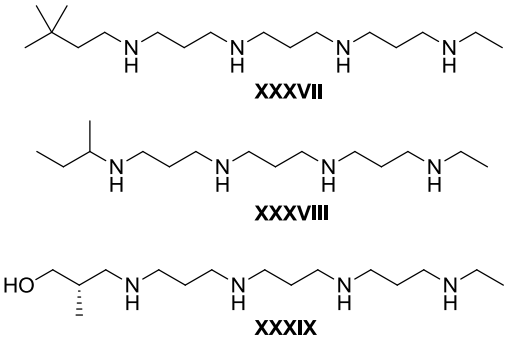

Despite similar structures, **XXXVII, XXXVIII** and **XXXIX** showed different behavior against H157, H82, H69 and A549 lung tumor cell lines. In particular, **XXXVII** did not produce significant SSAT induction, but initiated a 30-fold induction of SMO 3-6 times more effective than **XXXVIII** and **XXXIX.** These three compounds had also been evaluated in *in vivo* studies using an A549 human lung tumor xenograft model in athymic nu/nu Fox Chase mice. Compounds **XXXVII** and **XXXIX** were most potent in inhibiting tumor growth, although **XXXVII** was more toxic. The reduced toxicity showed by **XXXIX**

could be due to the presence of the hydroxyl group in agreement with the observations reported for **XXVI**.[31]

It is well known the affinity of polyamines for DNA as well as the importance of DNA intercalation for antitumor activity. To improve the anticancer properties of polyamines and in order to target DNA and/or Topoisomerase II (TOPO II) activity, Phanstiel *et al*. synthesized a series of polyamine-DNA intercalator conjugates.[274] They were composed of a Spm of Spd fragment covalently bonded to an aromatic nucleus (acridine or anthracene) via an aliphatic chain (examples could be represented by compounds **XL-XLIII**)

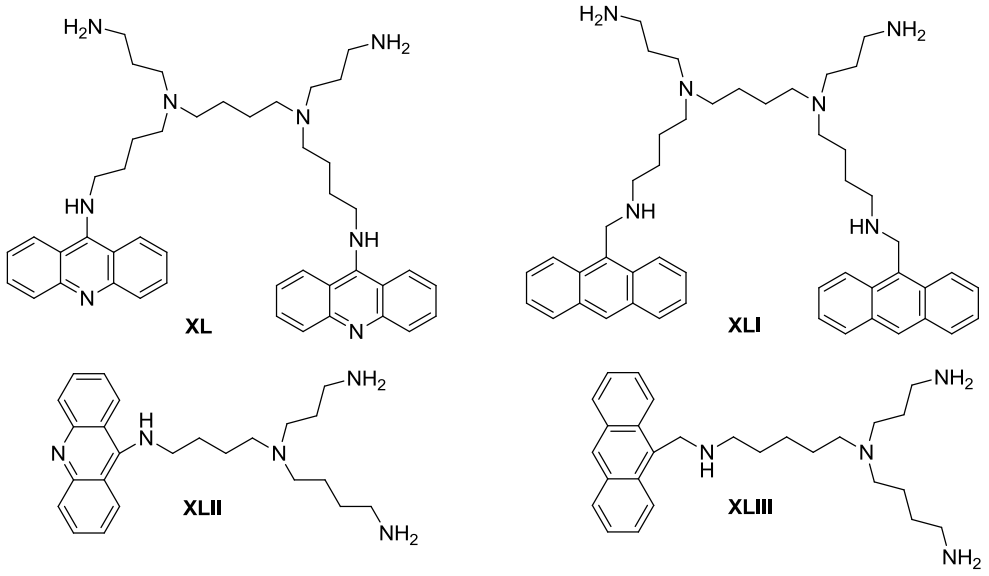

The *bis* ligands **XL** and **XLI** inhibited human DNA TOPO II activity at 5 μM, and they were more potent than their monosubstituted Spd counterparts **XLII** and **XLIII**. This was consistent with the observation that *bis*-intercating agents could bind DNA more efficiently than monointercalators. Also, *bis*-intercalators behaved as cytostatic agents, while monosubstituted were cytotoxic and, *in vitro* test in L1210 murine leukemia cells showed that anthracene conjugates were generally more toxic than the acridine ones.

It has been demonstrated that telomerase is an essential factor in tumorigenesis,[275,276] and it could be considered a potential target for the development of anticancer agents. Telomerase could be inhibited by different approaches,[277,278,279] included disturbance of the

telomere/telomerase interaction with molecules able to interact with four-stranded DNA structure like G-quadruplexes. Polyamines are able to interact with these kind of structure and recently it has been demonstrated that a small linear molecule, triethylene tetramine (TETA), could stabilize both inter- and intra-molecular G-quadruplex structures, leading to telomerase inhibition and acute cytotoxicity.

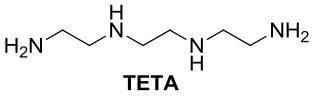

TETA

The exact binding mechanism of TETA to the quadruplex remains to be clarified, however TETA can interact with G-quadruplex both in presence or in absence of K^+ and the effect was more notable to intermolecular G-quadruplex.[280] Further studies showed the ability of TETA to inhibit the expression of c-myc by enhancing the stability of G-quadruplex formed by the nuclease-hypersensitivity element III_1 (NHE) in the c-myc promoter, which controls 80-90% of c-myc transcription.[281] More recently it has been reported that a long-term treatment with TETA, at 50 or 100 μM, induced marked senescence in MCF-7 cells. Also, the growth arrest was accompanied by the up-regulation of the expression of p53 and p21, which indicates their implication in senescence pathway.[282] Anyway, at low concentrations the ability of inhibit cell growth by TETA was limited, but it was able to potentiate antitumor activity of some traditional drugs like taxol, adriamycin, carboplatin and cyclophosphamide *in vitro* and *in vivo*. This fact suggested a potential role of TETA as chemosensitizer.[283]

CHAPTER 5
MAO-A AND PROSTATE CANCER

5.1 PROSTATE CANCER

Prostate canceris a form of cancer that develops in tissues of the prostate, a gland in the male reproductive system. Normally, most prostate cancers grow slowly; however, there are cases of aggressive forms. Prostate cancer is classified as an adenocarcinoma, or glandular cancer, that begins when normal semen-secreting prostate gland cells mutate into cancer cells.

In Italy, data referring to the year 2006, showed 46.000 new prostate cancer cases diagnosed. It is the second cause of cancer death after lung tumor[284] and it is the most common cancer affecting men in the United States. The first risk factor is the age: the majority of prostate cancers are diagnosed in older men (it is rarely seen in men younger than age 40). Race is the second most common risk factor: African-American men are at greatest risk for developing prostate cancer, while Asian/Pacific Islanders and American Indian/Native Alaskan men are at low risk of disease. Other risk factors include family history of prostate cancer, lifestyle, dietary factors and consumption of drugs.[285]

5.1.1 The Gleason Greading

The Gleason Greading was introduced in 1960s and 1970s by Dr. Donald F. Gleason and members of the Veterans Administration Cooperative Urological Research Group, and it is a prognostic indicator for the adenocarcinoma of the prostate together with other parameters like clinical stage and prostate-specific antigen (PSA).[286,287,288] This system is based on the histologic arrangement pattern of carcinoma cells, that is correlated with the degree of differenziation of the neoplastic cells.

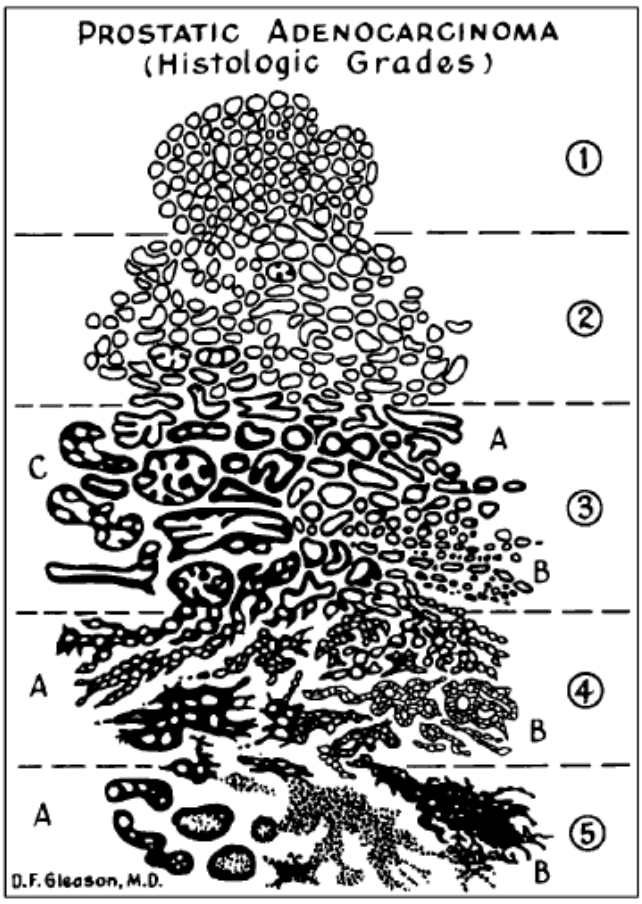

Figure 5.1: Gleason grades: standard drawing.[286]

Nine growth patterns were described into five grades, that are illustrated in Figure 5.1. Grade 1 cells are very well differentiated. The following grades are characterized by a minor differentiation until Grade 5, where cells are very poorly differentiated. The five grade patterns are used to generate a histologic score (Gleason Score), which can range from 2 to 10, by adding the primary grade pattern and the secondary grade pattern. The primary pattern is the one that is predominant in the tissue sample obtained by needle biopsy, and the secondary pattern is the second most common pattern. If only one pattern is present, that grade is multiplied by two to give the score.[286,289] In current practice, the vast majority of prostate cancers have a Gleason score of ≥ 6. Hence, tumors composed of patterns 3, 4, and 5 are considered clinically significant.[290]

The Gleason grade is also correlated with clinical end points of the pathology, like clinical stage, progression of metastatic disease, and survival. It is also important to predict response to a specific therapy, such as radiotherapy or surgery. Tumors with Gleason grade 3 patterns, have >95% chance of being surgically treated, while the progression from grade

3 to 4/5 marks a critical change from curable to lethal cancer.[286] There are 86 genes that distinguish grade 3 from grade 4/5 carcinomas, while grade 4 and 5 present high degree of similarity, thus they are grouped together.

Recently, a correlation between high levels of monoamine oxidase A (MAO-A) expression and poorly differentiated prostate cancer has been demonstrated. In this study MAO-A expression was elevated in Gleason 4 or 5 samples compared to Gleason 3 samples.[290]

5.2 MONOAMINE OXIDASE (MAO)

MAO are enzymes that catalyses the oxidative deamination of a range of monoamines, like 5-hydroxytryptamine (5-HT or serotonin), histamine, dopamine and adrenaline.[291]They exist in two isoenzymatic forms: MAO-A and MAO-B. They are associated with the mitochondrial outer membrane, and their presence vary from tissue to tissue.[292] Immunohistochemical studies have shown that serotonergic neurons and astrocytes contain mainly MAO-B, whereas catecholaminergic neurons contain mostly MAO-A.[293]

MAO can be found in peripheral tissues, like intestine, liver, and placenta, and in central and peripheral nervous system. Their physiological function seems to be correlated with the protection of the body by oxidizing amines from the blood.[294]

MAO-A and MAO-B have about 70% identity and they are covalently bound to a flavin adenine dinucleotide (FAD), in particular the 8α-*S*-cysteinyl FAD, by a thioether linkage. FAD is the redox cofactor, and is necessary for the redox activity of the enzyme.[295]

MAO-B has been the most studied isoform and its crystal structure has been obtained in 2001 (Figure 5.2).[296] The enzyme is composed of 520 amino acids and it is dimeric. The protein region responsible for membrane attachment is formed by the C-terminal amino acids 461-520. The C-terminal residues create an extended polypeptide chain that is followed by an α-helix forming the transmembrane helical segment. The substrate binding site is formed by a flat cavity of 420 $Å^3$ and includes a number of aromatic and aliphatic amino acids, providing an high hydrophobic environment. Close to the substrate cavity there is a smaller hydrophobic cavity, shielded by a loop (amino acids 99-112). The two cavities are separated by four residues. These observations suggest a mechanism that

initially involves the movement of loop 99-112 to open access of the substrate to the smaller cavity (termed the 'entrance cavity'). When substrate is in the 'entrance cavity', a movement of the four residues separating the two cavities allows its diffusion into the active site. In this context, loop 99-112 may function as a 'gating switch' to the entrance cavity.

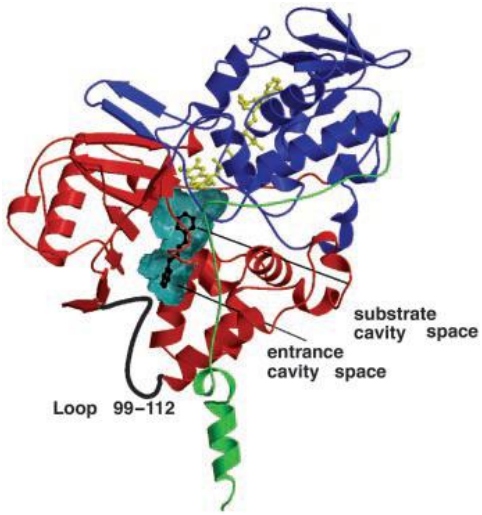

Figure 5.2: Overall three-dimensional structure of human MAO-B monomeric unit in complex with an inhibitor. The FAD-binding domain is in blue, the substrate-binding domain is in red, and the C-terminal membrane-binding region is in green. The FAD cofactor and the inhibitor are shown as yellow and black ball-and-stick models, respectively. The inhibitor binds in a cavity (shown as a cyan surface) that results from the fusion of the entrance and substrate cavities[297]

The major part of the cavity is hydrophobic, which allows for the binding of apolar substrates and inhibitors. The only hydrophilic section is near the flavin and is required for recognition and directionality of the substrate amine functionality. This hydrophilic region is located between Tyr-398 and Tyr-435, which, together with the flavin, form an aromatic cage for amine recognition.[297]

5.2.1 The oxidative mechanism of MAO

Monoamine oxidases A and B catalyze the oxidation of primary, secondary, and some tertiary amines to their corresponding protonated imines with concomitant reduction of O_2 to hydrogen peroxide (Figure 5.3) wchich can be responsible of oxidative stress.

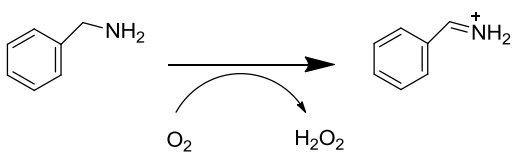

Figure 5.3: Oxidation of benzylamine, a primary amine

The detailed mechanism by which they catalyze amine oxidation is not well-defined, however several mechanisms have been proposed. The most widely quoted mechanisms for MAO catalysis are two: the Single Electron Transfer (SET) mechanism (Figure 5.4) proposed by Silverman *et al.*,[298] and the Polar Nucleophilic mechanism (Figure 5.5) proposed by Hamilton *et al.*[299] Both mechanisms produce a protonated imine (oxidation of amine) and a flavin semiquinone (reduction of FAD).[300]

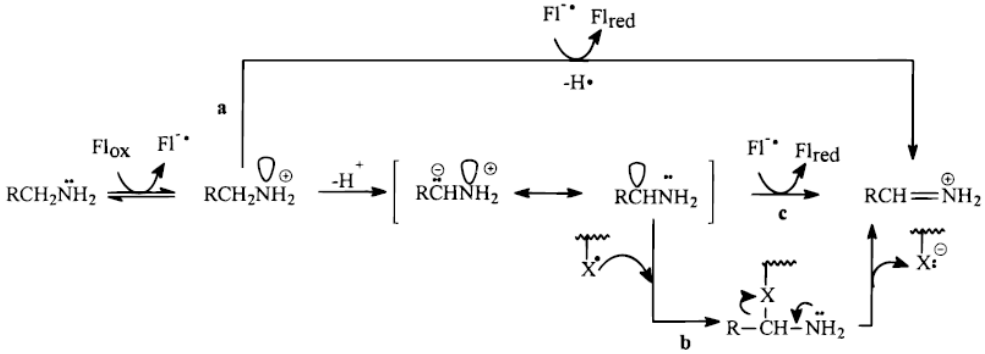

Figure 5.4: Proposed SET mechanism

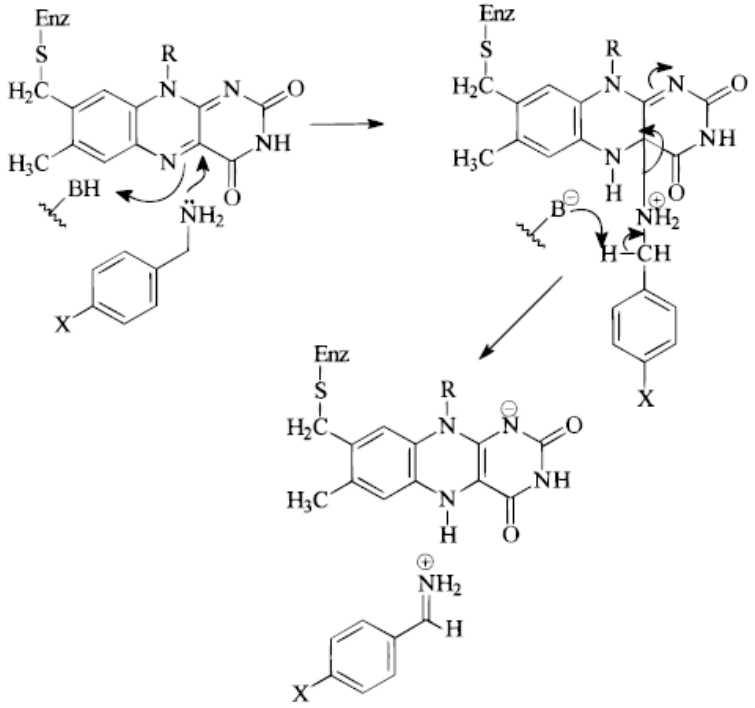

Figure 5.5: Proposed Polar Nucleophilic Mecanism

5.3 MAO INHIBITORS

MAO inhibitors are used mostly to treat major depressive disorders and central nervous system pathologies, like Parkinson disease.

The first MAO inhibitor endowed with antidepressant activity, was Iproniazid. This compound was initially developed as antitubercolosis agent. It was ineffective in this context (because developed resistance quickly), anyway it was observed to have 'psychoenergizing' effects in patients and was also shown to inhibit MAO. Consequently, several hydrazine derivative MAO inhibitors have been developed as antidepressants. Unfortunately, liver toxicity, hypertensive crises, haemorrhage and, in some cases, death resulted in withdrawal of many MAO inhibitors from the clinic.[294] Since liver toxicity was associated with the hydrazine ring, non-hydrazine inhibitors were developed, such as tranylcypromine and pargyline. However, these drugs induced hypertensive crises after the patient ate tyramine-rich foods such as aged cheese (hence, the 'cheese reaction'). In patients treated with these drugs, tyramine enter the circulation and potentiate sympathetic cardiovascular activity by releasing noradrenaline. Since 80% of intestinal MAO is MAO-A, this isoenzyme is primarily responsible for degradation of tyramine, and thus inhibition of MAO-A is associated with the 'cheese reaction'.[301]

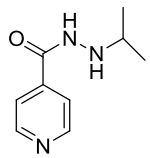
Iproniazid

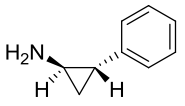
Tranylcypromine

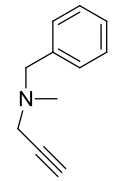
Pargyline

Nowadays there is a wide range of MAO inhibitors, included selective MAO-A and MAO-B inhibitors. Selective MAO-A inhibitors are effective in the treatment of depression, while selective MAO-B inhibitors together with L-DOPA are used in the treatment of Parkinson's disease.[294]

5.3.1 Selective MAO-A inhibitors

The prototype of MAO-A irreversible inhibitors is Clorgyline. This molecule presents an acetylenic group that is essential for the enzyme inhibition. Propargylamine derivatives are oxidized by MAO to the corresponding eyniminium species (Figure 5.6). They are

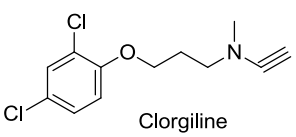
Clorgiline

highly electrophilic Michael acceptors, able to bind the flavin group with covalent bond and inactivate the enzyme at micromolar concentrations.[302]

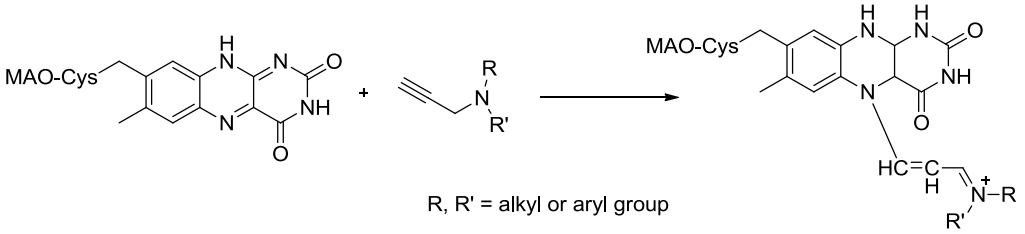

Figure 5.6: Proposed mechanism of covalent inactivation of MAO by propargylamine inhibitors [302]

Further investigations were aimed to find reversible, selective and more safe MAO-A inhibitors. The result was the discovery of Toloxatone, the first reversible competitive and selective MAO-A inhibitor introduced as an antidepressant in clinical practice.[303] Subsequently other inhibitors were developed, like Moclobemide[304] and Tetrindol.[305]

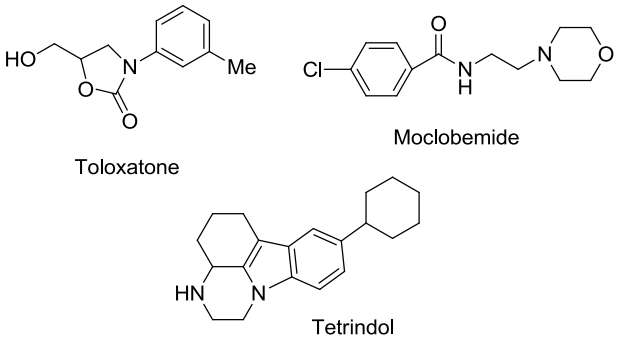

These inhibitors do not cause 'cheese reaction', because reversible inhibitors can block sufficient MAO-A in the central nervous system to obtain an antidepressant effect, while dietary tyramine is able to displace the inhibitor from peripheral MAO-A, allowing its metabolism.[306]

5.4 MAO-A ACTIVITY IN PROSTATE CANCER

The normal prostate tissue shows a high degree of cellular organization. It includes two morphologically distinct cell types: basal cells, luminal cells, and a number of intermediate states, differing in appearance, but also in biological properties. Luminal cells

are differentiated, androgen dependent and they have low proliferative capacity. On the other hand, basal cells are generally undifferentiated, androgen independent, and they present a high proliferative ability, attributes characteristic of stem cells.[307] It has been proposed that basal cells give rise to mature secretory luminal cells to maintain tissue homeostasis and, in normal prostatic epithelium cell exists at many stages in a continuum of differentiation progressing from stem cells to definitive basal and luminal cells.[308]

Neoplastic transformation in prostate cancer arise from intermediate stem cells, as shown in studies by Schalken and Van Leenders analyzing immunophenotypic keratin expression. Basal cell showed strong expression of keratin 5 and 14 in the presence of low keratin 8 and 18 levels, while luminal cells strongly expressed keratin 8 and 18. Other marker are p63 for basal cells and androgen receptors for secretory cells.[307,309]

Studies by True *et al*. demonstrated a very significant correlation between high levels of MAO-A expression and prostate cancer. They demonstrated that in laser captured prostate cancer (PCa) cells, MAO-A was one of the most highly over-expressed genes in high-grade PCa. Its expression was 2.4-fold higher in Gleason grade 4/5 compared with grade 3. MAO-A are also expressed in prostate normal basal cells. All these kind of cells are poorly differentiated.[290] This find points out that MAO-A could be a key factor in the increased lethality of high-grade prostate cancer,[310] and for this reason it is an interesting target for anticancer molecules.

The pattern of expression and the function of MAO-A in the human prostate cancer is not clearly understood. However, two hypothesis have been suggested. The first theory suggested MAO-A as protecting agents of prostatic epithelial cells from mitogenic activity of neurotransmitters of catecholamines. Limited evidence showed that noradrenaline and serotonin might stimulate prostate epithelial cell growth.[311,312] In this contest, MAO-A could inactivate these factors by oxidative degradation. The second hypothesis stated that MAO-A in prostatic basal epithelial cells prevent differentiation into secretory cells. The first hypothesis have been rejected, since relevant evidences demonstrated the implication of MAO-A in inhibiting cells differentiation.The study have been carried out by Zhao *et al*., using normal human prostatic cells from basal (E-PZ cells) and stromal (F-PZ cells) hepithelium.

To test the first hypothesis, the effects of Clorgyline on the growth of noradrenaline- and serotonin-treated E-PZ cells were evaluated and, in presence of 1 μM Clorgyline, noradrenaline and serotonin were not able to induce growth-promoting effects on E-PZ cells. To confirm this action, another experiment have been done, excluding hydrocortisone, that up-regulate MAO-A, and bovine pituitary extract from the culture medium, that contain monoamines that mask the effects of noradrenaline and serotonin. Even in these conditions no effects on the growth of basal epithelial cells were observed, indicating that inhibition of MAO-A did not affect the growth of basal epithelial cells or their response to noradrenaline or serotonin.

To verify the second theory, the effects of MAO-A inhibitions on the expression of androgen receptors (AR), a hallmark of secretory cells, have been examined using PCR, western blotting and immunofluorescence. Cells treated with 1 μM Clorgyline, showed increment of AR protein. Moreover, the use of Pargyline, a selective MAO-B inhibitor, did not induce AR expression, suggesting that induction of AR protein expression in E-PZ cells is Clorgyline-specific. Finally, in Clorgyline-treated E-PZ cells, MAO-A activity was reduced by 73% compared with cells grown in the control medium.

All these findings demonstrated that MAO-A inhibition induce differentiation of basal epithelial cells in secretory cells. This study also demonstrated that MAO-A is selectively expressed by basal epithelial cells in normal prostatic tissues, signifying a cell-specific function. Furthermore, inhibition of MAO-A activity induced AR expression at both mRNA and protein levels. Finally, inhibition of MAO-A repressed the expression of the basal epithelial cell marker, cytokeratin 14, and induced morphological changes resembling secretory differentiation.[309]

Further studies were carried out to evaluate the effect of Clorgyline on MAO-A in high grade prostate cancer cells (E-CA).[313] In particular, two type of E-CA were used: E-CA-88, derived from cancer composed of 80% Gleason grade 4 and 20% Gleason grade 3, and E-CA-90, from cancer of 100% Gleason grade 4. All the cells derived from patients without prior chemical, hormonal, or radiation therapy. Significance Analysis of Microarrays (SAM), identified 156 genes whose expression was significantly up-regulated by Clorgyline at 1 μM concentration. More than half of these genes, are usually suppressed by oncogenes like Erb2, Ras, Myc, etc. For instance, SAMD9, the gene most significantly

up-regulated by Clorgyline, is repressed in various neoplastic diseases.[314] Also, Clorgyline up-regulated AR as well as classic AR targets genes, like PSA, promoting differentiation of PCa cells.[315] In addition, Clorgyline was able to induce other genes associated with secretory differentiation, and repress genes associated with a basal cell phenothype. It has been suggested that this ability is mediated trough the down-regulation of EZH2, a critical component of the Polycomb Group (PcG) complex, that represses the expression of differentiation-related genes. The expression of PcG is associated with poor prognosis in PCa; EZH2 is over-expressed in metastatic prostate cancer and is a marker of aggressive diseases in clinically localized solid tumors.[316] This fact suggested that Clorgyline could improve patient outcome through up-regulation of PcG repressed genes.[313]

All these results support the possibility that antidepressant drugs that target MAO-A might find a new application in treating high-grade prostate cancer. However, further studies are needed to better understand all the mechanisms involved in differentiation patterns and correlation between MAO-A and prostate cancer.

CHAPTER 6
DISUBSTITUTED NDIs AS MULTITARGET DIRECTED LIGANDS

6.1 DRUG DESIGN

The design and synthesis of novel anticancer agents in one of the most active research field in medicinal chemistry. However, despite several effort have been done to find new potential molecules, drugs used in therapy actually present a number of side effects due to lack of selectivity.

Molecules able to reversibly interact with DNA represent the principal class of anticancer agents, since DNA is involved in cell proliferation and cancerogenetic process. In particular, a class of compounds termed intercalator can stabilize the double helix creating a non covalent bond with adjacent base pairs. Consequently, DNA cannot recognize associated proteins like transcription factors or polymerase, leading to replication problems and cell death. In this context, molecules bearing naphatalene diimide (NDI) scaffold are able to interact with DNA showing intercalating properties, stabilization of DNA triplexes and interaction with particular DNA structures termed G-quadruplex.[317,318,319]

Furthermore, it is well known that polyamines, protonated at physiological pH, are able to interact with the phosphate residues of DNA. Also, they are involved in cell cycle regulation and apoptotic processes. Polyamines can be considered as an universal template, since they can bind different targets and their affinity and selectivity can be modified by inserting appropriate substituents and varying the length of the polyamines backbone.[229]

Recently, a correlation between monoamine oxidase A (MAO-A) and prostate cancer have been demonstrated.[310] MAO-A is a mitochondrial enzyme that degrades monoamines, and its inhibitors are currently in use for the treatment of depression. Current experimental evidences show that MAO-A are highly expressed in basal cells of the prostatic epithelium where they inhibit differentiation in secretory cells, promoting abnormal cell growth. In particular, it has been suggested that over-expression of MAO-A is a key factor in progression from curable to lethal pancreatic cancer. Clorgyline, a MAO-A irreversible inhibitor, induce secretory differentiation of prostate cancer cells and it is able to down-regulate proteins that repress the expression of differentiation genes.[319] Therefore, MAO-A

inhibitors could find potential application in high grade prostate cancer, by promoting differentiation and inhibiting oncogenic pathways.

The aim of this work was to design and synthesize new molecular entities Multi-Target-Directed-Ligands (MTDLs) able to interact with different pathway involved in cancer pathogenesis. Cancer is a multifactorial disease, consequently molecules able to hit most of the therapeutics targets could be useful in treating this complex pathology.

Recently Tumiatti *et al*. published a series of NDI derivatives with antiproliferative activity and probably able to act as MTDLs, since they showed different biological properties.[19] These compounds were characterized by NDI scaffold (endowed with intercalation ability), properly functionalized with two basic side chains, to allow the interaction with the DNA phosphate groups. To improve the basicity of the two terminal nitrogen atoms, a 2-methoxy substituent was introduced on the two aromatic rings. The synthesized compounds presented side chains with different length, to explore their influence on the antiproliferative activity. Among all the derivatives, two lead compounds have been identified (**1** and **2**, Figure 6.1). They showed antiproliferative activity in the micromolar range on SKBR-3 CEM and HL60 cell lines. Also, they efficiently bound DNA, triggered caspase activation, caused p53 protein accumulation, down-regulated AKT, and finally caused ERK1/2 decrease and ERKs phosphorylation inhibition.

In this thesis, the study of structure-activity relationships of compounds **1** and **2** has been extended, synthesizing two series of compounds, correlated to compound **1** (odd numbers **3**, **5**, **7**, **9**, **11**, **13**, **15** and **17**) and **2** (even numbers **4**, **6**, **8**, **10**, **12**, **14**, **16** and **18**). The 2-methoxy groups on the phenyl ring have been shifted in position 3 or 4. Also, they were substituted with different chemical groups, characterized by different effects on the aromatic ring, in order to investigate their influence on the biological activities. The substituents inserted on the aromatic ring are chlorine, fluorine, nitro, trifluoromethyl, and methyl groups.

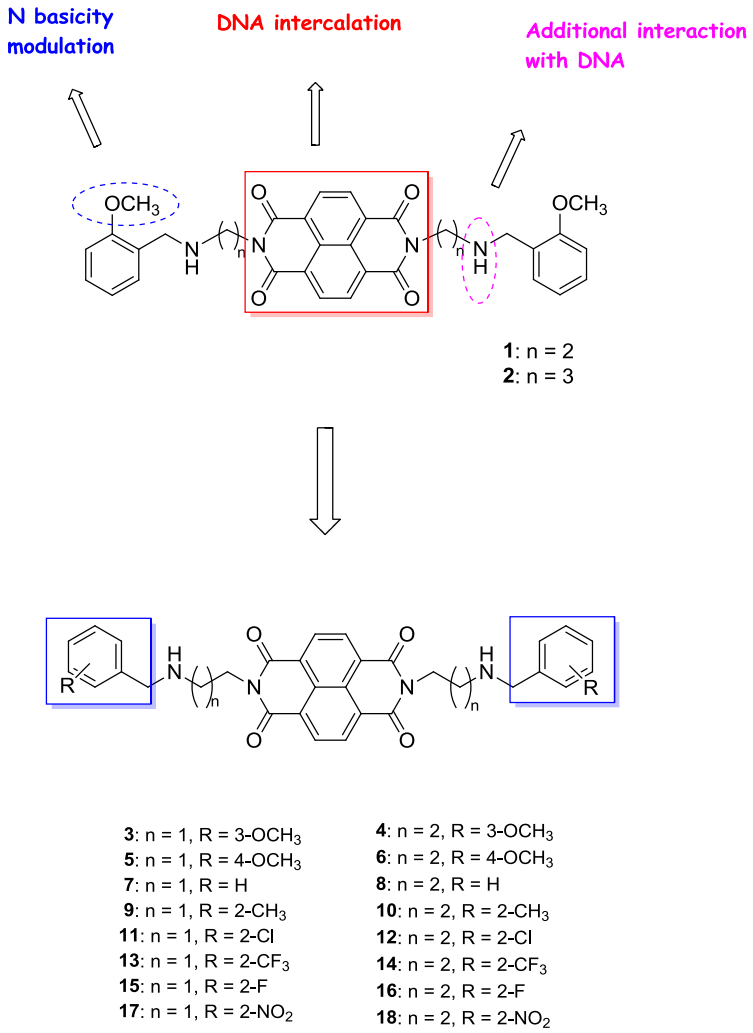

Figure 6.1: Drug design of compounds **3**-**18**

In addition, compounds bearing the trimethoxybenzyl moiety have been synthesized (**19**-**22** Figure 6.2), with the aim to investigate a possible interaction with additional targets. This group is a common pharmacophore in well-known anticancer compounds, such as Combretastatin A4, Colchicine and Podophyllotoxin, all acting on tubulin skeleton.

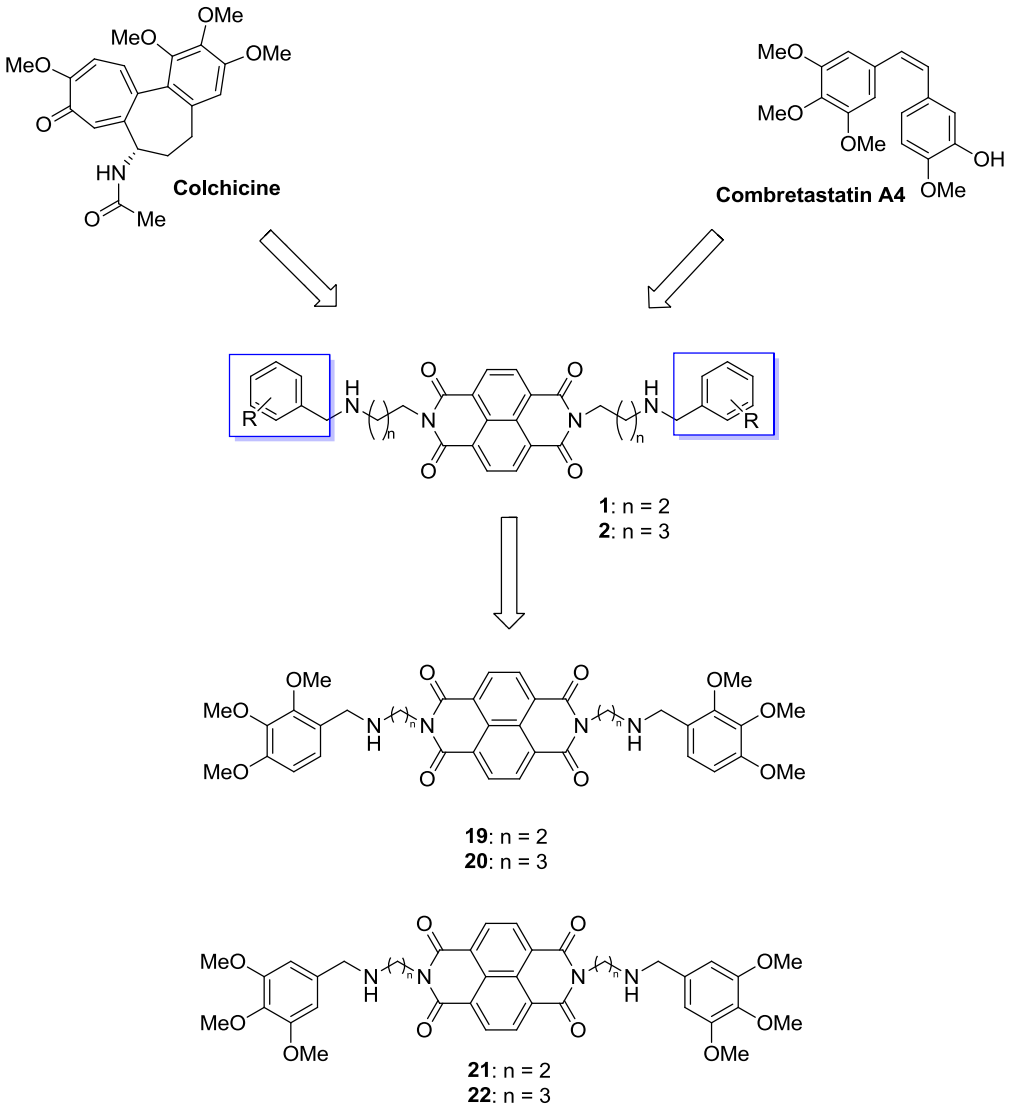

Figure 6.2: Drug design of compounds **19-22**

Finally, to explore the activity of these MTDLs specifically on prostate cancer, compounds bearing acetylene (**23**, **24** Figure 6.3) groups on the side chain have been synthesized. Acetylene group has been demonstrated to be essential for the inhibition of MAO-A. Moreover, to confirm the importance of the acetylene groups in MAO inhibition, derivatives characterized by two vinyl groups (**25**, **26** Figure 6.3) have beensynthesized.

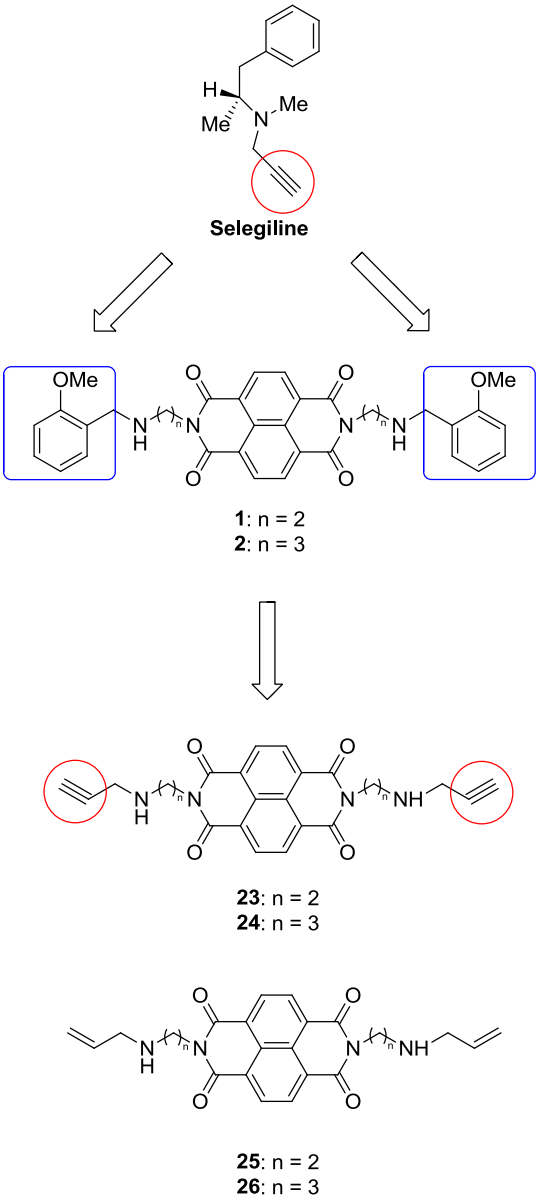

Figure 6.3: Drug design of compounds **23**-**26**

6.2 METHODS

6.2.1 Synthesis

Compounds **3-22** have been synthesized following the procedure reported in Scheme 6.1. The appropriate benzaldehydes were treated with 1,2-diaminoethane or 1,3-diaminopropane to afford the corresponding Schiff bases, reduced *in situ* with sodium borohydride to give compounds **27-46**. Condensation of such derivatives with naphthalenetetracarboxylic dianhydride led to the corresponding diamine-diimides **3-22**.

Compounds **23-26** have been synthesized following the procedure reported in Scheme 6.2. Propargyl bromide or allyl bromide were treated with 1,2-diaminoethane or 1,3-diaminopropane and potassium carbonate, to obtain the amines **47-50**. Condensation of such derivatives with naphthalenetetracarboxylic dianhydride led to the corresponding diamine-diimides **23-26**.

Di-*p*-toluensulfonates salts of the final compounds were prepared to obtain derivatives easier to handle.

Scheme 6.1

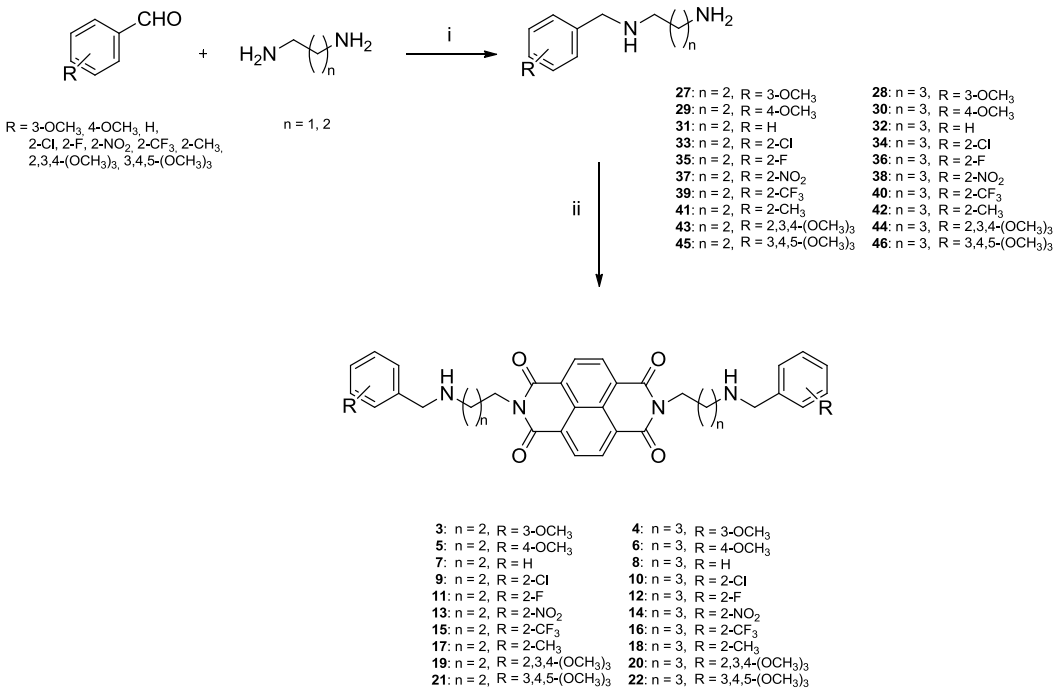

Conditions: (i) (a) toluene, reflux, 5 h; (b) $NaBH_4$, EtOH, room temp., 4 h, 24-36%; (ii) 1,4,5,8-Naphthalenetetracarboxylic dianhydride, i-PrOH, reflux, 24 h, 20-85%.

Scheme 6.2

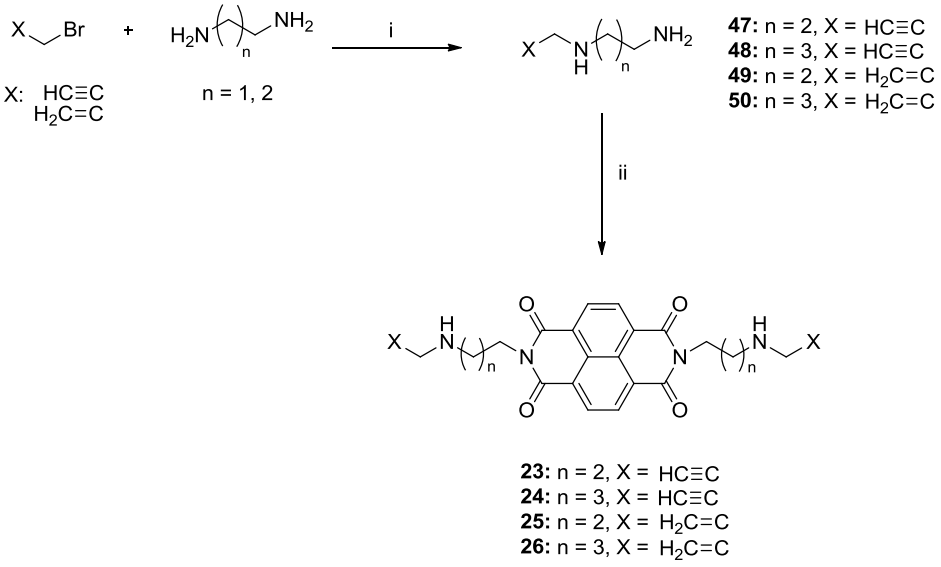

Conditions; (i) K_2CO_3, CH_3CN, room temp., 24h, 27-44%; (ii) 1,4,5,8-Naphthalenetetracarboxylic dianhydride, i-PrOH, reflux, 24 h, 31-42%.

6.2.2 Biology

Derivatives **1-3**, **5**, **7**, **8**, **10**, **12**, **19-22** were submitted for *in vitro* antiproliferative activity to the Developmental Therapeutics Program (DTP) at National Cancer Institute (NCI) for evaluation of their anticancer activity against 60 human cancer cell lines derived from nine human cancer cell types, that have been grouped in disease sub-panels including leukemia, non-small-cell lung, colon, central nervous system, melanoma, ovarian, renal, prostate, and breast tumor cell lines. Lead compounds **1** and **2** were used as reference.

Compounds **14**, **16** and **18**, not selected by the NCI, have been tested for growth inhibition on additional panel of tumor cell lines, including neuroblastoma (HTLA-230), ovarian carcinoma (OVCAR-3), melanoma (MZ2-Mel 3.0) and colon adenocarcinoma (SW620), by the MTT [3-(4,5-dimethylthiazolyil-2)-2,5-diphenyltetrazolium bromide] assay.

The DNA-binding activity of the strongly cytotoxic compounds **8**, **12, 20, 22** was determined using a fluorometric intercalator displacement method,[320] and it is expressed as the drug concentration reducing by 50% the fluorescence of DNA-bound Ethidium bromide (EC_{50}). This EC_{50} value allows to estimate the affinity ranking order of the ligands for calf thymus DNA.[321]

All the experimental part of the biology assays have been reported in other PhD thesis. However, as soon as possible it will be published a paper describing all the methods.

6.2.3 Computational studies

With the aim to investigate the binding mode of **20** for duplex and G-quadruplex DNA, docking simulation were performed using the available crystallographic structures from the Protein Data Bank (PDB).[322,323]

6.3 RESULTS AND DISCUSSION

As preliminary screening compounds **1**-**3**, **5**, **7**, **8**, **10**, **12**, **19**-**22** were submitted to the Developmental Therapeutics Program (DTP) at National Cancer Institute (NCI) for evaluation of their anticancer activity against different human cell lines, that have been grouped in disease sub-panels including leukemia, non-small-cell lung, colon, central nervous system, melanoma, ovarian, renal, prostate, and breast tumor cell lines. The compounds have been dissolved in dimethyl sulfoxide and evaluated at five concentrations at 10-fold dilution the highest being 10^{-4}M in comparison to our lead compounds **1** and **2**. The results are showed in Table 6.1 and they are expressed as the negative log of the molar concentration at three assay end points: the 50% growth inhibitory power (pGI_{50}), the cytostatic effect (pTGI = total growth inhibition), and the cytotoxic effect (pLC_{50}). For several compounds this five concentration assay was repeated twice and no significative differences were found. Also, compounds **14**, **16** and **18**, not selected by NCI, have been tested for growth inhibition on additional panel of tumor cell lines, including neuroblastoma (HTLA-230), ovarian carcinoma (OVCAR-3), melanoma (MZ2-Mel 3.0) and colon adenocarcinoma (SW620), by the MTT [3-(4,5-dimethylthiazolyil-2)-2,5-diphenyltetrazolium bromide] assay. Results are shown in Table 6.2.

Table 6.1. Growth Inhibition, Cytostatic and Cytotoxic Activity of **1**-**3**, **5**, **7**, **8**, **10**, **12**, and **19**-**22** in the 60-Cell Panel in comparison to Vincristine.

Compd[a]	modes	Leukemia	NSCLC	colon	CNS	melanoma	ovarian	renal	prostate	breast	MG-MID[b].
1	pGI_{50}	6.60	6.44	6.7	6.29	6.34	6.53	6.34	6.52	6.34	6.46
	pTGI	6.17	6.07	6.35	5.89	5.95	6.05	5.92	6.02	5.88	6.03
	pLC_{50}	5.36	5.72	6.14	5.54	5.58	5.37	5.47	5.47	5.35	5.55
2	pGI_{50}	6.75	6.69	6.94	6.67	6.72	6.68	6.67	6.73	6.64	6.72
	pTGI	6.10	6.26	6.51	6.23	6.41	6.12	6.27	6.36	6.19	6.27
	pLC_{50}	6.01	5.74	6.03	5.80	6.09	5.42	5.73	5.82	5.79	5.82
3	pGI_{50}	5.57	5.24	5.66	5.50	5.72	5.39	5.46	5.41	5.52	5.50
	pTGI	5.05	4.98	5.30	5.04	5.42	5.01	5.04	4.76	5.13	5.08
	pLC_{50}		4.52	4.77	4.73	5.09	4.70	4.51	4.20	4.84	4.67
5	pGI_{50}	6.54	6.40	6.75	6.46	6.61	6.57	6.44	6.39	6.49	6.52
	pTGI	5.83	5.84	6.28	5.96	6.22	6.06	5.91	5.78	5.98	5.98
	pLC_{50}	4.72	5.17	5.75	5.44	5.83	5.54	5.48	5.38	5.36	5.41
7	pGI_{50}	5.90	5.64	5.90	5.63	5.79	5.62	5.60	5.57	5.72	5.71
	pTGI	5.30	5.20	5.57	5.04	5.44	5.24	5.21	4.94	5.33	5.25
	pLC_{50}		4.99	5.23	4.63	5.22	4.78	4.67		4.79	4.90
8	pGI_{50}	6.85	6.68	7.03	6.81	6.76	6.79	6.75	6.74	6.65	6.78
	pTGI	6.05	6.23	6.53	6.42	6.44	6.30	6.29	6.37	6.16	6.31
	pLC_{50}	5.18	5.71	5.90	5.95	6.12	5.36	5.67	5.69	5.66	5.69
10	pGI_{50}	6.58	6.48	6.86	6.35	6.56	6.65	6.63	6.58	6.49	6.57
	pTGI	5.79	5.96	6.38	5.86	6.13	6.15	6.15	5.88	6.03	6.03
	pLC_{50}	5.36	5.49	5.76	5.50	5.68	6.59	5.77	5.68	5.63	5.72
12	pGI_{50}	6.77	6.75	7.03	6.79	6.77	6.79	6.80	6,74	6.66	6.79
	pTGI	5.88	6.36	6.56	6.42	6.47	6.31	6.37	6.35	6.20	6.32
	pLC_{50}	4.70	6.01	6.14	5.96	6.17	5.82	5.56	6.28	5.93	5.84
19	pGI_{50}	6.42	6.32	6.77	6.20	6.52	6.48	6.50	6.19	6.45	6.43
	pTGI	5.93	5.85	6.33	5.74	6.09	6.49	6.26	5.91	5.94	6.06
	pLC_{50}		5.49	5.96	5.05	5.73	6.53	6.34		5.62	5.82
20	pGI_{50}	6.89	6.90	7.06	6.96	6.98	6.85	6.74	6.99	6.82	6.91
	pTGI	6.22	6.48	6.64	6.57	6.68	6.43	6.36	6.63	6.38	6.49
	pLC_{50}	4.66	5.91	6.10	6.07	6.39	5.64	5.90	6.13	5.96	5.86
21	pGI_{50}	6.65	6.28	6.60	6.41	6.28	6.39	6.36	6.66	6.58	6.47
	pTGI	6.29	5.92	6.22	5.94	6.01	6.04	6.09	6.13	6.20	6.09
	pLC_{50}		5.56	5.60	5.43	5.67	5.71	5.79	5.66	5.70	5.64
22	pGI_{50}	6.48	6.33	6.60	6.34	6.38	6.32	6.18	6.38	6.40	6.38
	pTGI	5.71	5.86	6.08	5.85	5.98	5.95	5.73	5.87	5.89	5.88
	pLC_{50}	5.38	5.70	5.41	5.37	5.58	5.26	5.27	5.33	5.31	5.40
Vin[c]	pGI_{50}	7.00	6.60	7.00	6.90	6.80	6.50	6.50	6.90	6.50	6.74
	pTGI	4.80	4.80	5.40	5.20	5.10	4.70	4.70	5.20	5.10	5.00
	pLC_{50}	3.20	3.60	4.10	3.70	3.60	3.50	3.60	3.50	3.50	3.59

[a]**1**-**3**, **5**, **7**, **8**, **10**, **12**, and **19**-**22**, *bis(p*-toluensulfonate) salt; highest concentration = 10^{-4} M unless otherwise reported; only modes showing a value greater than 4.00 are reported. [b]Mean graph midpoint, i.e., the mean concentration for all cell lines. [c]Vincristine sulfate, highest concentration = 10^{-3} M. Data are expressed as the negative log of the molar concentration at three assay end points: the 50% growth inhibitory power (pGI_{50}), the cytostatic effect (pTGI = total growth inhibition) and the cytotoxic effect (pLC_{50}).

Table 6.2. Cytotoxic Activity of **2**, **14**, **16**, and **18** against HTLA-230, OVCAR-3, MZ2-Mel 3.0, and SV620 Cells.

compd[a]	HTLA	OVCAR	pIC_{50}[b] MZ2_Mel3.0	SV620	MG/MID[d]
2	7.0 ± 0.3	6.7 ± 0.2	6.1 ± 0.1	6.4 ± 0.2	6.5
14	6.0 ± 0.1	6.1 ± 0.2	5.8 ± 0.1	6.2 ± 0.2	6.0
16	na[c]	na[c]	na[c]	na[c]	na[c]
18	6.0 ± 0.1	5.7 ± 0.3	5.7 ± 0.1	6.0 ± 0.1	5.88

[a]*bis*(*p*-toluensulfonate) salt. [b]pIC_{50} values are the negative log of the molar concentration causing 50% growth inhibition, after 48 h of compounds exposure, evaluated by MTT method. [c]Not active at 10 μM. [d]Mean graph midpoint, i.e., the mean concentration for all cell lines. Results, derived from three different experiments in quadruplicate wells as compared to that of control cells, are expressed as mean ± S.E.M.

The analysis of the results showed in Table 6.1, showed that in compounds related to **1**, the removal of the methoxy group (**7**) or its shift to position 3, providing **3**, cause a decrease of cytotoxic activity of more than 10-folds. At the same time, its introduction in position 4 (**5**), restored completely the activity, which is comparable with that of the lead compound **1**. The introduction of two additional methoxy groups in position 3 and 4 (**19**) or in 4 and 5 (**21**), caused decrease of the cytotoxic activity in comparison with **1**.

On the other hand, the series of **2**-related compounds, showed different results. The substitution of the methoxy group with a hydrogen (**8**) or a fluorine (**12**) atom, did not cause any decrease in activity, but the presence of different substituents such as chlorine (**10**), nitro (**14**), trifluoromethyl (**16**) and methyl (**18**) groups in 2-position on the two aromatic rings determined a marked decrease of inhibitory activity on different cell lines in comparison with **2**. In particular, it is to note that **16** did not show any significant activity up to 10 μM (Table 6.2). Moreover, the pattern of the multisubstitution with three methoxy groups was different from that observed for **1**-series. Compounds **20** and **22**, characterized by 2,3,4- and 3,4,5-trimethoxy substitution, respectively, showed a different biological profile. In particular, the inhibitory activity of **22** is decreased in comparison with **2,** while **20** showed the highest levels of GI_{50}, emerging as the most potent among all the NDI derivatives towards the different tested cell lines. Notably, this compound displayed the highest values of cytotoxic activity against colon and prostate cells. These data were similar to those reported for Vincristine, a well-known anticancer agent (see Table 6.1).

As a result of this study, compound **20** resulted the most interesting derivative of the two series, so it was used as model compound for further investigations to elucidate its mechanism of action at cellular level.

With the aim to investigate if **20** could induce apoptosis, the activity of caspase proteases have been monitored on a proper substrate (Asp-Glu-Val-Asp (EVD), i.e. mainly effector caspases -3 and -7), which represents a marker of apoptotic cell death.[324] Treatment of HeLa cells with **20** for 24 h, increased caspase activity in a dose-dependent manner (Figure 6.4 A), in association to the increased number of cells committed to death.

The apoptotic process was also studied observing the cells nuclear morphology, which is another reliable indicator of apoptotic cell death. By DAPI staining in cells treated for 24 h with 2 μM of **20** (Figure 6.4 B) it was possible to detect several cells with characteristic hallmarks of apoptosis, i.e. chromatin condensation, nuclear fragmentation and/or condensation.[325]

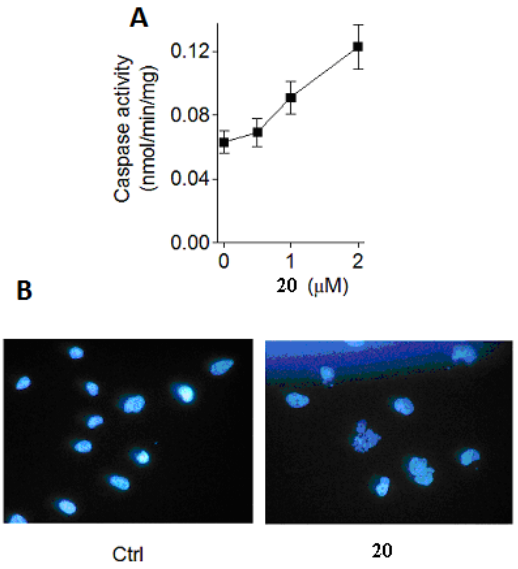

Figure 6.4: A. Effects of **20** on caspases activity. The cells were treated for 24 h with the indicated dose of **20**, afterward, cells were collected for caspase activity determination. Data are mean ± S.E.M. of three replicates. B. Morphological evaluation of nuclei stained with DAPI from control HeLa cells and cells treated with 2 μM of **20** for 24 h.

To confirm the ability of **20** to induce apoptosis, OVCAR 3.0 cells were treated with **20** by staining cells with Annexin V-FITC and PI. FACS was used to distinguish and quantitatively determine the percentage of dead, viable, apoptotic and necrotic cells. As shown in Figure 6.5 panel A, OVCAR 3.0 control and treated cells were gated into LR (Lower Right), UP (Upper Right), LL (Lower Left) and UL (Upper Left) quadrants. Cells in LR and UR were considered as early apoptotic (annexin+/PI-) and late apoptotic (annexin+/PI+) respectively. Cells in LL and UL were considered live (annexin-/PI-) and necrotic (annexin+/PI+), respectively. In particular, the percentage of apoptosis shown in the dot plot of flow cytometric analysis, increased gradually after 72 h according to the **20** concentration: 41% at 1.5 µM, 47% at 2.0 µM and 57% at 2.5 µM. These data, taken together with the above experiments, confirmed the apoptotic mode of cell death. The experiment was repeated three times with similar results. These results can also be visualized in Figure 6.5 panel B, where the extent of apoptosis was expressed as the sum of the percentages in LR and UR quadrants. Compound **20** was effective in inducing apoptosis in a dose and time dependent manner between the concentration of 1.5 µM and 2.5 µM. Compared to 24 h treatment with **20** at 2.5 µM, apoptosis gradually increased to about 3-fold after 72 h treatment, while at 2.0 µM and 1.5 µM the increase was about 5-fold and 6-fold after 72 h, respectively. The mean values and standard deviations calculated for untreated and treated cells at different concentrations in combination with the statistical analysis determined by Mann Whitney test demonstrated that the differences between control and treated cells are statistically significative at any time of treatment ($P = 0.0286$ vs control).

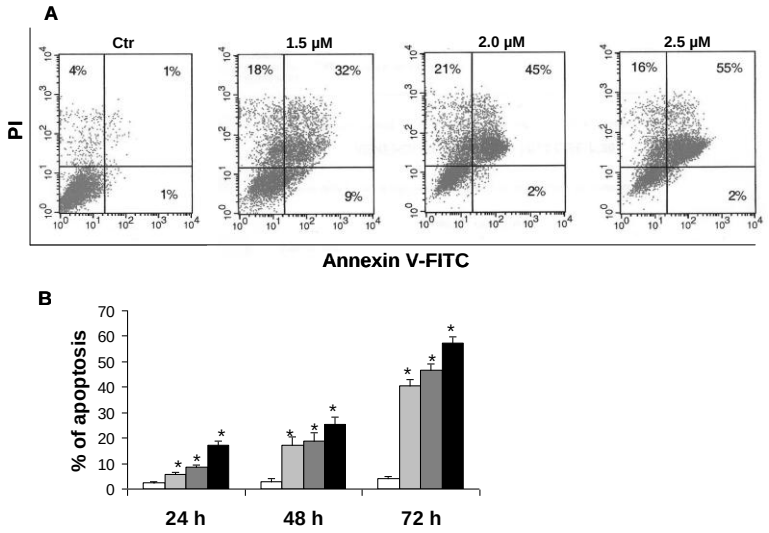

Figure 6.5: (A) Flow cytometry analysis of apoptosis induced by **20** at different concentrations in OVCAR 3.0 ovarian carcinoma cell line after 72 h of drug exposure, using Annexin V-FITC/PI double staining method. (B) Quantitative detection of **20**-induced apoptosis by Annexin V-FITC/PI staining on OVCAR 3.0 cell line at different times and concentrations. White columns: control; light grey columns: **20** at 1.5 µM; grey columns: **20** at 2.0 µM; black columns: **20** at 2.5 µM. Bars represent the mean number of triplicates wells from three independent experiments;

The involvement of some putative signal transduction pathways implicated in apoptosis induction by **20** also has been investigated. HeLa cells were treated with **20** for 20 hours, then ERK1/2 mitogen-activated protein kinases, that are generally associated with cell growth, were examined. As shown in Figure 6.6, **20** was able to down-regulate the p44 ERK2 protein, and to significantly inhibit the phosphorylation of both p42 and p44 ERKs, which are known to influence the survival of cancer cells.[326]

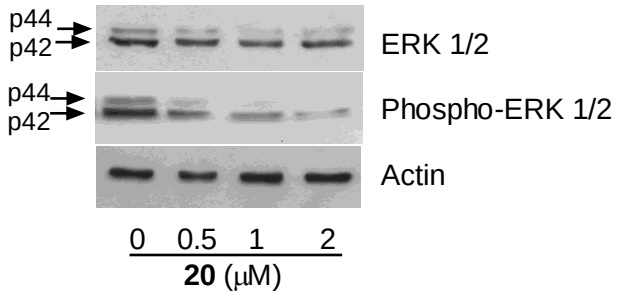

Figure 6.6: Effect of **20** on signal transduction pathway correlated to cell survival. HeLa cells were incubated for 20 h in the presence of the indicated concentration of **20**. The content and phosphorylation status of ERK 1/2 in cell extracts was determined by Western blotting (50 µg of protein/lane).

In order to detect whether oxidative stress would play a role in the cytotoxic mechanism of the novel derivative, the effect of the antioxidant N-acetylcysteine (NAC) on the survival of cells treated with **20** have been studied. Figure 6.7 shows that addition of 5 mM NAC to the culture medium completely inhibited HeLa cells death induced by **20**, suggesting the involvement of oxidative mechanisms in the cytotoxic action of **20**.

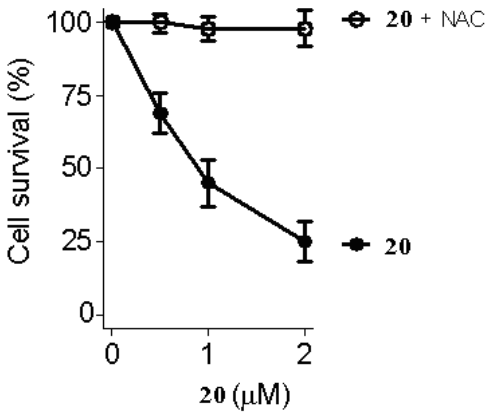

Figure 6.7: Effect on NAC on the survival of cells treated with **20**. Cell viability was measured in cells treated for 24 h with the indicated concentration of **20** in the absence or presence of 5 mM NAC. Results are mean ± S.E.M. of triplicate determinations.

As reported in the introduction, antiproliferative effects are often related to inhibition of cell cycle progression. For this reason, compound **20** was submitted to the bromodeoxyuridine (BrdU) assay. HTLA-230 neuroblastoma cells were treated with 1.5 μM of **20** for 24-48 hours. Then, the cells were pulsed labelled with BrdU and the DNA synthesis were examined. As shown in Figure 6.8, a time-dependent increase of the percentage of cells in G2/M phases (R4) has been observed. This evidence is accompanied by a nearly complete depletion of cells in S phase (R3). In particular, the percentage of cells in S phase decreases from 33% to 9.6%, while the percentage of cells accumulated in G2/M phases was of 30% after 48 h of treatment. Moreover, the percentage of cells in the sub-G1 fraction (R1), which contains apoptotic cells, increased at longer times of **20** exposure (from 0.9% to 15.2% after 48 h). Therefore, the cell cycle analysis showed a concomitant rise of

treated cells in G2/M fraction and a depletion of S fraction. These findings suggest delay in exit of daughter cells from the mitotic cycle leading to reduction of tumor cell number.

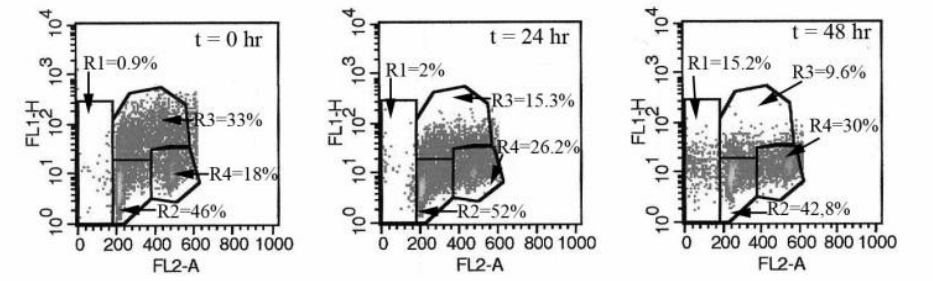

Figure 6.8: Effect of **20** on cell cycle progression in HTLA-230 neuroblastoma cells. BrdU uptake (fluorescein isothiocynate, y-axis) versus total cellular DNA content (propidium iodide, x-axis) was evaluated by densitometric fluorescence-activated cell sorter analysis. (R1 = sub-G1-phase cells; R2 = G1-phase cells; R3 = S-phase cells; R4 = G2/M-phase cells).

As reported above, derivatives **19-22** were designed by introducing the trimethoxyphenyl pharmacophore, peculiar of some anticancer agents such as Colchicine, Podophyllotoxin and Combretastatin A4, which affects the microtubules structure, with the aim to hit this specific and important biological target. To verify this biological activity, **19-22** and the reference compound **2** were tested both in cells and *in vitro* assays. Concerning the first series of assays, A549 cells were incubated for 20 hours with 100 times the GI_{50} of **19-22** and **2**. This assay did not show depolymerisation of the cytoplasmic microtubules (Figure 6.9). In particular, when the cells were treated with **21** and **2** (Figure 6.9, D, F), they became rounded and the microtubule cytoskeleton looked disorganized but no microtubule depolymerisation was observed. As control 2.5 μM Podophillotoxin was employed and the cellular microtubules completely depolymerised (results not shown).

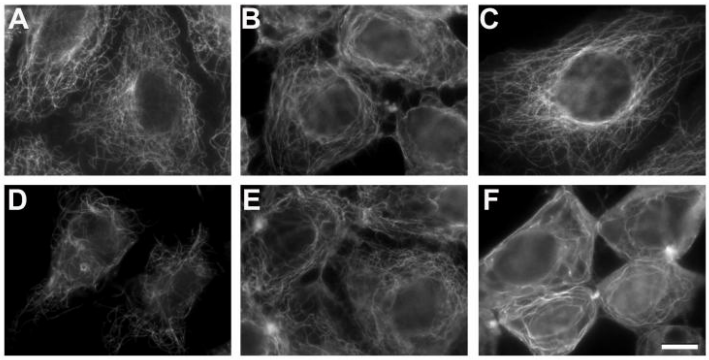

Figure 6.9: Effect of **19-22** and reference compound **2** on the cytoplasmic microtubule network of A549 lung carcinoma cells. A549 cells were incubated for 20 hours with either A, DMSO, B, 10 μM **20**, C, 50 μM **19**, D, 50 μM **21**, E, 20 μM **22**, or F, 20 μM **2**. Microtubules were stained with anti-tubulin monoclonal antibodies (DM1A). The bar is 10 μm.

Moreover, in *in vitro* assay the assembly of 25 μM tubulin in the presence of 30 μM of **2**, **19-21** has been tested. In the absence of compounds the critical concentration of tubulin required for assembly was 3.40 ± 0.83 μM. In the presence of a stabilizer (Docetaxel) the concentration was of course lower 1.24 ± 0.31 μM. In the presence of a destabilizer (Podophyllotoxin) the concentration required was lower 7.40 ± 0.79 μM. In the presence of the compounds **2**, **19-21** the required concentration was equal to those determined in the absence of drug (3.67 ± 0.90 μM, 3.65 ± 0.97 μM, 3.23 ± 0.86 μM, 3.50 ± 1.09 μM, respectively) and no effect on tubulin assembly was observed. These results demonstrated that **2**, **19-21** did not affect directly microtubules and tubulin. In particular, in A549 cells they were cytotoxic but they did not impair microtubules functions.

Since several NDI compounds are DNA intercalator, the ability of the most interesting compounds **8**, **12**, **20** and **22** to interact with double stranded DNA have been tested applying a fluorometric intercalator displacement method.[320] DNA-binding activity was expressed as the drug concentration able to reduce by 50% the fluorescence of DNA-bound ethidium bromide (EtBr). This EC_{50} value allows to estimate the affinity ranking order of the ligands for calf thymus DNA.[321] Table 6.3 shows that tested compounds were strong DNA-interacting molecules with modest modulation of the EC_{50} values.

Table 6.3. DNA interaction of **1**, **2**, **8**, **12**, **20** and **22** evaluated by EtBr displacement, fluorescence quenching melting on dsDNA and G4, and TAQ polymerase inhibition.

Compound	EtBr displacement EC_{50} (nM)[a] ctDNA	Fluorecence melting ΔTm (°C)[b] G4	dsDNA	TAQ inhibition IC_{50} (μM)[c]
1	93 ± 4[d]	16.1	6.2	> 40
2	122 ± 6	15.5	7.7	10 ±2
8	118 ± 8	18.5	11.3	3.5 ± 8
12	130 ± 8	16.4	8.1	> 40
20	166 ± 8	20.5	8.4	8 ± 1
22	159 ± 8	16.1	5.2	5 ± 1

[a]EC_{50} values are defined as the drug concentrations which reduce the fluorescence of the DNA-bound ethidium by 50%. [b]ΔTm corresponds to the increment in the DNA melting temperature induced by 2.5 μM drug concentration. Errors were ± 0.4 °C. [c]IC_{50} values are defined as the drug concentrations which reduce by 50% the amplification of a fragment of pBR322 mediated by TAQ polymerase. [d]Data reported in ref. [12]

G-quadruplex and duplex DNA recognition of the most active compound was also evaluated by fluorescence quenching melting assay using a G-quadruplex folded sequence based on the human telomeric sequence (G4) and a 18-bp random double stranded DNA (dsDNA). As shown in Table 6.3, all derivatives were able to significantly increase the tested DNAs melting temperatures in a concentration dependent manner (Figure 6.10). It emerged that the increment in the melting temperature was generally more intense for the G-quadruplex folded sequence than for the dsDNA template. However, on both substrates, the process appeared to reach saturation in the low micromolar range, which suggests a strong interaction with both DNA arrangements.

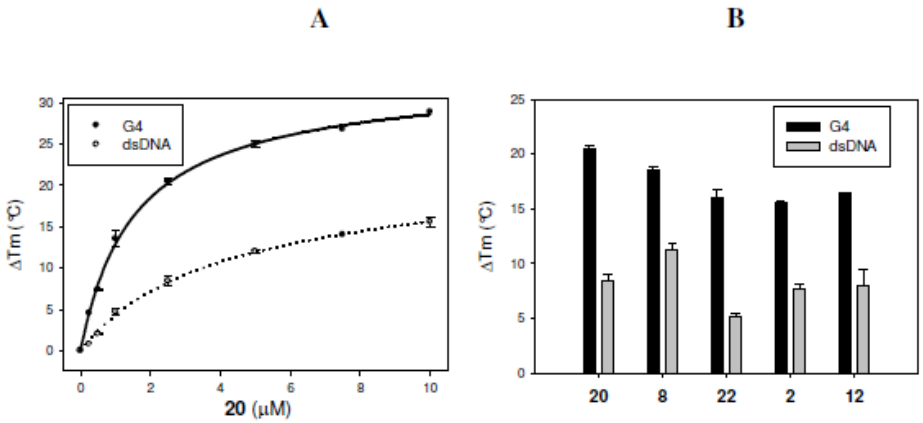

Figure 6.10: Variation of DNA (0.25 μM) thermal stability (ΔTm °C) produced by tested ligands in 50 mM potassium buffer, pH 7.4, evaluated by fluorescence quenching melting experiments. Heating rate 1 °C/min. PANEL A: increasing concentration of **20** on G-quadruplex folded telomeric sequence (G4) or double stranded (dsDNA) DNA; PANEL B: **2**, **8**, **12**, **20**, and **22** (2.5 μM) on G-quadruplex (black bars) and dsDNA (grey bars).

In particular, Table 6.3 shows that **20** appears to be the most efficient G-quadruplex binder whereas **8**, in agreement with EtBr displacement data, induced the most relevant stabilization on double stranded DNA. The difference between the recognition of the two DNA foldings slightly increments accordingly with the number of methoxy groups whereas, their substitution with a fluorine atom (**12**) does not significantly alter the DNA stabilization properties which, actually, parallels the cytotoxic activity.

Table 6.3 also show the inhibitor activity of derivatives **1**, **2**, **8**, **12**, **20**, and **22** on Taq Polymerase. The most potent derivative was **22**, with **2** and **20** slightly less potent, but in the same order. Interestingly, **1** and **12**, characterized by shorter side chains and by a fluorine atom on the aromatic rings, respectively, were the less potent of the all series, showing no activity up to 40 μM.

The interaction of all derivatives with both DNA duplex and quadruplex, was further confirmed by circular dichroism spectroscopy (CD), using NDI derivatives **2**, **8**, **12**, **20**, and **22**. A representative example is reported in Figure 6.11 for **20**. The addition of the NDI derivatives to a double stranded DNA, caused an increment of the intensities of the two major bands located at 275 and 245 nm (Figure 6.11, Panel B). This result confirmed an intercalation binding mode for NDI into the double helix. Using the human telomeric G-quadruplex as substrate, the binding of all the test ligands induced an increase of intensity of the DNA dichroic signal, in particular of the 295 band which is generally attributed to the antiparallel components of the nucleic acid structure (Figure 6.11, Panel A).

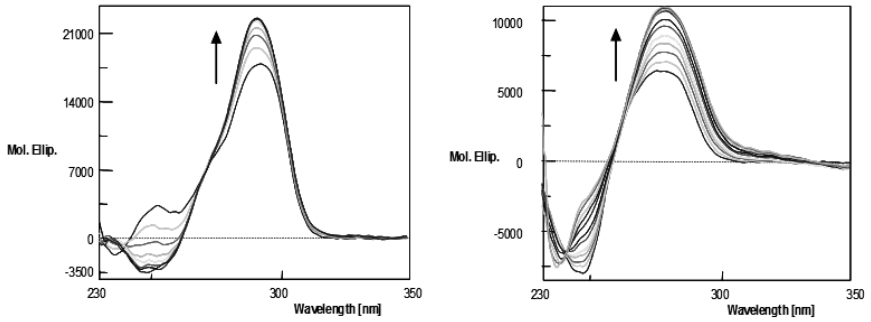

Figure 6.11: Modification of DNA CD spectra upon addition of **20**(0-20 μM) in 10 mM Tris, 50 mM KCl, pH 7.5. Arrows indicate spectrals changes upon ligand addition. Panel A: 4 μM G-quadruplex folded human telomeric sequence Tel22. Panel B: 45 μM ctDNA.

Quantitative analysis of the binding process towards the two substrates using **20** as model compound have been performed to obtain further information about DNA-binding. These data were obtained by UV-VIS titrations since addition of dsDNA or G-quadruplex DNA induced a significant reduction of the drug absorbance (Figure 6.12). The results are summarized in Table 6.4 and confirmed a relevant affinity of **20** toward both DNA substrates. In particular, the difference in K_a is likely not sufficient to preclude the recognition of one target in physiological conditions.

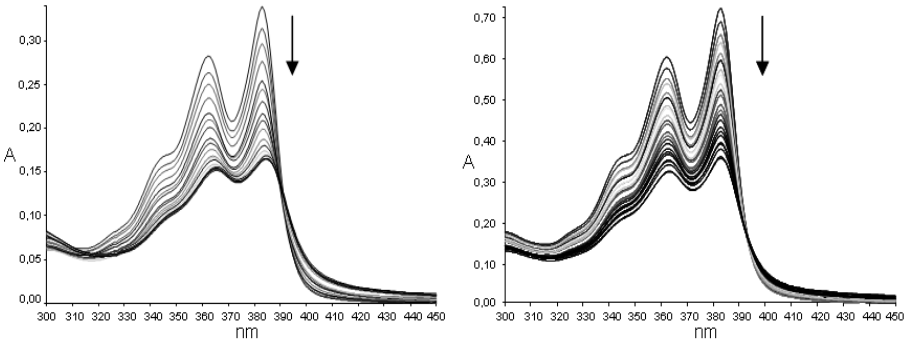

Figure 6.12: Titrations of **20** (10-20 μM) with DNA in 10 mM Tris, 50 mM KCl, pH 7.5. Panel A: human telomeric sequence folded in G-quadruplex; Panel B: ctDNA. Arrows indicate absorption spectra change upon DNA addition.

Table 6.4. Thermodynamic parameters for the DNA binding by **20** determined in 10 mM Tris, 20 mM KCl, pH 7.5, 37°C. n refears to the number of G-quadruplex or base pairs involved in the binding of one NDI molecule

	$Ka \cdot 10^{-6}$ (M^{-1})	n
G-quadruplex	6.94 ± 2.05	0.49
dsDNA	0.85 ± 0.07	2.62 ± 0.03

These data proved that stacking interactions are relevant for the DNA binding process. Indeed, dsDNA binding data analysis indicated a complex stoichiometry (n) of two base pairs for each bound drug molecule, which is in line with an intercalation binding mode. In the presence of G-quadruplex, two NDI molecules bound to one DNA structure. This likely corresponds to the stacking of the ligands one at each terminal tetrad.

Since test derivatives showed to be able to recognize telomeric G-quadruplex sequences, the telomerase activity in HeLa cells treated with **20**, the best G-quadruplex binder, has been evaluated. The results confirmed that **20** is able to reduce the activity of this enzyme thus confirming a cytotoxic mechanism which can result from the potential impairment of several biological pathways (Figure 6.13).

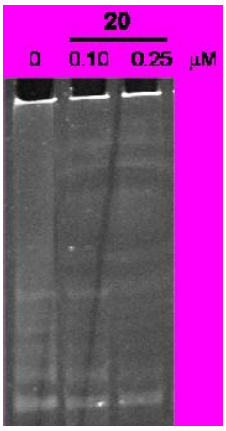

Figure 6.13: Reduction of telomerase activity in HeLa cell after treatment for 24 h with **20**. For each line, a cellular extract corresponding to 2 ng of total proteins was used.

With the aim to characterize the conformational profile and binding mode for duplex and G-quadruplex DNA, compound **20** have been submitted to molecular modeling studies. Analysis of the ionization state, showed that at pH 7.5 the bis cationic form, with both secondary amines protonated, was the most prevalent among all ionizable states. Consequently, the conformational study has been carried out with this ionization form, by the Monte Carlo search. The docking simulations were performed using the available crystallographic structures from the Protein Data Bank (PDB).[322,323] Docking models have been obtained with Autodock.

Figure 6.14 A shows the lowest energy pose of **20** within the DNA duplex. There is a synergy of attractive interactions due to the NDI core stacking (two contributions) within the guanine-citosine intercalation site, one hydrophobic contact and hydrogen bond within the minor groove and two hydrogen bonds within the major groove.

a)

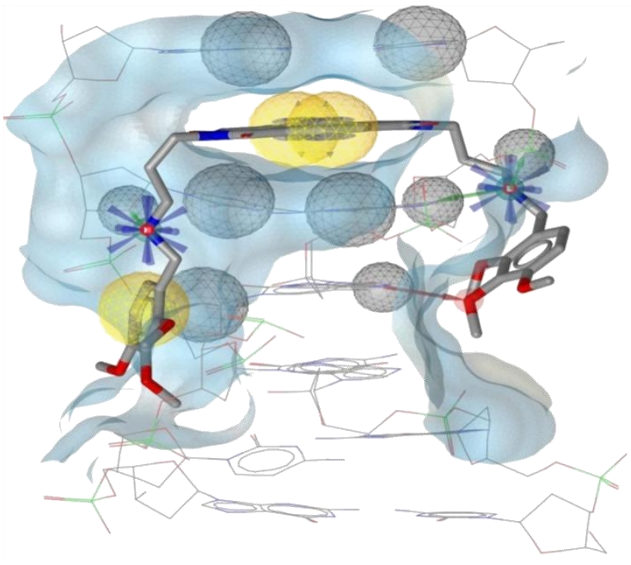

b)

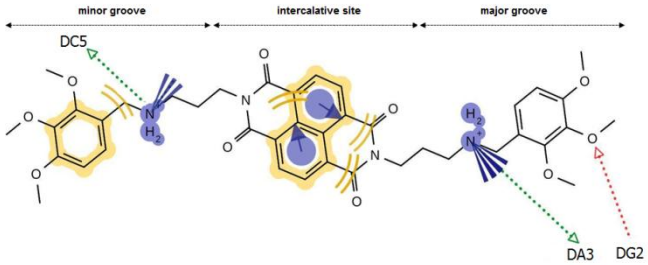

Figure 6.14: a) 3D representation of the best intercalative pose of compound **20** within the DNA duplex. The ligand and the DNA are respectively displayed as polytube and wireframe models. The gray surface represents target binding pocket. The hydrophobic features of the ligand are pointed as yellow spheres. The exclusion volume coats onto the target are shown as gray spheres. Intermolecular hydrogen bonds are displayed as red and green arrows, pointing respectively ligand acceptor and donor atoms. Positive ionizable target nitrogens are shown as blue features. The ligand aromatic rings detected to interact via π-π interactions are highlighted with blue circles with top/bottom triangles. b) 2D ligand representation with the main interaction features with the DNA duplex model. Three intermolecular hydrogen bonds are represented by dotted vectors. Electrostatic interacting nitrogens are shown as blue features. Hydrophobic interacting rings are highlighted in yellow. NDI core π-π stacked rings are depicted with blue circles and black arrows. The top ruler indicates the corresponding DNA duplex interaction area.

The molecular recognition obtained in the docking simulations of the ligand **20** with the DNA G-quadruplex model is shown in Figure 6.15a, where the 2:1 stoichiometry results in a sort of "sandwich-type interaction". In this ternary complex the first bound ligand assumed a semi-folded conformation, fitting the NDI core onto the DNA G-tetrads in top position by efficient end stacking interaction. Both the ionized nitrogen atoms were able to donate hydrogen bonds, respectively to the phosphate groups of dG14 and dG20 (Figure 6.15b). The second ligand recognized the G-tetrad in the bottom position by stacking of the NDI core, not properly detected as a pharmacophore feature (Figure 6.15c). The reason can be addressed to the misalignment among the aromatic cores of guanines and NDI (data not shown). The side chains of this second ligand assumed a more extended conformation each one realizing different DNA interactions. One appeared to be more involved than the other in stabilizing the interaction with the G-quadruplex bottom side. Actually, the ionized nitrogen atom and the trimethoxy aromatic ring of one side chain established one hydrogen bond with dG22 N3 and hydrophobic contacts with the DNA, respectively. Conversely, the second side chain engaged interaction only with the dG10 residue. Globally, the "sandwich-type" model seemed to be able to protect the unwinding process thus explaining the consistent stabilizing effect of **20** on the G-quadruplex.

a)

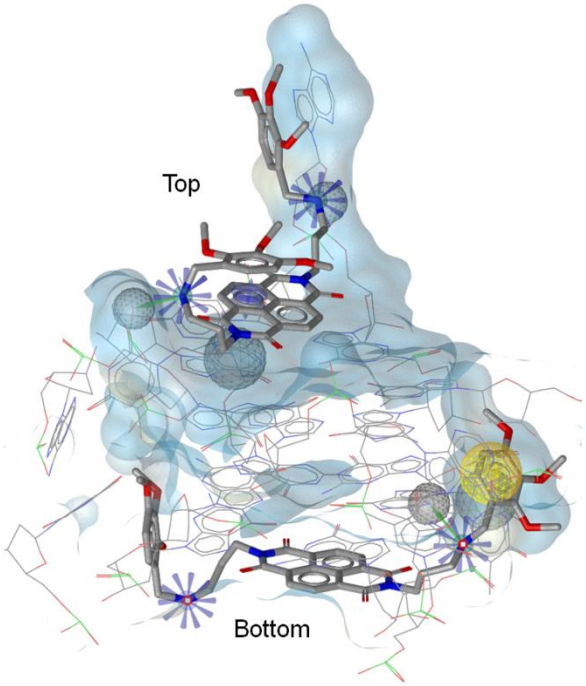

b)

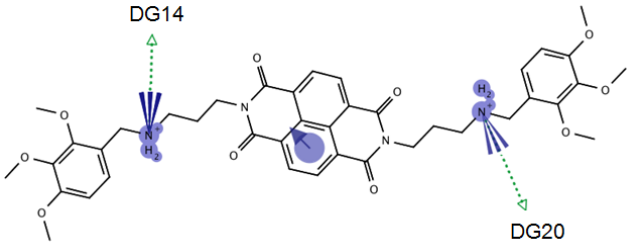

c)

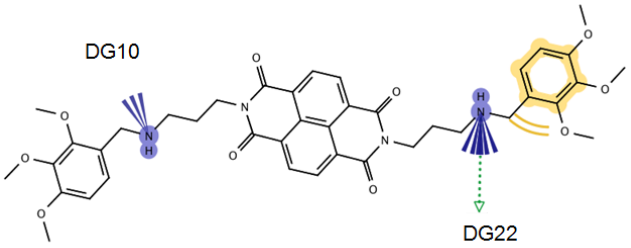

Figure 6.15: a) 3D representation of compound **20** top/bottom best poses obtained with the DNA G-quadruplex model. The gray surface represents target binding pocket. The exclusion volume coats onto the target are shown as gray spheres. The intermolecular donating hydrogen bonds are displayed as green arrows. Positive ionizable target nitrogens are shown as blue features. The ligand aromatic ring detected to interact via π-π interactions is highlighted with a blue circles with triangles. b) 2D ligand representation with the main interaction features with the DNA G-quadruplex model in top side. Two intermolecular hydrogen bonds are represented by dotted vectors. Electrostatic interacting nitrogen atoms are shown as blue features. The π-π stacked ring is depicted with blue circles and a black arrow.c) 2D ligand representation with the main interaction features with the DNA G-quadruplex model in bottom side. One intermolecular hydrogen bond is represented by a dotted vector. Electrostatic interacting nitrogen atoms are shown as blue features. Hydrophobic interacting rings are highlighted in yellow.

Compounds **23-26** were submitted to the Developmental Therapeutics Program (DTP) at National Cancer Institute (NCI) for evaluation of their anticancer activity against different human cell lines (Table 6.5), with the same procedure described above.

Table 6.5. Growth Inhibition, Cytostatic and Cytotoxic Activity of **23-26** in the 60-Cell Panel in comparison to lead compounds **1** and **2**.

Cmpd[a]	leukemia	NSCLC	colon	CNS	melanoma	ovarian	renal	prostate	breast	MG-MID[b]
23	5.23	5.45	5.65	5.43	5.56	5.50	5.40	5.21	5.35	5.42
24	6.46	6.49	6.54	6.37	6.55	6.39	6.41	6.50	6.13	6.43
25	6.12	6.15	6.25	6.14	6.10	6.12	6.13	6.12	6.14	6.14
26	6.43	6.38	6.49	6.31	6.14	6.33	6.34	6.37	6.44	6.36
1	6.60	6.44	6.70	6.29	6.34	6.53	6.34	6.52	6.34	6.46
2	6.75	6.69	6.94	6.67	6.72	6.68	6.67	6.73	6.64	6.72

[a]**23-26**, *bis*-hydrocloride salt; highest concentration = 10^{-4} M unless otherwise reported; only modes showing a value greater than 4.00 are reported. [b]Mean graph midpoint, i.e., the mean concentration for all cell lines. Data are expressed as the negative log of the molar concentration at three assay end points: the 50% growth inhibitory power (pGI_{50})

From the analysis of the results, derivatives with 3 methylene units emerged as the most potent compounds, as it was observed within lead compounds **1** and **2**. Also, the substitution of the methoxy group with a acetylene or vinyl group, resulted in reduction of cytotoxic activity. However, compounds bearing the acetylene group were more potent than those with vinyl. Consequently, compound **24** was the most active derivative of the series.

Since compounds **23-26** were designed by introducing functions able to irreversibly interact with MAO-A enzymes, their activity against this target compared with MAO-B have been evaluated at 50 μM concentration. (Table 6.6).

Table 6.6. Kinetic parameters of human MAO A and B in presence of compounds **24-26**

Cmpd	MAO A			MAO B		
	Vmax residue	Km (μM)	Vmax/Km residue	Vmax residue	Km (μM)	Vmax/Km residue
Control	1	523± 71	1			
24	0.55±0.17	1710± 750	0.23±0.03	0.77	369± 25	1.16
25	0.65±0.07	512± 102	0.60±0.06	0.93	374± 45	1.37
26	0.61±0.14	413± 146	0.73±0.07	0.86	449± 37	1.06

The preliminary data show that compound **24** was the more effective compound in MAO-A inhibition. In addition it is endowed with a good selectivity between MAO-A and MAO-B.

6.4 CONCLUSION

In this work it has been demonstrated that the cytostatic and cytotoxic activities of **1** and **2** were affected by the insertion of different substituents on the two aromatic rings confirming their possible influence on the biological effects. In particular, compound **20**, characterized by a chain length of three methylene units and by 2,3,4-trimethoxy groups on the two aromatic rings, was the most potent of the two series and showed an interesting biological profile. In fact, it displayed pGI_{50} values around 7, demonstrating an improvement of the cytotoxic activity towards multiple cancer lines, in comparison with lead compounds **1** and **2** and comparable with those of Vincristine. Nevertheless, the mechanism of action of **20** is distinct from vincristine. Indeed, **20** showed the ability to tightly bind DNA irrespectively to its structural arrangement, to inhibit Taq polymerase and telomerase, to trigger caspase activation by a possible oxidative mechanism, to downregulate ERK 2 protein and to inhibit ERKs phosphorylation, without acting directly on microtubules and tubuline.

All together these data point out that **20** interact with several targets involved in cancer development, therefore this study may represent a promising starting point for the development of new MTDLs hopefully useful for the cancer treatment.

6.5 EXPERIMENTAL SECTION

6.5.1 Chemistry

Melting point were taken in glass capillary tubes on a Buchi SMP-20 apparatus and are uncorrected. ESI-MS spectra were recorded on Perkin-Elmer 297 and WatersZQ 4000. ^{1}H NMR and ^{13}C NMR were recorded on Varian VRX 200 and 400 instruments. Chemical shift are reported in parts per millions (ppm) relative to peak of tetramethylsilane (TMS) and spin multiplicities are given as s (singlet), brs (broad singlet), d (doublet), t (triplet), q (quartet) or m (multiplet). The elemental analysis was performed with Perkin Elmer elemental analyzer 2400 CHN. From all new compounds satisfactory elemental analyses were obtained, confirming >95%purity. Chromatographic separations were performed on silica gel columns by flash (Kieselgel 40, 0.040-0.063 mm, Merck) column chromatography. Reactions were followed by thin layer chromatography (TLC) on Merck (0.25 mm) glass-packed precoated silica gel plates (60 F254) and then visualized in an iodine chamber or with a UV lamp. The term "dried" refers to the use of anhydrous sodium sulphate. Compounds were named following IUPAC rules as applied by Beilstein-Institute AutoNom (version 2.1), a PC integrated software package for systematic names in organic chemistry.

General Procedure for the Synthesis of 3-26: A mixture of the appropriate amine **27-50** and 1,4,5,8-Naphthalene-tetracarbocylic dianhydride in a 1:5 molar ratio in iso-propanol were refluxed for 2 hours. After cooling down, removal of the solvent gave residue that was purified by flash chromatography using as eluent a mixture of dichloromethane/methanol/33% acqueous ammonia (9:1:0.03) providing the desired products **3-26** that were converted into the corresponding bis-p-toluenesulfonates salt.

2,7-Bis-[2-(3-methoxy-benzylamino)-ethyl]benzo[lmn][3,8] phenanthroline-1,3,6,8-tetraone (3): yellow oil (70 mg, 28%); mp (bis-p-toluensulfonate salt): 152-155 °C; ^{1}H NMR ($CDCl_3$, 200 MHz, free base) δ = 1.58 (brs, 2H exchangeable with D2O), 3.06 (t, J = 6.2 Hz, 4H), 3.76 (s, 6H), 3.84 (s, 4H), 4.41 (t, J = 6.2 Hz, 4H), 6.85-6.89 (m, 4H), 7.18-7.29 (m, 4H), 8.78 ppm (s, 4H); ^{13}C NMR ($CDCl_3$, 50MHz): δ = 39.3, 46.1, 54.2, 55.8, 112.0, 113.2, 119.9, 125.6, 128.5, 129.1, 129.6, 158.5, 164.1 ppm; ESI-MS (m/z): 593 [M

+H]$^+$; Anal. calcd for $C_{48}H_{48}N_4O_{12}S_2$ • $2H_2O$: C 59.25, H 5.39, N 5.76, found: C 58.97, H 5.23, N 5.88.

2,7-Bis-[3-(3-methoxy-benzylamino)-propyl]-benzo[lmn][3,8] phenanthroline-1,3,6,8-tetraone (4): yellow oil (55 mg, 16%); mp (*bis-p*-toluensulfonate salt): 102-104 °C;^{1}H NMR ($CDCl_3$, 200 MHz, free base): δ = 1.99-2.10 (m, 4H + 2H exchangeable with D_2O), 2,77 (t, *J* = 6.6 Hz, 4H), 3.81 (s, 10H), 4.34 (t, *J* = 7.7 Hz, 4H), 6.75-6.80 (m, 2H), 6.88-6.92 (m, 4H), 7.17-7.25 (m, 2H), 8.76 ppm (s, 4H); ^{13}C NMR ($CDCl_3$,50MHz): δ = 28.2, 39.0, 46.5, 53.8, 55.3, 112.4, 113.7, 120.5, 126.6, 128.0, 129.4, 131.1, 158.7, 163.8 ppm; ESI-MS (m/z): 621 [M +H]$^+$; Anal. calcd for $C_{50}H_{52}N_4O_{12}S_2$ • $2H_2O$: C 59.99, H 5.64, N 5.60, found: C 59.79, H 5.56, N 5.73.

2,7-Bis-[2-(4-methoxy-benzylamino)-ethyl]-benzo[lmn][3,8] phenanthroline-1,3,6,8-tetraone (5): yellow oil (82 mg, 15.0 %); mp (*bis-p*-toluensulfonate salt): 124-126 °C; ^{1}H NMR ($CDCl_3$, 400 MHz, free base): δ = 1.54 (brs, 2H exchangeable with D_2O), 3.02 (t, *J* = 6.4 Hz, 4H), 3.74 (s, 6H); 3.76 (s, 4H); 4.37 (t, *J* = 6.4 Hz, 4H); 6.74-6.76 (m, 4H); 7.16-7.18 (m, 4H); 8.75 ppm (s, 4H); ^{13}C NMR ($CDCl_3$, 50MHz): δ = 38.1, 47.5, 52.6, 56.5, 112.3, 115.6, 121.3, 126.9, 127.5, 130.0, 159.9, 162.8 ppm; ESI-MS (m/z): 593 [M+H]$^+$; Anal. calcd for $C_{48}H_{48}N_4O_{12}S_2$ • $2H_2O$: C 59.25, H 5.39, N 5.76, found: C 59.42, H 5.11, N 5.59.

2,7-Bis-[3-(4-methoxy-benzylamino)-propyl]-benzo[lmn][3,8] phenanthroline-1,3,6,8-tetraone (6): yellow oil (67 mg, 21%); mp (*bis-p*-toluensulfonate salt): 134-136°C; ^{1}H NMR ($CDCl_3$, 200 MHz, free base): δ = 1.59 (brs, 2H exchangeable with D_2O), 2.00-2.35 (m, 4H), 2.75 (t, *J* = 6.4 Hz, 4H), 3.75 (s, 4H), 3.79 (s, 6H), 4.32 (t, *J* = 7.0 Hz, 4H), 6.80-6.84 (m, 4H), 7.20-7.28 (m, 4H), 8.77 ppm (s, 4H); ^{13}C NMR ($CDCl_3$, 50MHz): δ = 25.7, 37.4, 47.6, 51.9, 56.9, 111.6, 115.3, 121.8, 127.4, 128.9, 131.1, 159.1, 163.6 ppm; ESI-MS (m/z): 621 [M+H]$^+$; Anal. calcd for $C_{50}H_{52}N_4O_{12}S_2$ • $2H_2O$: C 59.99, H 5.64, N 5.60, found: C 59.75, H 5.47, N 5.67.

2,7-Bis-(2-benzylamino-ethyl)-benzo[lmn][3,8]phenanthroline-1,3,6,8-tetraone (7): yellow oil (82 mg, 30%); mp (*bis-p*-toluensulfonate salt): 163-165 °C; ^{1}H NMR ($CDCl_3$, 200 MHz, free base): δ = 1.58 (brs, 2H exchangeable with D_2O), 3.07 (t, *J* = 6.2 Hz, 4H), 3.88 (s, 4H), 4.42 (t, *J* = 6.6 Hz, 4H), 7.23-7.29 (m, 10H), 8.79 ppm (s, 4H); ^{13}C NMR ($CDCl_3$, 50 MHz): δ = 40.6, 46.9, 53.6, 126.7, 127.0, 128.2, 128.5, 131.1, 151.1,

152.0, 163.2 ppm; ESI-MS (m/z): 533 $[M+H]^+$; Anal. calcd for $C_{46}H_{44}N_4O_{10}S_2 \bullet 2H_2O$: C 60.51, H 5.30, N 6.14, found: C 60.79, H 5.63, N 6.44.

2,7-Bis-(3-benzylamino-propyl)-benzo[lmn][3,8]phenanthroline-1,3,6,8-tetraone (8): yellow oil (107 mg, 34%); mp (*bis*-*p*-toluensulfonate salt): 163-165 °C; ^{1}H NMR ($CDCl_3$, 200 MHz, free base): δ = 1.45-1.45 (m, 2H + 4H exchangeable with D_2O), 3.15 (t, *J* = 6.2 Hz, 4H), 3.76 (s, 4H), 4.32 (t, *J* = 6.6 Hz, 4H), 7.17-7.25 (m, 10H), 8.72 ppm (s, 4H); ^{13}C NMR ($CDCl_3$, 50 MHz): δ = 28.7, 41.7, 46.6, 54.1, 126.0, 127.6, 128.6, 129.5, 131.5, 150.8, 152.5, 163.6 ppm; ESI-MS (m/z): 561 $[M+H]^+$; Anal. calcd for $C_{48}H_{48}N_4O_{10}S_2 \bullet 2H_2O$: C 61.21, H 5.57, N 5.95, found: C 61.47, H 5.79, N 6.13.

2,7-Bis-[2-(2-chloro-benzylamino)-ethyl]-benzo[lmn][3,8] phenanthroline-1,3,6,8-tetraone (9): yellow oil (93 mg, 35%); mp (*bis*-*p*-toluensulfonate salt): 174 °C; ^{1}H NMR ($CDCl_3$, 200 MHz, free base): δ = 1.61 (brs, 2H exchangeable with D_2O), 3.06 (t, *J* = 6.6 Hz, 4H), 3.97 (s, 4H), 4.42 (t, *J* = 6.6 Hz, 4H), 7.17-7.19 (m, 4H), 7.28-7.35 (m, 4H), 8.78 ppm (s, 4H); ^{13}C NMR ($CDCl_3$, 50 MHz): δ = 37.1, 45.5, 53.2, 125.3, 126.9, 128.0, 129.4, 131.1, 131.9, 134.2, 137.9, 152.1, 162.1 ppm; ESI-MS (m/z): 601 $[M+H]^+$; Anal. calcd for $C_{46}H_{42}Cl_2N_4O_{10}S_2 \bullet 2H_2O$: C 56.27, H 4.72, N 5.71, found: C 56.44, H 4.91, N 5.91.

2,7-Bis-[3-(2-chloro-benzylamino)-propyl]-benzo[lmn][3,8] phenanthroline-1,3,6,8-tetraone (10): yellow oil (83 mg, 21%); mp (*bis*-*p*-toluensulfonate salt): 115 °C; ^{1}H NMR ($CDCl_3$, 200 MHz, free base): δ = 1.69 (brs, 2H exchangeable with D_2O), 1.95-2.08 (m, 4H), 2.78 (t, *J* = 7.0 Hz, 4H), 3.90 (s, 4H), 4.34 (t, *J* = 7.0 Hz, 4H), 7.16-7.24 (m, 4H), 7.28-7.40 (m, 4H), 8.76 ppm (s, 4H); ^{13}C NMR ($CDCl_3$, 50 MHz): δ = 28.4, 39.1, 46.6, 51.2, 126.7, 126.8, 128.3, 129.5, 130.1, 131.0, 133.8, 137.7, 151.2, 163.0 ppm; ESI-MS (m/z): 629 $[M+H]^+$; Anal. calcd for $C_{48}H_{46}Cl_2N_4O_{10}S_2 \bullet 2H_2O$: C 57.08, H 4.99, N 5.55, found: C 57.41, H 5.24, N 5.81.

2,7-Bis-[2-(2-fluoro-benzylamino)-ethyl]-benzo[lmn][3,8] phenanthroline-1,3,6,8-tetraone (11): yellow oil (62 mg, 27%); mp (*bis*-*p*-toluensulfonate salt): 174 °C dec; ^{1}H NMR ($CDCl_3$, 200 MHz, free base): δ = 1.62 (brs, 2H exchangeable with D_2O), 3.06 (t, *J* = 6.2 Hz, 4H), 3.85 (s, 4H), 4.41 (t, *J* = 6.2 Hz, 4H), 6.95-7.05 (m, 8H), 8.78 ppm (s, 4H); ^{13}C NMR ($CDCl_3$, 50 MHz): δ = 36.3, 45.1, 48.0, 114.9, 124.7, 126.1, 127.8, 128.0, 129.1,

130.1, 132.6, 151.7, 162.4 ppm; ESI-MS (m/z): 569 $[M+H]^+$; Anal. calcd for $C_{46}H_{42}F_2N_4O_{10}S_2 \bullet 2H_2O$: C 58.2, H 4.89, N 5.90, found: C 58.45, H 5.01, N 5.99.

2,7-Bis-[3-(2-fluoro-benzylamino)-propyl]-benzo[lmn][3,8] phenanthroline-1,3,6,8-tetraone (12): yellow oil (77 mg, 22%); mp (*bis-p*-toluensulfonate salt): 104-107 °C; ^{1}H NMR ($CDCl_3$, 200 MHz, free base): δ = 1.73 (brs, 2H exchangeable with D_2O), 1.90-2.08 (m, 4H), 2.77 (t, *J* = 7.0 Hz, 4H), 3.87 (s, 4H), 4.33 (t, *J* = 7.4 Hz, 4H), 6.97-7.21 (m, 4H), 7.23-7.37 (m, 4H), 8.76 ppm (s, 4H); ^{13}C NMR ($CDCl_3$, 50 MHz): δ = 28.3, 39.0, 46.5, 47.3, 115.5, 124.1, 126.7, 128.6, 128.8, 130.4, 130.5, 131.01, 151.1, 163.0 ppm; ESI-MS (m/z): 597 $[M+H]^+$; Anal. calcd for $C_{48}H_{46}F_2N_4O_{10}S_2 \bullet 2H_2O$: C 59.01, H 5.16, N 5.73, found: C 59.37, H 5.31, N 5.86.

2**,7-Bis-[2-(2-nitro-benzylamino)-ethyl]-benzo[lmn][3,8] phenanthroline-1,3,6,8-tetraone (13)**: yellow oil (53 mg, 26%); mp (*bis-p*-toluensulfonate salt): > 250 °C; ^{1}H NMR ($CDCl_3$, 200 MHz, free base): δ = 1.62 (brs, 2H exchangeable with D_2O), 3.08 (t, *J* = 6.2 Hz, 4H), 4.11 (s, 4H), 4.41 (t, *J* = 6.2 Hz, 4H), 7.28-7.54 (m, 6H), 7.80-7.85 (m, 2H), 8.78 ppm (s, 4H); ^{13}C NMR ($CDCl_3$, 50 MHz): δ = 40.3, 47.1, 50.6, 124.7, 126.7, 128.1, 131.0, 131.3, 133.0, 135.4, 149.3, 151.3, 163.2 ppm; ESI-MS (m/z): 623 $[M+H]^+$; Anal. calcd for $C_{46}H_{42}N_6O_{14}S_2 \bullet 2H_2O$: C 55.08, H 4.62, N 8.38, found: C 54.94, H 4.72, N 8.11.

2,7-Bis-[3-(2-nitro-benzylamino)-propyl]-benzo[lmn][3,8] phenanthroline-1,3,6,8-tetraone (14): yellow oil (71 mg, 24%); mp (*bis-p*-toluensulfonate salt): 90-95 °C; ^{1}H NMR ($CDCl_3$, 200 MHz, free base): δ = 1.83 (brs, 2H exchangeable with D_2O), 1.85-1.97 (m, 4H), 2.77 (t, *J* = 6.6 Hz, 4H), 4.06 (s, 4H), 4.32 (t, *J* = 7.0 Hz, 4H), 7.36-7.44 (m, 2H), 7.53-7.66 (m, 4H), 7.92-7.96 (m, 2H), 8.74 ppm (s, 4H); ^{13}C NMR ($CDCl_3$, 50 MHz): δ = 28.4, 39.0, 46.9, 50.8, 124.8, 126.6, 128.0, 131.1, 131.3, 133.2, 135.7, 149.2, 163.0 ppm; ESI-MS (m/z): 651 $[M+H]^+$; Anal. calcd for $C_{48}H_{46}N_6O_{14}S_2 \bullet 2H_2O$: C 55.91, H 4.89, N 8.15, found: C 55.81, H 4.67, N 8.23.

2,7-Bis-[2-(2-trifluoromethyl-benzylamino)-ethyl]-benzo[lmn] [3,8]phenanthroline-1,3,6,8-tetraone (15): yellow oil (102 mg, 25%); mp (*bis-p*-toluensulfonate salt): 122-126 °C; ^{1}H NMR ($CDCl_3$, 200 MHz, free base): δ = 1.59 (brs, 2H exchangeable with D_2O), 3.08 (t, *J* = 6.2 Hz, 4H), 4.03 (s, 4H), 4.43 (t, *J* = 6.2 Hz, 4H), 7.21-7.63 (m, 8H), 8.79 ppm (s, 4H); ^{13}C NMR ($CDCl_3$, 50 MHz): δ = 40.4, 47.1, 49.6, 103.2, 125.9, 126.0, 126.7, 127.0, 128.3, 130.2, 131.1, 131.9, 138.8, 163.1 ppm; ESI-MS

(m/z): 669 $[M+H]^+$; Anal. calcd for $C_{48}H_{42}F_6N_4O_{10}S_2 \bullet 2H_2O$: C 54.96, H 4.42, N 5.34, found: C 55.12, H 4.41, N 5.50.

2,7-Bis-[3-(2-trifluoromethyl-benzylamino)-propyl]-benzo[lmn] [3,8]phenanthroline-1,3,6,8-tetraone (16): yellow oil (91 mg, 27%); mp (*bis-p*-toluensulfonate salt): 119-121 °C; ^{1}H NMR ($CDCl_3$, 200 MHz, free base): δ = 1.58 (brs, 2H exchangeable with D_2O), 2.02-2.07 (m, 4H), 2.81 (t, *J* = 7.0 Hz, 4H), 3.98 (s, 4H), 4.35 (t, *J* = 6.2 Hz, 4H), 7.29-7.38 (m, 2H), 7.47-7.55 (m, 2H), 7.62-7.65 (m, 4H), 8.78 ppm (s, 4H); ^{13}C NMR ($CDCl_3$, 50 MHz): δ = 24.3, 41.4, 46.6, 49.1, 101.7, 123.7, 125.1, 126.1, 127.2, 128.7, 129.9, 131.4, 132.2, 139.9, 162.0 ppm; ESI-MS (m/z): 697 $[M+H]^+$; Anal. calcd for $C_{50}H_{46}F_6N_4O_{10}S_2 \bullet 2H_2O$: C 55.76, H 4.68, N 5.20, found: C 55.40, H 4.72, N 5.55.

2,7-Bis-[2-(2-methyl-benzylamino)-ethyl]-benzo[lmn][3,8] phenanthroline-1,3,6,8-tetraone (17): yellow oil (53 mg, 28%); mp (*bis-p*-toluensulfonate salt): 149-151 °C; ^{1}H NMR ($CDCl_3$, 200 MHz, free base): δ = 1.53 (brs, 2H exchangeable with D_2O), 2.27 (s, 6H), 3.08 (t, *J* = 6.4 Hz, 4H), 3.82 (s, 4H), 4.39 (t, *J* = 6.4 Hz, 4H,), 7.05-7.08 (m, 5H), 7.21-7.26 (m, 3H), 8.74 ppm (s, 4H); ^{13}C NMR ($CDCl_3$, 50 MHz): δ = 19.2, 40.7, 47.3, 51.5, 126.0, 126.8, 126.0, 127.1, 128.6, 130.4, 131.2, 136.5, 138.3, 163.3 ppm; ESI-MS (m/z): 561 $[M+H]^+$; Anal. calcd for $C_{48}H_{48}N_4O_{10}S_2 \bullet 2H_2O$: C 61.21, H 5.57, N 5.95, found: C 60.98, H 5.47, N 6.02.

2,7-Bis-[3-(2-methyl-benzylamino)-propyl]-benzo[lmn][3,8] phenanthroline-1,3,6,8-tetraone (18): yellow oil (44 mg, 37%); mp (*bis-p*-toluensulfonate salt): 137-140 °C; ^{1}H NMR ($CDCl_3$, 200 MHz, free base): δ = 1.64 (brs, 2H exchangeable with D_2O), 2.03 (m, 4H), 2.37 (s, 6H), 2.83 (t, *J* = 7.0 Hz, 4H), 3.80 (s, 4H), 4.34 (t, *J* = 7.0 Hz, 4H), 7.14-7.15 (m, 5H), 7.25-7.28 (m, 3H), 8.76 ppm (s, 4H); ^{13}C NMR ($CDCl_3$, 50 MHz) δ = 18.9, 28.2, 39.0, 46.9, 51.4, 125.7, 126.4, 126.5, 126.8, 128.2, 130.1, 130.8, 136.2, 138.1, 162.8 ppm; ESI-MS (m/z): 589 $[M+H]^+$; Anal. calcd for $C_{50}H_{52}N_4O_{10}S_2 \bullet 2H_2O$: C 61.97, H 5.82, N 5.78, found: C 61.74, H 5.59, N 5.71.

2,7-Bis-[2-(2,3,4-trimethoxy-benzylamino)-ethyl]-benzo[lmn][3,8] phenanthroline-1,3,6,8-tetraone (19): yellow oil (96 mg, 27%); mp (*bis-p*-toluensulfonate salt): 221-224 °C dec; ^{1}H NMR ($CDCl_3$, 400 MHz, free base): δ = 1.90 (brs, 2H exchangeable with D_2O), 3.01 (t, *J* = 12.8 Hz, 4H), 3.49-3.90 (m, 22H), 4.38 (t, *J* = 8.7 Hz, 4H), 6.56-6.58 (d, *J* = 8.4 Hz, 2H), 6.92-6.94 (d, *J* = 8.4 Hz, 2H), 8.75 ppm (s, 4H); ^{13}C

NMR ($CDCl_3$, 100 MHz): δ = 40.1, 46.4, 48.4, 50.2, 55.8, 60.6, 106.8, 124.1, 125.2, 126.5, 126.6, 130.7, 141.9, 151.9, 153.0, 163.2 ppm; ESI-MS (m/z): 735 $[M+Na]^+$; Anal. calcd for $C_{52}H_{56}N_4O_{16}S_2 \bullet 2H_2O$: C 57.13, H 5.53, N 5.13, found: C 56.81, H 5.32, N 5.42.

2,7-Bis-[3-(2,3,4-trimethoxy-benzylamino)-propyl]-benzo[lmn] [3,8]phenanthroline-1,3,6,8-tetraone (20): yellow oil (69 mg, 46%); mp (*bis-p*-toluensulfonate salt): 237 °C dec; ^1H NMR ($CDCl_3$, 400 MHz, free base): δ = 1.96-2.0 (m, 4H + 2H exchangeable with D_2O), 2.74 (t, *J* = 8.0Hz, 4H), 3.73 (s, 4H), 3.82 (s, 6H), 3.84 (s, 6H), 3.90 (s, 6H), 4.29 (t, *J* = 8.0 Hz, 4H), 6.56-6.58 (d, *J* = 8.0 Hz, 2H), 6.92-6.94 (d, *J* = 8.0 Hz, 2H), 8.73 ppm (s, 4H); ^{13}C NMR ($CDCl_3$, 100 MHz): δ = 28.1, 38.9, 46.4, 48.4, 55.8, 60.6, 60.9, 106.8, 123.9, 125.7, 126.3, 126.4, 130.7, 141.9, 151.9, 152.8, 162.6 ppm; ESI-MS (m/z): 741 $[M+H]^+$; Anal. calcd for $C_{54}H_{60}N_4O_{16}S_2 \bullet 2H_2O$: C 57.85, H 5.53, N 5.13, found: C 58.06, H 5.65, N 5.17.

2,7-Bis-[2-(3,4,5-trimethoxy-benzylamino)-ethyl]-benzo[lmn] [3,8]phenanthroline-1,3,6,8-tetraone (21)*:* yellow oil (121 mg, 39% yield); mp (*bis-p*-toluensulfonate salt): 199-201 °C; ^1H NMR ($CDCl_3$, 200 MHz, free base): δ = 1.52 (brs, 2H exchangeable with D_2O), 3.04 (t, *J* = 6.4 Hz, 4H), 3.74-3.80 (m, 22H), 4.38 (t, *J* = 6.3 Hz, 4H), 6.52 (s, 4H), 8.74 ppm (s, 4H); ^{13}C NMR ($CDCl_3$, 50 MHz): δ = 40.2, 46.7, 53.6, 55.9, 60.7, 104.7, 126.5, 126.6, 129.7, 130.8, 135.8, 136.6, 150.9, 153.0, 162.9 ppm; ESI-MS (m/z): 735 $[M+Na]^+$; Anal. calcd for $C_{52}H_{56}N_4O_{16}S_2 \bullet 2H_2O$: C 57.13, H 5.53, N 5.13, found: C 56.95, H 5.41, N 5.31.

2,7-Bis-[3-(3,4,5-trimethoxy-benzylamino)-propyl]-benzo[lmn] [3,8]phenanthroline-1,3,6,8-tetraone (22): yellow oil (130 mg, 85%); mp (*bis-p*-toluensulfonate salt): 199-201 °C; ^1H NMR ($CDCl_3$, 200 MHz, free base): δ = 1.99-2.06 (m, 4H + 2H exchangeable with D_2O), 2.78 (t, *J* = 6.8 Hz, 4H), 3.77 (s, 4H), 3.82 (s, 6H), 3.87 (12H), 4.32 (t, *J* = 6.9 Hz, 4H), 6.59 (s, 4H), 8.74 ppm (s, 4H); ^{13}C NMR ($CDCl_3$, 50 MHz): δ = 27.6, 38.4, 45.9, 49.7, 53.5, 55.6, 60.3, 104.5, 125.9, 126.0, 130.3, 135.2, 136.2, 150.6, 152.6, 162.3 ppm; ESI-MS (m/z): 741 $[M+H]^+$; Anal. calcd for $C_{54}H_{60}N_4O_{16}S_2 \bullet 2H_2O$: C 57.85, H 5.75, N 5.00, found: C 57.64, H 5.89, N 5.19.

2,7-bis(2-(prop-2-yn-1-ylamino)ethyl)benzo[lmn][3,8]phenanthroline-1,3,6,8(2H,7H)-tetraone (23): yellow solid (27%); m.p. (*bis-p*-toluensulfonate salt): 152

°C; ^{1}H NMR (200MHz, $CDCl_3$) δ 1.57 (brs, 2H exchangeable with D_2O), 2.19-2.21 (m, 2H), 3.16 (t, 4H), 3.45 (s, 4H), 4.41 (t, 4H), 8.78 (s, 4H); ESI-MS (m/z): 429 $(M+H)^+$.

2,7-bis(3-(prop-2-yn-1-ylamino)propyl)benzo[lmn][3,8]phenanthroline-1,3,6,8(2H,7H)-tetraone (24): white solid, (35%); m.p. (*bis*-*p*-toluensulfonate salt): 187 °C; ^{1}H NMR (200MHz, $CDCl_3$) δ 1.53 (brs, 2H exchangeable with D_2O), 1.93-2.00 (m, 4H), 2.15-2.17 (m, 2H), 2.82 (t, 4H), 3.45 (s, 4H), 4.31 (t, 4H), 8.77 (s, 4H); ESI-MS (m/z): 457 $(M+H)^+$.

2,7-bis(2-(allylamino)ethyl)benzo[lmn][3,8]phenanthroline-1,3,6,8(2H,7H)-tetraone (25): white solid, (44%); m.p. (*bis*-*p*-toluensulfonate salt): 182 °C; ^{1}H NMR (200MHz, $CDCl_3$) δ 1.53 (brs, 2H exchangeable with D_2O), 3.04 (t, 4H), 3,31-3,34 (m, 4H), 4.39 (t, 4H),5.07-5.23 (m, 4H), 5.82-5.95 (m, 2H), 8.76 (s, 4H); ESI-MS (m/z): 433 $(M+H)^+$.

2,7-bis(3-(allylamino)propyl)benzo[lmn][3,8]phenanthroline-1,3,6,8(2H,7H)-tetraone (26): white solid, (41%); m.p. (*bis*-*p*-toluensulfonate salt): 152 °C; ^{1}H NMR (200MHz, $CDCl_3$) δ 1.56 (brs, 2H exchangeable with D_2O), 8.79 (s, 4H); ESI-MS (m/z): 461 $(M+H)^+$.

General Procedure for the Synthesis of 27-46: A mixture of the appropriate diamine and aldehyde (in a 5:1 molar ratio) in toluene was refluxed in a Dean-Stark apparatus for 5 h. Following solvent removal, the residue was taken up in EtOH, $NaBH_4$ (1:2.5 molar ratio) was added at 0 °C, and the stirring was continued at room temperature for 4 h. The solvent was then removed and the residue was dissolved in dichloromethane and washed with brine. Removal of the dried solvent gave a residue that was purified by flash chromatography using as eluent a mixture of dichloromethane/methanol/33% acqueous ammonia (9:1:0.1), providing the desired products **27-46**.

***N*^{1}-(3-Methoxy-benzyl)-ethane-1,2-diamine (27)**: yellow oil; (560 mg, 22%); ^{1}H NMR ($CDCl_3$, 400 MHz): δ = 1.74 (brs, 3H exchangeable with D_2O), 2.69 (t, *J* = 6 Hz, 2H), 2.81 (t, *J* = 5.6 Hz, 2H), 3.77 (s, 2H), 3.80 (s, 3H), 6.77-6.80 (m, 1H), 6.88-6.90 (m, 2H), 7.21-7.26 ppm (m, 1H); ^{13}C NMR ($CDCl_3$, 100 MHz): δ = 41.3, 51.3, 53.5, 54.9, 112.1, 113.4, 120.2, 129.1, 141.8, 159.5.

***N*^{1}-(3-Methoxy-benzyl)-propane-1,3-diamine (28)**: yellow oil (430 mg, 60%); ^{1}H NMR ($CDCl_3$, 400 MHz): δ = 1.42 (brs, 3H exchangeable with D_2O), 1.61-1.75 (m, 2H),

2.68-2.84 (m, 4H), 3.79 (s, 2H), 3.83 (s, 3H), 6.78-6.83 (m, 1H), 6.90-6.93 (m, 2H), 7.22-7.30 ppm (m, 1H); ^{13}C NMR ($CDCl_3$, 100 MHz): δ = 33.6, 40.5, 47.2, 54.0, 55.0, 113.4, 120.3, 129.3, 142.2, 151.1, 159.7 ppm.

***N*^{1}-(4-Methoxy-benzyl)-ethane-1,2-diamine (29)**: yellow oil (512 mg, 21%); ^{1}H NMR ($CDCl_3$, 200 MHz): δ = 1.53 (brs, 3H exchangeable with D_2O), 2.68-2.74 (m, 2H), 2.82-2.88 (m, 2H), 3.77 (s, 2H), 3.82 (s, 3H), 6.86-6.91 (m, 2H), 7.26-7.30 ppm (m, 2H); ^{13}C NMR ($CDCl_3$, 50 MHz): δ = 41.7, 51.8, 53.3, 55.3, 113.8, 129.3, 132.7, 158.6 ppm.

***N*^{1}-(4-Methoxy-benzyl)-propane-1,3-diamine (30)**: yellow oil (670 mg, 51%); ^{1}H NMR ($CDCl_3$, 200 MHz): δ = 1.64-1.71 (m, 2H); 1.74 (brs, 3H exchangeable with D_2O), 2.67-2.82 (m, 4H), 3.74 (s, 2H), 3.81 (s, 3H), 6.85-6.90 (m, 2H), 7.23-7.27 ppm (m, 2H); ^{13}C NMR ($CDCl_3$, 50 MHz): δ = 33.2, 40.3, 46.9, 53.3, 55.0, 113.6, 129.2, 132.3, 158.5 ppm.

***N*^{1}-Benzyl-ethane-1,2-diamine (31)**: yellow oil (597 mg, 22%); ^{1}H NMR ($CDCl_3$, 200 MHz): δ = 1.70 (brs, 3H exchangeable with D_2O), 2.69-2.74 (m, 2H), 2.81-2.86 (m, 2H), 3.82 (s, 2H), 7.30-7.36 ppm (m, 4H); ^{13}C NMR ($CDCl_3$, 50 MHz): δ = 41.5, 51.6, 53.8, 127.0, 128.2, 128.4, 140.3 ppm.

***N*^{1}-Benzyl-propane-1,3-diamine (32)**: yellow oil (770 mg, 30%); ^{1}H NMR ($CDCl_3$, 200 MHz): δ = 1.55-1.63 (m, 2H + 3H exchangeable with D_2O), 2.65-2.73 (m, 2H), 2.84-2.89 (m, 2H), 3.9 (s, 2H), 7.28-7.36 ppm (m, 5H); ^{13}C NMR ($CDCl_3$, 50 MHz): δ = 27.7, 41.1, 50.9, 53.3, 126.5, 128.8, 129.2, 140.5 ppm.

***N*^{1}-(2-Chloro-benzyl)-ethane-1,2-diamine (33)**: yellow oil (620 mg, 25%); ^{1}H NMR ($CDCl_3$, 200 MHz): δ = 1.64 (brs, 3H exchangeable with D_2O), 2.80 (t, *J* = 5.4 Hz, 2H), 2.91 (t, *J* = 5.2 Hz, 2H), 3.99 (s, 2H), 7.30-7.48 ppm (m, 4H); ^{13}C NMR ($CDCl_3$, 50 MHz): δ = 41.8, 51.4, 52.0, 127.1, 128.5, 129.7, 130.4, 138.0, 151.1 ppm.

***N*^{1}-(2-Chloro-benzyl)-propane-1,3-diamine (34)**: yellow oil (790 mg, 35%); ^{1}H NMR ($CDCl_3$, 200 MHz): δ = 1.32-144 (m, 2H + 3H exchangeable with D_2O), 2.36-2.51 (m, 4H), 3.57 (s, 2H), 6.87-6.94 (m, 2H), 7.02-7.13 ppm (m, 2H); ^{13}C NMR ($CDCl_3$, 50 MHz): δ = 33.3, 40.3, 47.0, 51.1, 126.6, 128.0, 129.2, 129.8, 133.4, 137.7 ppm.

***N*^{1}-(2-Fluoro-benzyl)-ethane-1,2-diamine (35)**: yellow oil (530 mg, 29%); ^{1}H NMR ($CDCl_3$, 400 MHz): δ = 1.45 (brs, 3H exchangeable with D_2O), 2.68 (t, *J* = 6 Hz, 2H,), 2.81 (t, *J* = 6 Hz, 2H), 3.85 (s, 2H), 7.00-7.05 (m, 1H), 7.08-7.12 (m, 1H), 7.20-7.26 (m, 1H),

7.32-7.36 ppm (m, 1H); ^{13}C NMR ($CDCl_3$, 100 MHz): δ = 41.4, 46.8, 51.4, 115.1, 123.8, 127.1, 128.4, 130.1, 162.15 ppm.

***N*^{1}-(2-Fluoro-benzyl)-propane-1,3-diamine (36)**: yellow oil (560 mg, 55%); ^{1}H NMR ($CDCl_3$, 400 MHz): δ = 1.63-1.70 (m, 2H), 2.09 (brs, 3H exchangeable with D_2O), 2.70 (t, *J* = 6.4 Hz, 2H), 2.80 (t, *J* = 6.8 Hz, 2H), 3.83 (s, 2H), 6.99-7.04 (m, 1H), 7.07-7.11 (m, 1H), 7.19-7.26 (m, 1H), 7.29-7.34 ppm (m, 1H); ^{13}C NMR ($CDCl_3$, 100 MHz): δ = 32.9, 40.5, 47.3, 47.4, 115.3, 124.2, 127.2, 128.8, 130.5, 160.1 ppm.

***N*^{1}-(2-Nitro-benzyl)-ethane-1,2-diamine (37)**: yellow oil (850 mg, 59%); ^{1}H NMR ($CDCl_3$, 400 MHz): δ = 1.71 (brs, 3H exchangeable with D_2O), 2.71 (t, *J* = 5.2 Hz, 2H), 2.83 (t, *J* = 5.8 Hz, 2H), 4.06 (s, 2H), 7.39-7.46 (m, 1H), 7.54-7.62 (m, 2H), 7.92-7.96 ppm (m, 1H); ^{13}C NMR ($CDCl_3$, 100 MHz): δ = 41.8, 50.7, 52.0, 124.8, 128.0, 131.2, 133.1, 135.7, 147.8 ppm.

***N*^{1}-(2-Nitro-benzyl)-propane-1,3-diamine (38)**: yellow oil (440 mg, 35%); ^{1}H NMR ($CDCl_3$, 400 MHz): δ = 1.55-1.60 (m, 2H), 1.84 (brs, 3H exchangeable with D_2O), 2.59-2.74 (m, 4H), 3.94 (s, 2H), 7.28-7.36 (m, 1H), 7.49-7.52 (m, 2H), 7.81-7.85 ppm (m, 1H); ^{13}C NMR ($CDCl_3$, 100 MHz): δ = 33.2, 40.4, 47.5, 50.9, 124.7, 127.9, 131.2, 133.1, 135.7, 149.2 ppm.

***N*^{1}-(2-Trifluoromethyl-benzyl)-ethane-1,2-diamine (39)**: yellow oil (620 mg, 67%); ^{1}H NMR ($CDCl_3$, 400 MHz): δ = 1.77 (brs, 3H exchangeable with D_2O), 2.73 (t, *J* = 6.2 Hz, 2H), 2.81 (t, *J* = 6.4 Hz, 2H), 3.96 (s, 2H), 7.28-7.65 ppm (m, 4H); ^{13}C NMR ($CDCl_3$, 100 MHz): δ = 41.4, 49.7, 51.7, 125.7, 126.8, 127.3, 127.8, 128.4, 130.2, 131.8 ppm.

***N*^{1}-(2-Trifluoromethyl-benzyl)-propane-1,3-diamine (40)**: yellow oil(560 mg, 47%); ^{1}H NMR ($CDCl_3$, 200 MHz): δ = 1.54 (brs, 3H exchangeable with D_2O), 1.63-1.76 (m, 2H), 2.72-2.85 (m, 4H), 3.97 (s, 2H), 7.29-7.67 ppm (m, 4H); ^{13}C NMR ($CDCl_3$, 100 MHz): δ = 31.3, 39.9, 47.4, 49.8, 125.7, 125.8, 126.9, 130.2, 131.9, 138.7 ppm.

***N*^{1}-(2-Methyl-benzyl)-ethane-1,2-diamine (41)**: yellow oil (420 mg, 23%); ^{1}H NMR $CDCl_3$, 400 MHz); δ = 1.57 (brs, 3H exchangeable with D_2O), 2.72 (s, 3H), 2.72-2.75 (m, 2H), 2.81-2.84 (m, 2H), 3.77 (s, 2H), 7.14-7.17 (m, 3H), 7.26-7.30 ppm (m, 1H); ^{13}C NMR ($CDCl_3$, 100 MHz): δ = 18.6, 41.2, 51.1 51.7 125.5 126.5, 127.9 129.8, 135.8, 137.9 ppm.

***N*^{1}-(2-Methyl-benzyl)-propane-1,3-diamine (42)**: yellow oil (510 mg, 42%); ^{1}H NMR ($CDCl_3$, 200 MHz): δ = 1.58-1.64 (m 2H), 2.01 (brs, 3H exchangeable with D_2O), 2.29 (s, 3H), 2.64-2.75 (m, 4H), 3.69 (s, 2H), 7.09-7.14 (m, 3H), 7.21-7.24 ppm (m, 1H); ^{13}C NMR ($CDCl_3$, 100 MHz): δ = 17.6, 31.8, 38.9, 46.4, 50.4, 124.5, 125.5, 126.9, 128.8, 134.8, 137.2 ppm.

***N*^{1}-(2,3,4-Trimethoxy-benzyl)-ethane-1,2-diamine (43)**: yellow oil (760 mg, 88%); ^{1}H NMR ($CDCl_3$, 200 MHz): δ 2.1 (brs, 3H exchangeable with D_2O), 2.66-2.75 (m, 2H), 2.84 (t, *J* = 5.3 Hz, 2H), 3.74 (s, 2H), 3.85-3.92 (m, 9H), 6.61-6.65 (d, *J* = 8.4 Hz, 1H,), 6.94-6.98 ppm (d, *J* = 8.4 Hz, 1H); ^{13}C NMR ($CDCl_3$, 100 MHz): δ = 44.3, 45.7, 53.2, 56.1, 56.8, 57.1, 108.2, 116.8, 119.5, 131.6, 147.3, 149.5 ppm.

***N*^{1}-(2,3,4-Trimethoxy-benzyl)-propane-1,3-diamine (44)**: yellow oil (505 mg, 51%); ^{1}H NMR ($CDCl_3$, 200 MHz): δ = 1.61-1.71 (m, 2H), 2.09 (brs, 3H exchangeable with D_2O), 2.64 (t, *J* = 7.0 Hz, 2H), 2.75 (t, *J* = 6.6 Hz, 2H,), 3.71 (s, 2H), 3.83-3.91 (m, 9H), 6.59-6.63 (d, *J* = 8.4 Hz, 1H), 6.9-6.94 ppm (d, *J* = 8.8, 1H); ^{13}C NMR ($CDCl_3$, 100 MHz): δ = 22.7, 41.0, 43.3, 51.1, 54.0, 57.2, 57.5, 107.1, 116.3, 121.1, 130.2, 145.4, 148.5 ppm.

***N*^{1}-(3,4,5-Trimethoxy-benzyl)-ethane-1,2-diamine (45)**: yellow oil (720 mg, 82%); ^{1}H NMR ($CDCl_3$, 200 MHz): δ = 2.3 (brs, 3H exchangeable with D_2O), 2.68 (t, *J* = 5.4 Hz, 2H), 2.78 (t, *J* = 5.2 Hz, 2H), 3.67-3.80 (m, 11H), 6.52 ppm (s, 2H); ^{13}C NMR ($CDCl_3$, 50 MHz): δ = 40.8, 50.9, 53.5, 55.5, 60.2, 104.4, 135.6, 136.2, 152.6 ppm.

***N*^{1}-(3,4,5-Trimethoxy-benzyl)-propane-1,3-diamine (46)**: yellow oil (810 mg, 91%); ^{1}H NMR ($CDCl_3$, 400 MHz): δ = 1.64 (brs, 3H exchangeable with D_2O), 1.2-1.76 (m, 2H), 2.69 (t, *J* = 6.6 Hz, 2H), 2.81 (t, *J* = 7.0 Hz, 2H), 3.64 (s, 3H), 3.70 (s, 2H), 3.79 (s, 3H), 3.83 (s, 3H), 6.55 ppm (s, 2H); ^{13}C NMR ($CDCl_3$, 100 MHz): δ = 31.0, 39.4, 46.4, 53.5, 55.7, 60.3, 104.7, 135.2, 136.3, 152.7 ppm.

General Procedure for the Synthesis of 47-50: To a solution of diamine (3 eq) in CH_3CN (15 mL) were added K_2CO_3 (1 eq) and propargyl or vinyl bromide (1 eq). The mixture was stirred for 24 h at room temperature under nitrogen atmosphere. The insoluble salts were removed by filtration and the solvent removed in vacuo. The crude material was purified by flash column chromatography using as eluent a mixture of dichloromethane/methanol/33% acqueous ammonia (7:3:0.3), providing the desired products **47-50**.

***N^1*-(prop-2-yn-1-yl)ethane-1,2-diamine (47):** yellow oil, (42%); ^{1}H NMR (200MHz, $CDCl_3$) δ 1.79 (brs, 3H exchangeable with D_2O), 2.24 (s, 1H), 2.78-2.89 (m, 4H), 3.47-3.48 (m, 2H).

***N^1*-(prop-2-yn-1-yl)propane-1,3-diamine (48):** yellow oil, (49%); ^{1}H NMR (200MHz, $CDCl_3$)δ 1.55-1.62 (m, 2H+3H exchangeable with D_2O), 2.17-2.19 (m, 1H), 2.67-2.76 (m, 4H), 3.37 (s, 2H).

***N^1*-allylethane-1,2-diamine (49):** yellow oil, (37%); ^{1}H NMR (200MHz, $CDCl_3$)δ 2.72 (brs, 3H exchangeable with D_2O), 2.59-2.77 (m, 2H), 2.65-2.77 (m, 4H), 3.24-3.27 (m, 2H), 5.08 (m, 2H), 5.82-5.99 (m, 1H).

***N^1*-allylpropane-1,3-diamine (50)**: yellow oil, (31%); ^{1}H NMR (200MHz, $CDCl_3$)δ 1.27 (brs, 3H exchangeable with D_2O), 1.69-1.79 (m, 2H), 2.74-2.87 (m, 4H), 3.28-3.31 (m, 2H), 5.10-5.25 (m, 2H), 5.84-5.95 (m, 1H).

CHAPTER 7
TETRASUBSTITUTED NDIs AS G-QUADRUPLEX-BINDING LIGANDS

7.1 DRUG DESIGN

Telomeres are complex structures located at the end of chromosome, and their maintenance is fundamental for cell viability. During cell replication, the enzyme telomerase is able to replicate them. However, in physiological conditions, telomere became shorter with age, resulting in cell death. On the other hand, cancer cells over-express telomerase, leading to a prolonged cell life. Since telomeres comprise repeated short G-rich tracts, they are able to fold into particular DNA structures called G-quadruplex. Stabilization of G-quadruplex by small molecules, could indirectly inhibit telomerase and telomere maintenance in cancer cells, and also displace the protein hPOT1 from the telomere, leading to end-to-end fusion of chromosomes, cell cycle arrest, and apoptosis. G-quadruplexes can be formed also in promoter regions of oncogenes such as *c-myc* and *c-kit*, and their stabilization can down-regulate the oncogene expression.

NDIs are very potent G-quadruplex ligands with high cellular toxicity. They possess a π-acidic core, ideal for performing π-π stacking interactions with G-tetrads, and when they are functionalized with four side chains bearing amine end groups, they have the potential to interact with the grooves at the sides of the G-quadruplex, as demonstrated by X-ray crystallography.[141, 327]

Neidle and coworkers described a series of NDIs with high affinity for human telomeric quadruplex DNA.[328,143] These compounds also showed high potency for growth inhibition in a panel of cancer cell lines, concomitant with telomerase inhibition. In particular, derivative with *N*-methyl-piperazine end-groups, showed exceptional potency in a panel of pancreatic cancer cell lines,[143] with a lead compound (BMSG-SH-3) having IC_{50} values in nanomolar range. BMSG-SH-3 has been evaluated in a pancreatic cancer xenograf model, revealing significant anti-tumor activity, with a 50% reduction in tumor volume, together with telomerase inhibition.[329]

The aim of this work was to find new potent G-quadruplex binding ligands with improved antiproliferative activity. In this study the SAR of NDIs have been expanded. Analogues of the lead compound BMSG-SH-3, in which the *N*-methyl-piperazine groups on two side-arms of the NDI core have been changed with other substituents, have been synthesized.

Since a reduction in highly cationic nature of these compounds could improve cellular uptake and tumor distribution properties, the principal substituent inserted on the side-arms was the morpholine group (compounds **1d**, **1f-h**), because it is less basic than the protonated *N*-methyl-piperazine ring, with a pK of 8.5 compared to that for the latter, of 9.2. Also, it is endowed with approximately equivalent size and so it could be bind in the same region of groove space. Only two side-chain have been changed, since the complete removal of cationic groups result in loss of quadruplex affinity. The series was further extended with NDI compounds each having two methoxy, furan, tetrahydrofuran, and tetrahydropyran end-groups (compounds **1a-c**, **1e**).

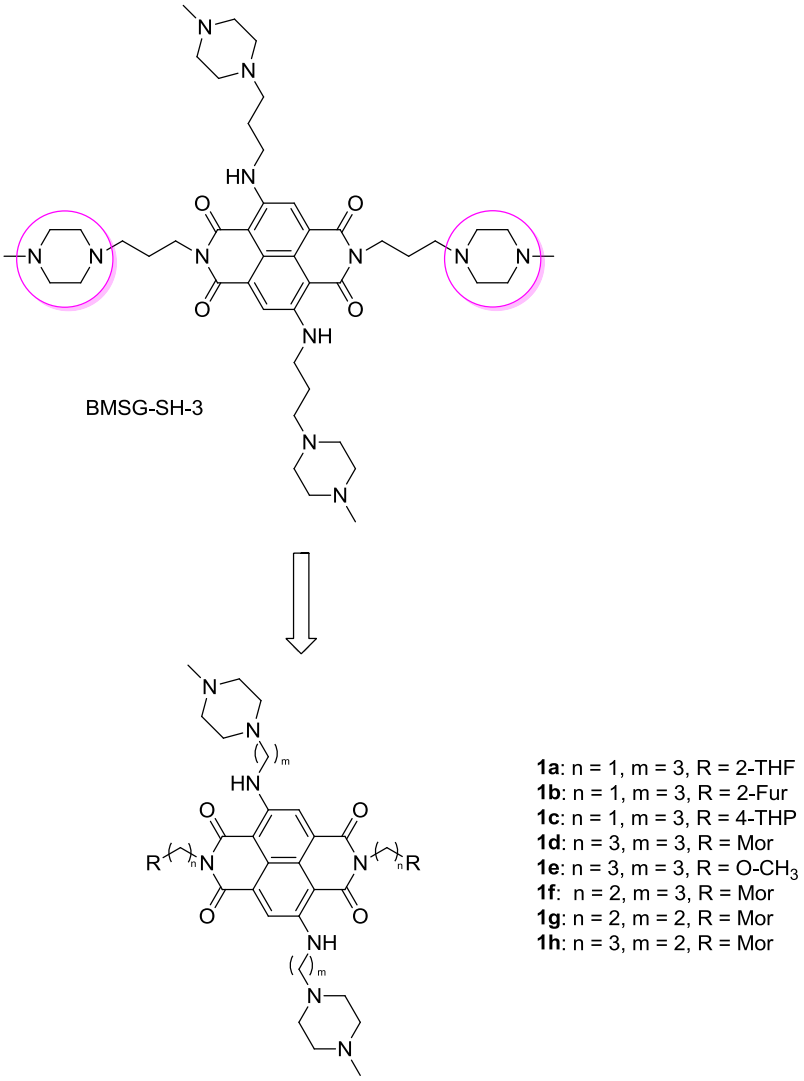

Figure 7.1: Drug Design of compounds **1a-h**

7.2 METHODS

7.2.1 Synthesis

Compounds **1a-h** were synthesized according to Scheme 7.1.

The 2,6-dibromonaphthalene-1,4,5,8-tetracarboxylic dianhydride (**3**) was obtained by reacting Naphthalenetetracarbocylic dianhydride with dibromoisocyanuric acid in sulphuric acid as reported in literature.[330]

The appropriate commercially available amine was condensed with **3** in acetic acid to obtain the disubstituted naphthalene diimide compounds **2a-f**.

Finally, such compounds were treated with 1-(3-Aminopropyl)-4-methylpiperazine or 1-(2-aminoethyl)-4-methylpiperazine in *N*-Methylpyrrolidone (NMP) to obtain the final products **1a-h**.

Scheme 7.1

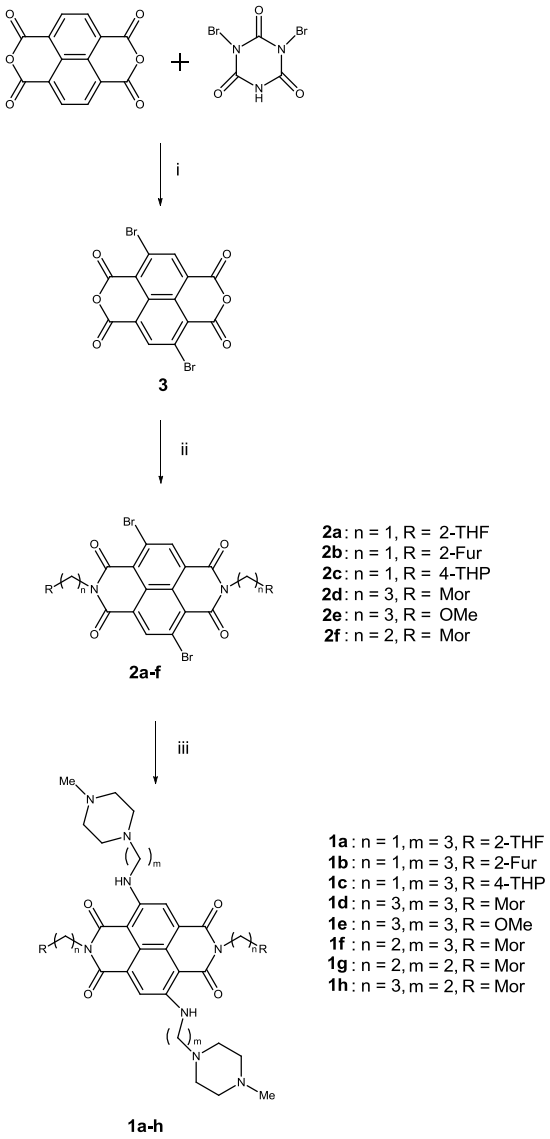

Conditions: i) H_2SO_4, 130 °C, 15h ref; ii) Amine, CH_3COOH, 100 °C, 5h; iii) Amine, NMP, 120 °C, overnight in a sealed tube. (Abbreviations: NMP = 1-Methyl-2-pyrrolidinone, THF = Tetrahydrofuran, Fur = Furan, THP = Tetrahydropyran, Mor = Morpholine).

7.2.2 Biophysical Evaluation

The G-quadruplex binding ability of compounds **1a-h** was assessed by Fluorescence Resonance Energy Transfer (FRET) melting technique. Values are expressed as the melting temperature difference between the nucleotide with drug and the negative control (ΔT_m).

To obtain information about the mode of binding of NDI compounds to G-quadruplex, the crystal structure of **1d** with the human telomeric 22-mer quadruplex sequence d[AGGG(TTAGGG)$_3$] has been carried out. The crystal structure was solved by molecular replacement using the PHASER program, with the native 22-mer telomeric quadruplex crystal structure 1KF1 as a search model. Programs CHIMERA23 and PYMOL24 were used for structure drawing.

7.2.3 Biology

Derivatives were tested for *in vitro* antiproliferative activity in a panel of cancer cell lines. The antiproliferative activity has been evaluated by the Sulforhodamine B short-term cytotoxicity assay (SRB). Values are showed as the concentration required to inhibit cell growth by 50% (IC_{50}).

7.3 RESULTS AND DISCUSSION

Compounds **1a-h** were firstly evaluated for their ability to stabilize G-quadruplex DNA with the high-throughput FRET melting technique. The sequences used for the screening are F21T (telomeric), and promoter region of HSP90A and HSP90B. Tloop is a DNA-duplex sequence used as control. The results in Table 7.1 shows that only compounds with morpholino rings were able to perform a significant telomeric quadruplex stabilization. All of them, produced high T_m changes, comparable to that noted for the lead compound BMSG-SH-3. In particular, compounds **1f** and **1g** composed by two methylene unit and characterized by a morpholino ring, were the most selective for quadruplex over duplex DNA.

None of the other etherocycles or acyclic ether compounds had any effect on quadruplex or duplex stability except compound **1a** and **1e**, which did not interact with F21T sequence, but they showed a large stabilizing effect on HSP90 promoter quadruplex sequences.

Table 7.1. G-quadruplex stabilization of compounds **1a-h** in the FRET melting temperature assay. Values are snown as ΔT_m in °C

Compd	T-loop	htel	HSP90A	HSP90B
1a	0.2	0.2	27.1	21.0
1b	0.3	0.2	0.9	1.1
1c	0.2	0.1	0.7	0.8
1d	4.9	26.6	33.1	28.6
1e	0.0	0.5	29.0	23.8
1f	0.8	27.0	33.9	29.1
1g	1.7	24.7	30.6	27.6
1h	8.1	27.8	31.9	31.1
BMSG-SH-3	1.3	28.3	36.3	32.0

Preliminary biological evaluation has been obtained by the SRB assay (Table 7.2). The cell growth inhibition ability of compounds **1a-h** has been assayed in a panel of cancer cell lines comprising: A549 (lung), RCC4 (renal), MIA-Paca-2 (pancreatic), 786-0 (renal)

and MCF-7 (breast). Among all the tested compounds, **1a** was devoid of activity. However, all the other derivatives without morpholino groups, showed some activity in micromolar range. In particular, compound **1e** showed up to 10-fold selectivity for the renal cancer cell line 786-0.

All the morpholino compounds displayed sub-micromolar activity in at least some of the cancer cell lines used, and the two compounds **1d** and **1h**, with a linker composed by three methylene unit showed an interesting activity against MIA-Paca-2 pancreatic carcinoma and A549 lung adenocarcinoma cell lines at the 10-20 nM level. Indeed, compared with BMSG-SH-3, the selectivity of these compounds *vs* the normal line WI-38 was modest. However, MTD (maximum tolerated dose) and xenograf experiments will be performed to verify whether this low selectivity could be related to the therapeutic window.

Table 7.2. Short term cytotoxicity of compounds **1a-h** in a panel of cancer cell lines (WI-38 is a normal fibroblast line), determined by 96 h SRB assay. Values are shown as IC_{50} in μM.

Cell line	1a	1b	1c	1d	1e	1f	1g	1h	BMSG-SH-3
A549	inactive	2.41±0.01	2.92±0.01	<0.01±0.005	2.54±0.01	1.55±0.02	4.93±0.05	<0.01±0.006	0.11±0.02
RCC4	inactive	3.11±0.06	8.38±0.50	0.56±0.05	10.51±0.14	1.75±0.18	5.10±0.70	0.28±0.06	n/a
MIA-PaCa2	inactive	2.83±0.01	2.50±0.01	0.01±0.01	2.79±0.09	0.04±0.01	n/a	0.01±0.01	0.11±0.02
786-0	inactive	1.10±0.03	1.20±0.03	0.32±0.01	7.17±0.41	0.63±0.06	1.48±0.17	n/a	n/a
MCF-7	inactive	2.61±0.06	3.12±0.13	0.07±0.007	5.62±0.15	0.17±0.01	0.18±0.03	0.03±0.01	0.17±0.03
WI-38	inactive	6.84±0.05	12.65±0.11	0.23±0.01	3.32±0.50	0.61±0.02	1.17±0.11	2.46±0.02	9.0±3.2

To investigate the binding mode of **1d** at G-quadruplex, crystallographic studies have been performed. The co-crystal structure of compound **1d** with the human telomeric sequence d[AGGG(TTAGGG)$_3$] has been obtained (Figure 7.2 A): it is a 2:2 complex in

which the ligand molecule bound at each end of the 5'-5' quadruplex dimer, stacked over the terminal G-quartets. The two aniline substituents are both oriented such they formed intramolecular hydrogen bonds with adjacent carbonyl oxygen atoms, effectively extending the π-π overlap with the G-quartet.

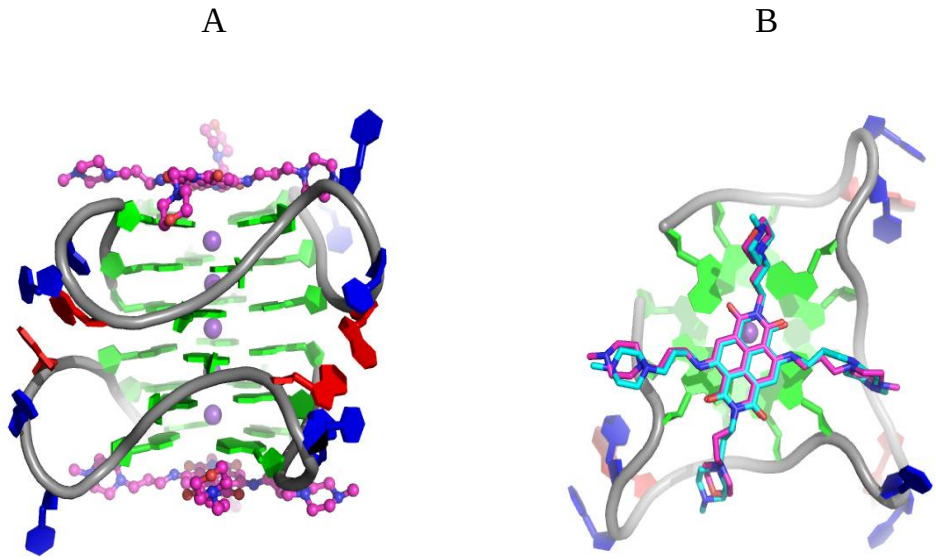

Figure 7.2: Crystal structure of the 2:2 complex between compound **1d** and the telomeric quadruplex. A. The 2:2 stoichiometry and the end-stacking of the bound compound (colored mauve). Potassium ions are shown as small spheres. B. A view projected onto the G-quartet, with compound **1d** superimposed on the previously-determined position of compound BMSG-SH-3.

Figure 7.2 B shows that the chromophore and side-chains of compound **1d** are almost superimposed over the position observed for the lead compound BMSG-SH-3 in its co-crystal structure. This correspondence even extends to the orientation of the end-groups. One nitrogen atom ring of the *N*-methyl-piperazine group (presumably the one that is protonated), is directly hydrogen-bounded to a phosphate oxygen atom (Figure 7.3 A), whereas the morpholino ring close to the adjacent groove did not show direct hydrogen bonds to the quadruplex backbone. For this group, it is evident the hydrogen-bond from the ring to a network of two water molecules and then to a neighboring phosphate group (Figure 7.3 B). Presumably this fact contributes to the stabilization of the side-chain.

A B

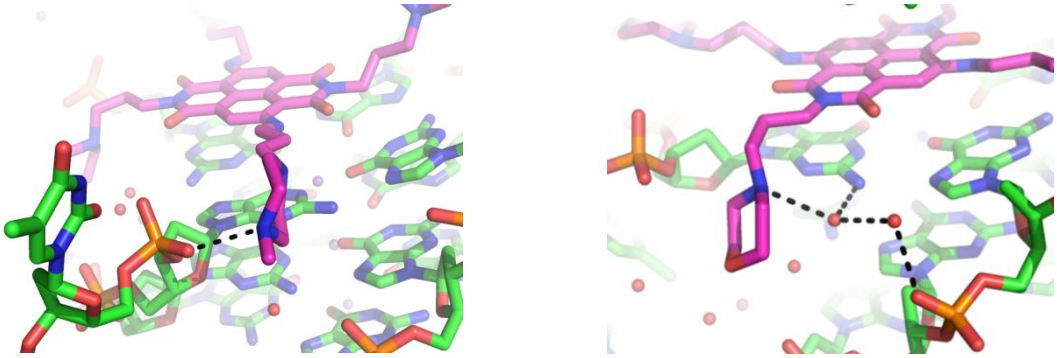

Figure 7.3: A. View of the hydrogen bonding between a N-methyl-piperazine ring nitrogen atom and a phosphate group in a groove. B. View of one morpholino group of compound **1d** bound in the groove, showing hydrogen bonding to two water molecules, which then contact a phosphate group and N2 of a guanine base.

7.4 CONCLUSION

In this work the structure-activity relationships of BMSG-SH-3 have been expanded. In particular, it has been demonstrated that the substitution of two *N*-methyl-piperazine moiety with two morpholino groups led to compounds endowed with high cytotoxic activity, correlated with G-quadruplex stabilization properties. Compounds **1d** and **1h,** bearing morpholino end-groups, were the most potent, showing growth inhibition ability in a panel of cancer cell line, superior to that of the lead compound BMSG-SH-3. In particular, they were the most potent inhibitors of cell growth in Mia-Paca-2 (pancreatic) and A549 (lung) cell lines, where they showed IC_{50} values at the 10-20 nM range. Furthermore, compound **1e** displayed an interesting biological profile characterized by a 10-fold selectivity for 786-0 (renal) cell lines.

Moreover, the morpholino compounds **1d** and **1h**, were able to interact with the G-quadruplex formed in telomeres and HSP90 promoter regions at 1 μM concentration with high ΔT_m values. The ability of **1d** to bind telomeric G-quadruplex has been confirmed by the co-crystal structure of this compound with the human telomeric G-quadruplex. The structure also allowed to elucidate the binding mode of the molecule to this important target.

The lack of quadruplex binding activity shown by the other compounds, strongly suggests that a suitable hydrogen-bonding ability is a minimal requirement for all four end-groups contained in these NDI derivatives.

Compounds **1d** and **1h** will be further investigated to better clarify their activity towards telomerase, and their mechanism(s) of action. Compound **1d** is currently being evaluated in a xenograft model of pancreatic cancer, which is very difficult to combat.

7.5 EXPERIMENTAL SECTION

7.5.1 Chemistry

All chemicals, reagents and solvents were purchased from Sigma-Aldrich, Alfa Aesar, Lancaster Synthesis and Fluorochem (UK) and used without further purification. Solvents were supplied by VWR and Fisher scientific. Column chromatography was performed using BDH silica gel (BDH 153325P). HPLC analysis was carried out with a Gilson apparatus combining a 322 PUMP and an Agilent 1100 SERIES detector, using a C18 5μ (100 x 4.6 mm) column (41622271 (W), YMC, Japan), at a flow of 1 mL/min. Preparative HPLC was carried out with a Gilson apparatus combining a 322 PUMP and a UV/VIS-155 detector with detection at 280 nm, using a C18 5μ (100 x 20 mm) column (201022272) (W), YMC, Japan, at a flow of 20 mL/min. Water and methanol with 0.1 % formic acid were used as solvents for HPLC. For the purification of compounds **1d**, **1f-h**, the following method was used: 100 % aqueous for 5 min after injection, gradually decreased to 60 % aqueous over 25 min. For compounds **1a-c** and **1e**, the following method was used: 100% aqueous for 2 min after injection, gradually decreased to 20% aqueous over 17 minutes. For the HPLC purity analysis of compounds **1a-h**, the method used was: 100 % aqueous for 5 min after injection, to 60 % aqueous over 18 min as well as 100 % aqueous for 5 min after injection, to 60 % aqueous over 43 min. Purity for final compounds was greater than 95% (HPLC, 280 nm). NMR spectra were recorded at 400 MHz (^{1}H NMR) or 500 MHz (^{13}C NMR) on a Bruker spectrometer. NMR spectra were analyzed with MestReC 4.5.6.0 with chemical shifts using TMS as a standard (δ = 0 ppm). NMR multiplicity abbreviations are s (singlet), bs (broad singlet), d (doublet), t (triplet), q (quartet), 5q (quintet), and m (multiplet). Coupling constants J are reported as observed in Hertz (Hz). High Resolution Mass spectra (HRMS) were measured on a Micromass Q-TTOF Ultima Global tandem mass spectrometer run under electrospray ionisation (ESI), and processed using the MassLab 3.2 software. For compounds **2a-f** no ^{13}C NMRs were obtained due to solubility issues.

Compound **3** was prepared according to literature procedures.[330] Analytical data and ^{1}H and ^{13}C NMR spectra matched literature values.

General Procedure for the Synthesis of compounds 2a-f. 2,6-dibromonaphthalene-1,4,5,8-tetracarboxylic dianhydride (**3**) (0.47 mmol) and the suitable amine (1.9 mmol) were suspended in acetic acid (14 ml) and refluxed for 5 h. After having been cooled to room temperature the precipitate was filtered and washed with water (50 mL) to give the title compound.

4,9-dibromo-2,7-bis((tetrahydrofuran-2-yl)methyl)benzo[lmn][3,8]phenanthroline-1,3,6,8(2H,7H)-tetraone (2a): from tetrahydrofurfurylamine as starting material; orange semi-solid (0.077 g, 28% yield). ^{1}H NMR (400 MHz, $CDCl_3$, TMS): δ 8.76 (s, 2H), 4.51-4.39 (m, 4H), 4.13-4.09 (m, 2H), 3.99-3.93 (m, 2H), 3.79-3.73 (m, 2H), 2.15-2.03 (m, 4H), 1.99-1.88 (m, 2H), 1.80-1.71 (m, 2H).

4,9-dibromo-2,7-bis(furan-2-ylmethyl)benzo[lmn][3,8]phenanthroline-1,3,6,8(2H,7H)-tetraone (2b): from furfurylamine as starting material; orange semi-solid (0.160 g, 39% yield). ^{1}H NMR (400 MHz, DMSO, TMS): δ 8.80-8.73 (m, 2H), 7.58-7.57 (m, 2H), 6.46-6.40 (m, 4H), 5.28-5.26 (m, 4H).

4,**9-dibromo-2,7-bis((tetrahydro-2H-pyran-4-yl)methyl)benzo[lmn][3,8]phenanthroline-1,3,6,8(2H,7H)-tetraone (2c):** from 4-(aminomethyl)tetrahydropyran (0.2 g, 2.1 mmol) as starting material; orange semi-solid (0.1 g, 23% yield). The compound was used without further purification. No analytical data provided for this compound due to solubility issues.

4,9-dibromo-2,7-bis(3-morpholinopropyl)benzo[lmn][3,8]phenanthroline-1,3,6,8(2H,7H)-tetraone (2d): from 3-morpholinopropylamine as starting material; orange semi-solid (0.15 g, 32% yield). ^{1}H NMR (400 MHz, $CDCl_3$, TMS): δ 8.99-8.76 (m, 2H), 4.33-4.28 (m, 4H), 3.54-3.52 (m, 8H), 2.53-2.50 (m, 4H), 2.45-2.37 (m, 8H), 2.00-1.92 (m, 4H).

4,9-dibromo-2,7-bis(3-methoxypropyl)benzo[lmn][3,8]phenanthroline-1,3,6,8(2H,7H)-tetraone (2e): from 3-methoxypropylamine as starting material; orange semi-solid (0.1 g, 25% yield). ^{1}H NMR (400 MHz, $CDCl_3$, TMS): δ 8.99 (s, 2H), 4.36-4.30 (m, 4H), 3.55-3.51 (m, 4H), 3.31-3.28 (m, 6H), 2.06-2.00 (m, 4H).

4,9-dibromo-2,7-bis(2-morpholinoethyl)benzo[lmn][3,8]phenanthroline-1,3,6,8(2H,7H)-tetraone (2f): from 4-(2-aminoethyl)morpholine as starting material; orange semi-solid (0.2 g, 14% yield). ^{1}H NMR (400 MHz, $CDCl_3$, TMS): δ 8.99 (s,1H),

8.76 (s, 1H), 4.37 (t, 4H, J=6.4 Hz), 3.66-3.64 (m, 8H), 2.74-2.70 (m, 4H), 2.58-2.53 (m, 8H).

General Procedure for the Synthesis of compounds 1a-h. The appropriate disubstituted naphthalene diimied (**2a-h)** (0.067 mmol), 1-(3-Aminopropyl)-4-methylpiperazine or 1-(2-aminoethyl)-4-methylpiperazine (0.3 mmol), and NMP (0.5 mL) were suspended in a microwave reaction vessel. The tube was flushed with argon, sealed and heated overnight (120 °C). After having been cooled to room temperature, the solvent was concentrated *in vacuo* and the crude mixture was purified by preparative HPLC to obtain the title compound.

4,9-bis((3-(4-methylpiperazin-1-yl)propyl)amino)-2,7-bis((tetrahydrofuran-2-yl)methyl) benzo[lmn] [3,8]phenanthroline-1,3,6,8(2H,7H)-tetraone (1a): from **2a** as starting material; blue semi-solid (0.02 g, 40% yield). ^{1}H NMR (400 MHz, $CDCl_3$, TMS): δ 9.49-9.43 (m, 2H), 8.18 (s, 2H), 4.46-4.41 (m, 2H), 4.37-4.33 (m, 2H), 4.16-4.07 (m, 2H), 3.98-3.93 (m, 2H), 3.77-3.71 (m, 2H), 3.59-3.57 (m, 4H), 2.96-2.82 (m, 8H), 2.78-2.65 (m, 8H), 2.60-2.56 (m, 10H), 2.11-2.00 (m, 4H), 1.98-1.88 (m, 8H). ^{13}C NMR (100 MHz, $CDCl_3$, TMS): δ 166.2, 163.3, 149.2, 125.8, 121.3, 118.6, 101.9, 76.4, 67.9, 55.4, 54.3, 51.7, 44.8, 43.7, 41.4, 29.6, 26.4, 25.3. HRMS (ES^+) calculated for $(M+2H)^{2+}$ $C_{40}H_{56}N_8O_6$ 746.4480, found 746.4450.

2,7-bis(furan-2-ylmethyl)-4,9-bis((3-(4-methylpiperazin-1-yl)propyl)amino)benzo[lmn][3,8] phenanthroline-1,3,6,8(2H,7H)-tetraone (1b): from **2b** as starting material; blue semi-solid (0.03 g, 16% yield). ^{1}H NMR (400 MHz, $CDCl_3$, TMS): δ 9.45 (t, 2H, J=5.4 Hz), 8.19 (s, 2H), 7.32-7.31 (m, 2H), 6.39-6.38 (m, 2H), 6.32-6.31 (m, 2H), 5.36 (s, 4H), 3.59 (q, 4H, J=6 Hz), 3.04 (bs, 8H), 2.73 (bs, 8H), 2.59-2.56 (m, 10H), 1.93 (5q, 4H, J=6.4 Hz, 6 Hz). ^{13}C NMR (100 MHz, $CDCl_3$, TMS): δ 165.5, 162.7, 150.2, 149.2, 142.0, 125.7, 121.2, 118.7, 110.6, 109.0, 101.8, 55.2, 53.3, 50.9, 43.8, 41.4, 36.3, 26.2. HRMS (ES^+) calculated for $(M+H)^+$ $C_{40}H_{48}N_8O_6$ 737.3775, found 737.3742.

4,9-bis((3-(4-methylpiperazin-1-yl)propyl)amino)-2,7-bis((tetrahydro-2H-pyran-4-yl)methyl)benzo [lmn][3,8]phenanthroline-1,3,6,8(2H,7H)-tetraone (1c): from **2c** as starting material; blue semi-solid (0.025 g, 20% yield). ^{1}H NMR (400 MHz, $CDCl_3$, TMS): δ 9.41 (t, 2H, J=5.4 Hz), 8.18 (s, 2H), 4.14 (d, 4H, J=7.2 Hz), 3.99-3.96 (m, 4H), 3.59 (q, 4H, J=6.4 Hz, 6 Hz), 3.38-3.32 (m, 4H), 2.54-2.50 (m, 16H), 2.30 (s, 6H), 2.20-2.10 (m,

2H), 1.97 (5q, 4H, J=6.8 Hz, 7.2 Hz), 1.66-1.48 (m, 12H). ^{13}C NMR (100 MHz, $CDCl_3$, TMS): δ 166.4, 163.4, 149.3, 125.7, 121.2, 118.6, 101.8, 67.7, 55.8, 55.1, 53.3, 46.1, 45.4, 41.4, 34.4, 30.9, 26.7. HRMS (ES^+) calculated for $(M+2H)^{2+}$ $C_{42}H_{60}N_8O_6$ 774.4792, found 774.4806.

4,9-bis((3-(4-methylpiperazin-1-yl)propyl)amino)-2,7-bis(3-morpholinopropyl) benzo[lmn][3,8] phenanthroline-1,3,6,8(2H,7H)-tetraone (1d): from **2d** as starting material; blue semi-solid (0.015 g, 12% yield). ^{1}H NMR (400 MHz, $CDCl_3$, TMS): δ 9.38 (t, 2H, J=5.4 Hz), 8.12 (s, 2H), 4.24 (t, 4H, J=6.8 Hz), 3.61 (t, 8H, J=4.4 Hz), 3.57 (q, 4H, J=6.8 Hz, 6.4 Hz), 2.53-2.44 (m, 30H), 2.30 (s, 6H), 1.99-1.88 (m, 8H). ^{13}C NMR (100 MHz, $CDCl_3$, TMS): δ 166.1, 163.1, 149.1, 125.7, 121.1, 118.3, 101.9, 67.0, 56.5, 55.8, 55.0, 53.6, 53.2, 46.0, 41.3, 38.8, 26.7, 24.7. HRMS (ES^+) calculated for $(M+H)^+$ $C_{44}H_{66}N_{10}O_6$ 831.5245, found 831.5242.

2,7-bis(3-methoxypropyl)-4,9-bis((3-(4-methylpiperazin-1-yl)propyl)amino)benzo[lmn][3,8] phenanthroline-1,3,6,8(2H,7H)-tetraone (1e): from **2e** as starting material; blue semi-solid (0.018 g, 27% yield). ^{1}H NMR (500 MHz, $CDCl_3$, TMS): δ 9.37 (t, 2H, J=5.4 Hz), 8.06 (s, 2H), 4.24 (t, 4H, J=7 Hz), 3.55-3.49 (m, 8H), 3.33 (s, 6H), 2.77-2.51 (m, 20H), 2.34 (s, 6H), 2.00-1.92 (m, 8H). ^{13}C NMR (125 MHz, $CDCl_3$, TMS): δ 165.9, 162.9, 149.0, 125.5, 121.0, 118.2, 101.7, 70.6, 58.6, 55.7, 54.6, 52.7, 45.5, 41.4, 37.9, 28.2, 26.6. HRMS (ES^+) calculated for $(M+H)^+$ $C_{38}H_{56}N_8O_6$ 721.4401, found 721.4437.

4,9-bis((3-(4-methylpiperazin-1-yl)propyl)amino)-2,7-bis(2-morpholinoethyl) benzo[lmn][3,8] phenanthroline-1,3,6,8(2H,7H)-tetraone (1f): from **2f** as starting material; blue semi-solid (0.018 g, 15% yield). ^{1}H NMR (400 MHz, $CDCl_3$, TMS): δ 9.36 (t, 2H, J=5.4 Hz), 8.14 (s, 2H), 4.45 (t, 4H, J=6.8 Hz), 3.84-3.82 (m, 8H), 3.64 (q, 4H, J=6.4 Hz, 5.6 Hz), 3.24 (bs, 8H), 3.03-2.84 (m, 20H), 2.75 (s, 6H), 2.73-2.69 (m, 4H), 2.00 (5q, 4H, J=6.8 Hz, 6.4 Hz). ^{13}C NMR (100 MHz, $CDCl_3$, TMS): δ 166.0, 163.1, 149.2, 125.7, 121.2, 118.4, 101.9, 65.4, 55.4, 54.6, 52.9 (x2C), 50.0, 43.3, 40.9, 35.7, 25.9. HRMS (ES^+) calculated for $(M+H)^+$ $C_{42}H_{62}N_{10}O_6$ 803.4932, found 803.4963.

4,9-bis((2-(4-methylpiperazin-1-yl)ethyl)amino)-2,7-bis(2-morpholinoethyl)benzo[lmn][3,8] phenanthroline-1,3,6,8(2H,7H)-tetraone (1g): from **2f** as starting material; blue semi-solid (0.020 g, 17% yield). ^{1}H NMR (400 MHz, $CDCl_3$,

TMS): δ 9.59-9.56 (m, 2H), 8.19 (s, 2H), 4.41 (t, 4H, J=6.4 Hz), 3.77-3.62 (m, 12H), 3.13 (bs, 8H), 2.91-2.66 (m, 30H). ^{13}C NMR (100 MHz, $CDCl_3$, TMS): δ 165.9, 163.0, 148.9, 125.8, 121.4, 118.7, 102.3, 66.6, 55.9, 55.9, 53.7, 53.6, 50.2, 43.7, 40.2, 36.8. HRMS (ES^+) calculated for $(M+2H)^{2+}$ $C_{40}H_{58}N_{10}O_6$ 776.4698, found 776.4660.

4,9-bis((2-(4-methylpiperazin-1-yl)ethyl)amino)-2,7-bis(3-morpholinopropyl) benzo [lmn][3,8] phenanthroline-1,3,6,8(2H,7H)-tetraone (1h): from **2d** as starting material; blue semi-solid (0.025 g, 7% yield). ^{1}H NMR (500 MHz, $CDCl_3$, TMS): δ 9.49-9.47 (m, 2H), 8.09 (s, 2H), 4.17-4.20 (m, 10H), 3.66 (t, 6H, J=4 Hz), 3.55 (q, 4H, J=5.5 Hz, 5.5 Hz), 3.02 (bs, 6H), 2.81-2.78 (m, 10H), 2.62-2.59 (m, 16H), 1.98-1.92 (m, 4H). ^{13}C NMR (125 MHz, $CDCl_3$, TMS): δ 166.0, 163.1, 148.9, 125.8, 121.3, 118.7, 102.3, 66.1, 56.0, 55.9, 53.6, 53.0, 50.3, 43.6, 40.1, 38.44, 24.1. HRMS (ES^+) calculated for $(M+H)^+$ $C_{42}H_{62}N_{10}O_6$ 803.4932, found 803.4952.

7.5.2 Biophysical Evaluation

7.5.2.1 Fluorescence Resonance Energy Transfer (FRET)

The following oligonucleotide sequences, all purchased from Eurogentec, were used: F21T: (5'-FAM-GGG TTA GGG TTA GGG TTA GGG-TAMRA-3'), HSP90a: (5'-FAM-GGG-CCA AAG GGA AGG GGT GGG-TAMRA-3'), HSP90b: (5'-FAM-GGGCGG GCC AAA GGG AAG GGG-TAMRA-3'), T-Loop: (5'-FAM-TAT AGC TATA TTT TTT TATA GCT ATA-TAMRA-3'). TAMRA (6-carboxytetramethylrhodamine) is the acceptor fluorophore, and FAM (6-carboxyfluorescein) is the donor fluorophore. From 50 μM stock solutions, 400 nM solutions in FRET buffer (60 mM potassium cacodylate pH 7.4) were prepared. The nucleotides were annealed by heating the samples to 90 °C for 10 min and allowing them to cool down to RT within 4 h. 10 mM solutions of the compounds in deionised water were prepared and diluted to double of the required concentrations with FRET buffer. In RT-PCR 96 well plates (MJ Research, Waltham, MA), each well was loaded with 50 μL of nucleotide solution and 50 μL of drug solution. Drug concentrations of 0.1, 0.2, 0.5, 1, 2, 5 and 10 μM were used, and every drug concentration was repeated 3 times. Measurements were made on a DNA Engine Opticon (MJ Research) with excitation at 450 – 495 nm and detection at 515 – 545 nm. The flourescence was read at intervals of

0.5 °C over the range 30 – 100 °C. Before each reading the temperature was held constant for 30 s. The raw data were processed using Origin (Version 7.0, OriginLab Corp.). The graphs were smoothed using a 10-point running average and normalized. The melting temperatures were obtained by determining the maxima of the first derivative of the smooth melting curves. The value ΔT is the melting temperature difference between the nucleotide with drug and the negative control.

7.5.2.2 Crystallography

The DNA G-quadruplex forming sequence d(AGGG[TTAGGG]$_3$) was initially dissolved in water to a final concentration of 2.5 mM single-stranded DNA (ssDNA). Buffer and salts were then added to the DNA to final concentrations of 2 mM ssDNA, 50 mM potassium chloride and 20 mM potassium cacodylate (pH 6.5). The buffered DNA was then annealed, which involved heating the sample to 85^{o}C in a heat block for 5 minutes followed by slow cooling to room temperature overnight. A stock solution of compound in water was mixed separately with the DNA 22-mer at equimolar ratios, and crystals grown in standard hanging drops. Crystals of the **1d**-DNA complex were grown at 12^{o}C in a drop containing 20 % PEG400, 100 mM lithium sulfate and 50 mM sodium cacodylate (pH 6.5). Crystals were flash-frozen in liquid nitrogen and data collected at the Diamond Light Source synchrotron. All datasets were processed and scaled using the XDS, SCALA and XIA2 programs.[331] The crystal structure was solved by molecular replacement using the PHASER program. .Model building and refinement were performed using the COOT and REFMAC5[332] programs. Initial $2F_o$-F_c maps showed clear electron density for the core G-quartets and potassium ions, as well as residual density for the loops and other regions omitted from the initial search model. A large region of electron density was visible in both F_o-F_c and $2F_o$-F_c maps above the 3' G-quartet, into which the naphthalene compound could be readily fitted. The structure was refined to a resolution of 2.3 Å, with final R_{work} and R_{free} values of 25.8 % and 28.8 % respectively. Programs CHIMERA[333] and PYMOL[334] were used for structure drawing.

7.5.3 Biology

7.5.3.1 Cell Culture

The cell lines MCF7, A549, MIA-Paca-2 (European Collection of Cell Cultures), WI38 (American Type Culture Collection), and RCC4 (HPA Culture Collection, UK) were maintained in monolayer culture in 75 cm^2 flasks (TPP, Switzerland) under a humidified 5 % CO_2 atmosphere at 37°C. For the cell lines MCF7 and A549, the medium Dulbecco's MEM (GIBCO 21969, Invitrogen, UK) supplemented with L-glutamine (2 mM, GIBCO 25030, Invitrogen, UK), essential amino acids (1 %, GIBCO 11140, Invitrogen, UK), and foetal calf serum (10 %, S1810, Biosera, UK) was used. For MIA-Pa-Ca-2 and RCC4, Dulbecco's MEM, supplemented with L-glutamine (2 mM) and foetal calf serum (10 %) was used. The medium MEM (M2279, Sigma, UK) with added L-glutamine (2 mM), essential amino acids (1 %) and foetal calf serum (10 %) was used for the cell line WI38. The medium RPMI 1640 (GIBCO 31870, Invitrogen, UK) with L-glutamine (2 mM) and 15 % foetal calf serum was used for the cell line 786-0. To passage the cells, they were washed with PBS (GIBCO 14040, Invitrogen, UK), treated with trypsine (GIBCO 25300, Invitrogen, UK), and re-seeded into fresh medium, resulting in an initial cell density of approximately 1x104 cells/mL medium. Cells were counted using a Neubauer haemocytometer (Assistant, Germany) by microscopy or a MacsQuant flow cytometer (Miltenyi Biotech, Germany) on a suspension of cells obtained by washing with PBS, trypsinisation, centrifugation at 8 °C at 8000 rpm for 3 minutes, and re-suspension in fresh medium.

7.5.3.2 Sulforhodamine B (SRB) short-term cytotoxicity assay

The cells were counted and diluted to the required concentration in 20 mL medium. For the cell lines A549, and MIA-Pa-Ca-2, 2000 cells with 160 µL media were seeded into each well of a 96 well plate (Nunc, Denmark). For WI38, 6000 cells per well, and for RCC4, MCF7 and 786-0, 4000 cells per well were used due to their higher doubling time. After incubation for 24 hours, the compounds to be tested, dissolved in 40 µL of medium, were added at different concentrations, and the cells incubated for 96 hours. The medium was then removed and the cells fixed by incubation with TCA (10 %, Sigma-Aldrich, UK)

in water for 30 min. After removal of the TCA, the cells were washed with deionised water 5 times and dried at 60 °C for 1 h. Cells were then incubated with SRB (80 µL, 0.4 % in 1 % acetic acid, Acros Organics, UK) for 15 min at RT. The SRB was removed, the wells washed with 1 % acetic acid (200 µL), and dried at 60 °C for 1 h. Tris-base (100 µL, 10 mM, Acros Organics, UK) solution was added to each well, and the plates were gently shaken for 5 min. The absorbance at 540 nm was measured with a plate reader (Spectrostar Omega, BMG Labtech, Germany). The data were normalised to the value of 100 for the control experiment (untreated cells), and the IC_{50} values were obtained by interpolation from a plot done with Origin (Version 7.0, OriginLab Corp.), as the concentration leading to an absorbance intensity of 50 %.

Bibliography

1. National Cancer Institute
2. World Health Organization
3. Avendaño, C.; Menéndez, J.C., Medicinal Chemistry of Anticancer Drugs, Elsevier Science.
4. Gottesman, M. M.; Fojo, T.; Bates, S. E., Multidrug resistance in cancer: role of ATP-dependent transporters. *Nature reviews. Cancer* **2002,** *2* (1), 48-58.
5. Engel, J. B.; Schally, A. V.; Dietl, J.; Rieger, L.; Honig, A., Targeted therapy of breast and gynecological cancers with cytotoxic analogues of peptide hormones. *Molecular pharmaceutics* **2007,** *4* (5), 652-8.
6. Wang, M. H.; Padhye, S. S.; Guin, S.; Ma, Q.; Zhou, Y. Q., Potential therapeutics specific to c-MET/RON receptor tyrosine kinases for molecular targeting in cancer therapy. *Acta pharmacologica Sinica* **2010,** *31* (9), 1181-8.
7. Saijo, N., Progress in cancer chemotherapy with special stress on molecular-targeted therapy. *Japanese journal of clinical oncology* **2010,** *40* (9), 855-62.
8. Jordan, V. C., Tamoxifen: catalyst for the change to targeted therapy. *Eur J Cancer* **2008,** *44* (1), 30-8.
9. Sanchez-Munoz, A.; Perez-Ruiz, E.; Jimenez, B.; Ribelles, N.; Marquez, A.; Garcia-Rios, I.; Alba Conejo, E., Targeted therapy of metastatic breast cancer. *Clinical & translational oncology : official publication of the Federation of Spanish Oncology Societies and of the National Cancer Institute of Mexico* **2009,** *11* (10), 643-50.
10. Weinstein, I. B.; Joe, A., Oncogene addiction. *Cancer research* **2008,** *68* (9), 3077-80; discussion 3080.
11. Friday, B. B.; Adjei, A. A., K-ras as a target for cancer therapy. *Biochimica et biophysica acta* **2005,** *1756* (2), 127-44.
12. Croce, C. M., Oncogenes and cancer. *The New England journal of medicine* **2008,** *358* (5), 502-11.
13. Gonzalez, V.; Hurley, L. H., The c-MYC NHE III(1): function and regulation. *Annual review of pharmacology and toxicology* **2010,** *50*, 111-29.
14. Lennartsson, J.; Jelacic, T.; Linnekin, D.; Shivakrupa, R., Normal and oncogenic forms of the receptor tyrosine kinase kit. *Stem Cells* **2005,** *23* (1), 16-43.
15. Workman, P.; Burrows, F.; Neckers, L.; Rosen, N., Drugging the cancer chaperone HSP90: combinatorial therapeutic exploitation of oncogene addiction and tumor stress. *Annals of the New York Academy of Sciences* **2007,** *1113*, 202-16.
16. O'Boyle, N. M.; Meegan, M. J., Designed Multiple Ligands for Cancer Therapy. *Current medicinal chemistry* **2011**.
17. Roth, B. L.; Sheffler, D. J.; Kroeze, W. K., Magic shotguns versus magic bullets: selectively non-selective drugs for mood disorders and schizophrenia. *Nature reviews. Drug discovery* **2004,** *3* (4), 353-9.
18. Cavalli, A.; Bolognesi, M. L.; Minarini, A.; Rosini, M.; Tumiatti, V.; Recanatini, M.; Melchiorre, C., Multi-target-directed ligands to combat neurodegenerative diseases. *Journal of medicinal chemistry* **2008,** *51* (3), 347-72.
19. Tumiatti, V.; Milelli, A.; Minarini, A.; Micco, M.; Gasperi Campani, A.; Roncuzzi, L.; Baiocchi, D.; Marinello, J.; Capranico, G.; Zini, M.; Stefanelli, C.; Melchiorre, C., Design, synthesis, and biological evaluation of substituted naphthalene imides and diimides as anticancer agent. *Journal of medicinal chemistry* **2009,** *52* (23), 7873-7.
20. Knox, A. J.; Price, T.; Pawlak, M.; Golfis, G.; Flood, C. T.; Fayne, D.; Williams, D. C.; Meegan, M. J.; Lloyd, D. G., Integration of ligand and structure-based virtual screening for the identification of the first dual targeting agent for heat shock protein 90 (Hsp90) and tubulin. *Journal of medicinal chemistry* **2009,** *52* (8), 2177-80.
21. Zhang, Y. M.; Cockerill, S.; Guntrip, S. B.; Rusnak, D.; Smith, K.; Vanderwall, D.; Wood, E.; Lackey, K., Synthesis and SAR of potent EGFR/erbB2 dual inhibitors. *Bioorganic & medicinal chemistry letters* **2004,** *14* (1), 111-4.

22. Karaman, M. W.; Herrgard, S.; Treiber, D. K.; Gallant, P.; Atteridge, C. E.; Campbell, B. T.; Chan, K. W.; Ciceri, P.; Davis, M. I.; Edeen, P. T.; Faraoni, R.; Floyd, M.; Hunt, J. P.; Lockhart, D. J.; Milanov, Z. V.; Morrison, M. J.; Pallares, G.; Patel, H. K.; Pritchard, S.; Wodicka, L. M.; Zarrinkar, P. P., A quantitative analysis of kinase inhibitor selectivity. *Nature biotechnology* **2008,** *26* (1), 127-32.
23. Tang, Y.; Hamed, H.; Cruichshanks, N.; Fisher, P. B.; Grant, S.; Dent, P., Obatoclax and Lapatinib Interact to Induce Toxic Autophagy Through NOXA. *Molecular pharmacology* **2012**.
24. Hurley, L. H., DNA and its associated processes as targets for cancer therapy. *Nature reviews. Cancer* **2002,** *2* (3), 188-200.
25. Balasubramanian, S.; Hurley, L. H.; Neidle, S., Targeting G-quadruplexes in gene promoters: a novel anticancer strategy? *Nature reviews. Drug discovery* **2011,** *10* (4), 261-75.
26. sandwalk.blogspot.com/2007/07/ethidium-bromide-binds-to-dna.html
27. Martinez, R.; Chacon-Garcia, L., The search of DNA-intercalators as antitumoral drugs: what it worked and what did not work. *Current medicinal chemistry* **2005,** *12* (2), 127-51.
28. Brana, M. F.; Cacho, M.; Gradillas, A.; de Pascual-Teresa, B.; Ramos, A., Intercalators as anticancer drugs. *Current pharmaceutical design* **2001,** *7* (17), 1745-80.
29. Braña, M.F.; Beralanga, J.M.C.; Roldan, C.M. DE PATENT 2, 318, 136, 1973
30. Feigon, J.; Denny, W. A.; Leupin, W.; Kearns, D. R., Interactions of antitumor drugs with natural DNA: 1H NMR study of binding mode and kinetics. *Journal of medicinal chemistry* **1984,** *27* (4), 450-65.
31. Rosell, R.; Carles, J.; Abad, A.; Ribelles, N.; Barnadas, A.; Benavides, A.; Martin, M., Phase I study of mitonafide in 120 hour continuous infusion in non-small cell lung cancer. *Investigational new drugs* **1992,** *10* (3), 171-5.
32. Malviya, V. K.; Liu, P. Y.; Alberts, D. S.; Surwit, E. A.; Craig, J. B.; Hannigan, E. V., Evaluation of amonafide in cervical cancer, phase II. A SWOG study. *American journal of clinical oncology* **1992,** *15* (1), 41-4.
33. Hsiang, Y. H.; Jiang, J. B.; Liu, L. F., Topoisomerase II-mediated DNA cleavage by amonafide and its structural analogs. *Molecular pharmacology* **1989,** *36* (3), 371-6.
34. Innocenti, F.; Iyer, L.; Ratain, M. J., Pharmacogenetics of anticancer agents: lessons from amonafide and irinotecan. *Drug metabolism and disposition: the biological fate of chemicals* **2001,** *29* (4 Pt 2), 596-600.
35. Brana, M. F.; Castellano, J. M.; Moran, M.; Emling, F.; Kluge, M.; Schlick, E.; Klebe, G.; Walker, N., Synthesis, structure and antitumor activity of new benz[d,e]isoquinoline-1,3-diones. *Arzneimittel-Forschung* **1995,** *45* (12), 1311-8.
36. Zee-Cheng, R. K.; Cheng, C. C., N-(Aminoalkyl)imide antineoplastic agents. Synthesis and biological activity. *Journal of medicinal chemistry* **1985,** *28* (9), 1216-22.
37. Sami, S. M.; Dorr, R. T.; Alberts, D. S.; Remers, W. A., 2-substituted 1,2-dihydro-3H-dibenz[de,h]isoquinoline-1,3-diones. A new class of antitumor agent. *Journal of medicinal chemistry* **1993,** *36* (6), 765-70.
38. Sami, S. M.; Dorr, R. T.; Alberts, D. S.; Solyom, A. M.; Remers, W. A., Analogues of amonafide and azonafide with novel ring systems. *Journal of medicinal chemistry* **2000,** *43* (16), 3067-73.
39. Brana, M. F.; Cacho, M.; Ramos, A.; Dominguez, M. T.; Pozuelo, J. M.; Abradelo, C.; Rey-Stolle, M. F.; Yuste, M.; Carrasco, C.; Bailly, C., Synthesis, biological evaluation and DNA binding properties of novel mono and bisnaphthalimides. *Organic & biomolecular chemistry* **2003,** *1* (4), 648-54.
40. Brana, M. F.; Cacho, M.; Garcia, M. A.; de Pascual-Teresa, B.; Ramos, A.; Dominguez, M. T.; Pozuelo, J. M.; Abradelo, C.; Rey-Stolle, M. F.; Yuste, M.; Banez-Coronel, M.; Lacal, J. C., New analogues of amonafide and elinafide, containing aromatic heterocycles: synthesis, antitumor activity, molecular modeling, and DNA binding properties. *Journal of medicinal chemistry* **2004,** *47* (6), 1391-9.
41. Li, Z.; Yang, Q.; Qian, X., Novel thiazonaphthalimides as efficient antitumor and DNA photocleaving agents: effects of intercalation, side chains, and substituent groups. *Bioorganic & medicinal chemistry* **2005,** *13* (16), 4864-70.
42. Brana, M. F.; Castellano, J. M.; Moran, M.; Perez de Vega, M. J.; Romerdahl, C. R.; Qian, X. D.; Bousquet, P.; Emling, F.; Schlick, E.; Keilhauer, G., Bis-naphthalimides: a new class of antitumor agents. *Anti-cancer drug design* **1993,** *8* (4), 257-68.
43. Brana, M. F.; Castellano, J. M.; Moran, M.; Perez de Vega, M. J.; Perron, D.; Conlon, D.; Bousquet, P. F.; Romerdahl, C. A.; Robinson, S. P., Bis-naphthalimides 3: synthesis and antitumor

activity of N,N'-bis[2-(1,8-naphthalimido)-ethyl] alkanediamines. *Anti-cancer drug design* **1996,** *11* (4), 297-309.
44. Gallego, J.; Reid, B. R., Solution structure and dynamics of a complex between DNA and the antitumor bisnaphthalimide LU-79553: intercalated ring flipping on the millisecond time scale. *Biochemistry* **1999,** *38* (46), 15104-15.
45. Patten, A. D.; Sun, J. H.; Ardecky, R. J. U.S. Patent 5,086,059, 1992
46. Nitiss, J. L.; Zhou, J.; Rose, A.; Hsiung, Y.; Gale, K. C.; Osheroff, N., The bis(naphthalimide) DMP-840 causes cytotoxicity by its action against eukaryotic topoisomerase II. *Biochemistry* **1998,** *37* (9), 3078-85.
47. Liu, Z. R.; Hecker, K. H.; Rill, R. L., Selective DNA binding of (N-alkylamine)-substituted naphthalene imides and diimides to G+C-rich DNA. *Journal of biomolecular structure & dynamics* **1996,** *14* (3), 331-9.
48. Verdun, R. E.; Karlseder, J., Replication and protection of telomeres. *Nature* **2007,** *447* (7147), 924-31.
49. Mueller, H. J., The remaking of chromosomes. Collecting Net. 1938, 13, 181-198
50. McClintock, B., The Stability of Broken Ends of Chromosomes in Zea Mays. *Genetics* **1941,** *26* (2), 234-82.
51. Martinez, P.; Blasco, M. A., Telomeric and extra-telomeric roles for telomerase and the telomere-binding proteins. *Nature reviews. Cancer* **2011,** *11* (3), 161-76.
52. O'Sullivan, R. J.; Karlseder, J., Telomeres: protecting chromosomes against genome instability. *Nature reviews. Molecular cell biology* **2010,** *11* (3), 171-81.
53. de Lange, T., Shelterin: the protein complex that shapes and safeguards human telomeres. *Genes & development* **2005,** *19* (18), 2100-10.
54. de Lange, T., How telomeres solve the end-protection problem. *Science* **2009,** *326* (5955), 948-52.
55. Cerni, C., Telomeres, telomerase, and myc. An update. *Mutation research* **2000,** *462* (1), 31-47.
56. Hayflick, L., The Limited in Vitro Lifetime of Human Diploid Cell Strains. *Experimental cell research* **1965,** *37*, 614-36.
57. Cohen, S. B.; Graham, M. E.; Lovrecz, G. O.; Bache, N.; Robinson, P. J.; Reddel, R. R., Protein composition of catalytically active human telomerase from immortal cells. *Science* **2007,** *315* (5820), 1850-3.
58. Venteicher, A. S.; Abreu, E. B.; Meng, Z.; McCann, K. E.; Terns, R. M.; Veenstra, T. D.; Terns, M. P.; Artandi, S. E., A human telomerase holoenzyme protein required for Cajal body localization and telomere synthesis. *Science* **2009,** *323* (5914), 644-8.
59. Venteicher, A. S.; Meng, Z.; Mason, P. J.; Veenstra, T. D.; Artandi, S. E., Identification of ATPases pontin and reptin as telomerase components essential for holoenzyme assembly. *Cell* **2008,** *132* (6), 945-57.
60. Smogorzewska, A.; de Lange, T., Regulation of telomerase by telomeric proteins. *Annual review of biochemistry* **2004,** *73*, 177-208.
61. Flores, I.; Canela, A.; Vera, E.; Tejera, A.; Cotsarelis, G.; Blasco, M. A., The longest telomeres: a general signature of adult stem cell compartments. *Genes & development* **2008,** *22* (5), 654-67.
62. Harley, C. B.; Futcher, A. B.; Greider, C. W., Telomeres shorten during ageing of human fibroblasts. *Nature* **1990,** *345* (6274), 458-60.
63. Blackburn, E. H., Telomere states and cell fates. *Nature* **2000,** *408* (6808), 53-56.
64. Kim, N. W.; Piatyszek, M. A.; Prowse, K. R.; Harley, C. B.; West, M. D.; Ho, P. L.; Coviello, G. M.; Wright, W. E.; Weinrich, S. L.; Shay, J. W., Specific association of human telomerase activity with immortal cells and cancer. *Science* **1994,** *266* (5193), 2011-5.
65. Bryan, T. M.; Reddel, R. R., Telomere dynamics and telomerase activity in in vitro immortalised human cells. *Eur J Cancer* **1997,** *33* (5), 767-73.
66. Bhattacharyya, S.; Sandy, A.; Groden, J., Unwinding protein complexes in ALTernative telomere maintenance. *Journal of cellular biochemistry* **2010,** *109* (1), 7-15.
67. Biessmann, H.; Mason, J. M., Telomerase-independent mechanisms of telomere elongation. *Cellular and molecular life sciences : CMLS* **2003,** *60* (11), 2325-33.

68. Opresko, P. L.; Sowd, G.; Wang, H., The Werner syndrome helicase/exonuclease processes mobile D-loops through branch migration and degradation. *PloS one* **2009,** *4* (3), e4825.
69. Temime-Smaali, N.; Guittat, L.; Wenner, T.; Bayart, E.; Douarre, C.; Gomez, D.; Giraud-Panis, M. J.; Londono-Vallejo, A.; Gilson, E.; Amor-Gueret, M.; Riou, J. F., Topoisomerase IIIalpha is required for normal proliferation and telomere stability in alternative lengthening of telomeres. *The EMBO journal* **2008,** *27* (10), 1513-24.
70. Sen, D.; Gilbert, W., Formation of parallel four-stranded complexes by guanine-rich motifs in DNA and its implications for meiosis. *Nature* **1988,** *334* (6180), 364-6.
71. Phan, A. T., Human telomeric G-quadruplex: structures of DNA and RNA sequences. *The FEBS journal* **2010,** *277* (5), 1107-17.
72. Parkinson, G. N.; Lee, M. P.; Neidle, S., Crystal structure of parallel quadruplexes from human telomeric DNA. *Nature* **2002,** *417* (6891), 876-80.
73. Phan, A. T.; Patel, D. J., Two-repeat human telomeric d(TAGGGTTAGGGT) sequence forms interconverting parallel and antiparallel G-quadruplexes in solution: distinct topologies, thermodynamic properties, and folding/unfolding kinetics. *Journal of the American Chemical Society* **2003,** *125* (49), 15021-7.
74. Schultze, P.; Hud, N. V.; Smith, F. W.; Feigon, J., The effect of sodium, potassium and ammonium ions on the conformation of the dimeric quadruplex formed by the Oxytricha nova telomere repeat oligonucleotide d(G(4)T(4)G(4)). *Nucleic acids research* **1999,** *27* (15), 3018-28.
75. Kotch, F. W.; Fettinger, J. C.; Davis, J. T., A lead-filled G-quadruplex: insight into the G-Quartet's selectivity for Pb(2+) over K(+). *Organic letters* **2000,** *2* (21), 3277-80.
76. Kankia, B. I.; Marky, L. A., Folding of the thrombin aptamer into a G-quadruplex with Sr(2+): stability, heat, and hydration. *Journal of the American Chemical Society* **2001,** *123* (44), 10799-804.
77. Phillips, K.; Dauter, Z.; Murchie, A. I.; Lilley, D. M.; Luisi, B., The crystal structure of a parallel-stranded guanine tetraplex at 0.95 A resolution. *Journal of molecular biology* **1997,** *273* (1), 171-82.
78. Arnott, S.; Chandrasekaran, R.; Marttila, C. M., Structures for polyinosinic acid and polyguanylic acid. *The Biochemical journal* **1974,** *141* (2), 537-43.
79. Sundquist, W. I.; Klug, A., Telomeric DNA dimerizes by formation of guanine tetrads between hairpin loops. *Nature* **1989,** *342* (6251), 825-9.
80. Gellert, M.; Lipsett, M. N.; Davies, D. R., Helix formation by guanylic acid. *Proceedings of the National Academy of Sciences of the United States of America* **1962,** *48*, 2013-8.
81. Burge, S.; Parkinson, G. N.; Hazel, P.; Todd, A. K.; Neidle, S., Quadruplex DNA: sequence, topology and structure. *Nucleic acids research* **2006,** *34* (19), 5402-15.
82. Li, L.; Rao, J. N.; Guo, X.; Liu, L.; Santora, R.; Bass, B. L.; Wang, J. Y., Polyamine depletion stabilizes p53 resulting in inhibition of normal intestinal epithelial cell proliferation. *American journal of physiology. Cell physiology* **2001,** *281* (3), C941-53.
83. Patel, D. J.; Phan, A. T.; Kuryavyi, V., Human telomere, oncogenic promoter and 5'-UTR G-quadruplexes: diverse higher order DNA and RNA targets for cancer therapeutics. *Nucleic acids research* **2007,** *35* (22), 7429-55.
84. Wang, Y.; Patel, D. J., Solution structure of the human telomeric repeat d[AG3(T2AG3)3] G-tetraplex. *Structure* **1993,** *1* (4), 263-82.
85. Baker, E. S.; Bernstein, S. L.; Gabelica, V.; De Pauw, E.; Bowers, M. T., G-quadruplexes in telomeric repeats are conserved in a solvent-free environment. *International journal of mass spectrometry* **2006,** *253* (3), 225-237.
86. Henderson, E.; Hardin, C. C.; Walk, S. K.; Tinoco, I., Jr.; Blackburn, E. H., Telomeric DNA oligonucleotides form novel intramolecular structures containing guanine-guanine base pairs. *Cell* **1987,** *51* (6), 899-908.
87. Hanahan, D.; Weinberg, R. A., The hallmarks of cancer. *Cell* **2000,** *100* (1), 57-70.
88. Heinrich, M. C.; Corless, C. L.; Demetri, G. D.; Blanke, C. D.; von Mehren, M.; Joensuu, H.; McGreevey, L. S.; Chen, C. J.; Van den Abbeele, A. D.; Druker, B. J.; Kiese, B.; Eisenberg, B.; Roberts, P. J.; Singer, S.; Fletcher, C. D.; Silberman, S.; Dimitrijevic, S.; Fletcher, J. A., Kinase mutations and imatinib response in patients with metastatic gastrointestinal stromal tumor. *Journal of clinical oncology : official journal of the American Society of Clinical Oncology* **2003,** *21* (23), 4342-9.
89. Lipps, H. J.; Rhodes, D., G-quadruplex structures: in vivo evidence and function. *Trends in cell biology* **2009,** *19* (8), 414-22.

90. Renciuk, D.; Kejnovska, I.; Skolakova, P.; Bednarova, K.; Motlova, J.; Vorlickova, M., Arrangements of human telomere DNA quadruplex in physiologically relevant K+ solutions. *Nucleic acids research* **2009,** *37* (19), 6625-34.
91. Paramasivan, S.; Rujan, I.; Bolton, P. H., Circular dichroism of quadruplex DNAs: applications to structure, cation effects and ligand binding. *Methods* **2007,** *43* (4), 324-31.
92. Martino, L.; Pagano, B.; Fotticchia, I.; Neidle, S.; Giancola, C., Shedding light on the interaction between TMPyP4 and human telomeric quadruplexes. *The journal of physical chemistry. B* **2009,** *113* (44), 14779-86.
93. Schaffitzel, C.; Berger, I.; Postberg, J.; Hanes, J.; Lipps, H. J.; Pluckthun, A., In vitro generated antibodies specific for telomeric guanine-quadruplex DNA react with Stylonychia lemnae macronuclei. *Proceedings of the National Academy of Sciences of the United States of America* **2001,** *98* (15), 8572-7.
94. Paeschke, K.; Juranek, S.; Simonsson, T.; Hempel, A.; Rhodes, D.; Lipps, H. J., Telomerase recruitment by the telomere end binding protein-beta facilitates G-quadruplex DNA unfolding in ciliates. *Nature structural & molecular biology* **2008,** *15* (6), 598-604.
95. Shaw, T. J.; Keszthelyi, E. J.; Tonary, A. M.; Cada, M.; Vanderhyden, B. C., Cyclic AMP in ovarian cancer cells both inhibits proliferation and increases c-KIT expression. *Experimental cell research* **2002,** *273* (1), 95-106.
96. Rankin, S.; Reszka, A. P.; Huppert, J.; Zloh, M.; Parkinson, G. N.; Todd, A. K.; Ladame, S.; Balasubramanian, S.; Neidle, S., Putative DNA quadruplex formation within the human c-kit oncogene. *Journal of the American Chemical Society* **2005,** *127* (30), 10584-9.
97. Fernando, H.; Reszka, A. P.; Huppert, J.; Ladame, S.; Rankin, S.; Venkitaraman, A. R.; Neidle, S.; Balasubramanian, S., A conserved quadruplex motif located in a transcription activation site of the human c-kit oncogene. *Biochemistry* **2006,** *45* (25), 7854-60.
98. Phan, A. T.; Kuryavyi, V.; Burge, S.; Neidle, S.; Patel, D. J., Structure of an unprecedented G-quadruplex scaffold in the human c-kit promoter. *Journal of the American Chemical Society* **2007,** *129* (14), 4386-92.
99. Wei, D.; Parkinson, G. N.; Reszka, A. P.; Neidle, S., Crystal structure of a c-kit promoter quadruplex reveals the structural role of metal ions and water molecules in maintaining loop conformation. *Nucleic acids research* **2012**.
100. Hsu, S. T.; Varnai, P.; Bugaut, A.; Reszka, A. P.; Neidle, S.; Balasubramanian, S., A G-rich sequence within the c-kit oncogene promoter forms a parallel G-quadruplex having asymmetric G-tetrad dynamics. *Journal of the American Chemical Society* **2009,** *131* (37), 13399-409.
101. Kuryavyi, V.; Phan, A. T.; Patel, D. J., Solution structures of all parallel-stranded monomeric and dimeric G-quadruplex scaffolds of the human c-kit2 promoter. *Nucleic acids research* **2010,** *38* (19), 6757-6773.
102. Ou, T. M.; Lu, Y. J.; Tan, J. H.; Huang, Z. S.; Wong, K. Y.; Gu, L. Q., G-quadruplexes: targets in anticancer drug design. *ChemMedChem* **2008,** *3* (5), 690-713.
103. Neidle, S., Human telomeric G-quadruplex: the current status of telomeric G-quadruplexes as therapeutic targets in human cancer. *The FEBS journal* **2010,** *277* (5), 1118-25.
104. Sun, D.; Thompson, B.; Cathers, B. E.; Salazar, M.; Kerwin, S. M.; Trent, J. O.; Jenkins, T. C.; Neidle, S.; Hurley, L. H., Inhibition of human telomerase by a G-quadruplex-interactive compound. *Journal of medicinal chemistry* **1997,** *40* (14), 2113-6.
105. Perry, P. J.; Reszka, A. P.; Wood, A. A.; Read, M. A.; Gowan, S. M.; Dosanjh, H. S.; Trent, J. O.; Jenkins, T. C.; Kelland, L. R.; Neidle, S., Human telomerase inhibition by regioisomeric disubstituted amidoanthracene-9,10-diones. *Journal of medicinal chemistry* **1998,** *41* (24), 4873-84.
106. Perry, P. J.; Gowan, S. M.; Reszka, A. P.; Polucci, P.; Jenkins, T. C.; Kelland, L. R.; Neidle, S., 1,4- and 2,6-disubstituted amidoanthracene-9,10-dione derivatives as inhibitors of human telomerase. *Journal of medicinal chemistry* **1998,** *41* (17), 3253-60.
107. Gutierrez, P. L., The metabolism of quinone-containing alkylating agents: free radical production and measurement. *Frontiers in bioscience : a journal and virtual library* **2000,** *5*, D629-38.
108. Perry, P. J.; Read, M. A.; Davies, R. T.; Gowan, S. M.; Reszka, A. P.; Wood, A. A.; Kelland, L. R.; Neidle, S., 2,7-Disubstituted amidofluorenone derivatives as inhibitors of human telomerase. *Journal of medicinal chemistry* **1999,** *42* (14), 2679-84.
109. Harrison, R. J.; Gowan, S. M.; Kelland, L. R.; Neidle, S., Human telomerase inhibition by substituted acridine derivatives. *Bioorganic & medicinal chemistry letters* **1999,** *9* (17), 2463-8.

110. Gowan, S. M.; Heald, R.; Stevens, M. F.; Kelland, L. R., Potent inhibition of telomerase by small-molecule pentacyclic acridines capable of interacting with G-quadruplexes. *Molecular pharmacology* **2001,** *60* (5), 981-8.
111. Leonetti, C.; Amodei, S.; D'Angelo, C.; Rizzo, A.; Benassi, B.; Antonelli, A.; Elli, R.; Stevens, M. F.; D'Incalci, M.; Zupi, G.; Biroccio, A., Biological activity of the G-quadruplex ligand RHPS4 (3,11-difluoro-6,8,13-trimethyl-8H-quino[4,3,2-kl]acridinium methosulfate) is associated with telomere capping alteration. *Molecular pharmacology* **2004,** *66* (5), 1138-46.
112. Biroccio, A.; Rizzo, A.; Elli, R.; Koering, C. E.; Belleville, A.; Benassi, B.; Leonetti, C.; Stevens, M. F.; D'Incalci, M.; Zupi, G.; Gilson, E., TRF2 inhibition triggers apoptosis and reduces tumourigenicity of human melanoma cells. *Eur J Cancer* **2006,** *42* (12), 1881-8.
113. Salvati, E.; Leonetti, C.; Rizzo, A.; Scarsella, M.; Mottolese, M.; Galati, R.; Sperduti, I.; Stevens, M. F.; D'Incalci, M.; Blasco, M.; Chiorino, G.; Bauwens, S.; Horard, B.; Gilson, E.; Stoppacciaro, A.; Zupi, G.; Biroccio, A., Telomere damage induced by the G-quadruplex ligand RHPS4 has an antitumor effect. *The Journal of clinical investigation* **2007,** *117* (11), 3236-47.
114. Gavathiotis, E.; Heald, R. A.; Stevens, M. F.; Searle, M. S., Drug recognition and stabilisation of the parallel-stranded DNA quadruplex d(TTAGGGT)4 containing the human telomeric repeat. *Journal of molecular biology* **2003,** *334* (1), 25-36.
115. Phatak, P.; Cookson, J. C.; Dai, F.; Smith, V.; Gartenhaus, R. B.; Stevens, M. F.; Burger, A. M., Telomere uncapping by the G-quadruplex ligand RHPS4 inhibits clonogenic tumour cell growth in vitro and in vivo consistent with a cancer stem cell targeting mechanism. *British journal of cancer* **2007,** *96* (8), 1223-33.
116. Read, M.; Harrison, R. J.; Romagnoli, B.; Tanious, F. A.; Gowan, S. H.; Reszka, A. P.; Wilson, W. D.; Kelland, L. R.; Neidle, S., Structure-based design of selective and potent G quadruplex-mediated telomerase inhibitors. *Proceedings of the National Academy of Sciences of the United States of America* **2001,** *98* (9), 4844-9.
117. Reed, J.; Gunaratnam, M.; Beltran, M.; Reszka, A. P.; Vilar, R.; Neidle, S., TRAP-LIG, a modified telomere repeat amplification protocol assay to quantitate telomerase inhibition by small molecules. *Analytical biochemistry* **2008,** *380* (1), 99-105.
118. Gowan, S. M.; Harrison, J. R.; Patterson, L.; Valenti, M.; Read, M. A.; Neidle, S.; Kelland, L. R., A G-quadruplex-interactive potent small-molecule inhibitor of telomerase exhibiting in vitro and in vivo antitumor activity. *Molecular pharmacology* **2002,** *61* (5), 1154-62.
119. Burger, A. M.; Dai, F.; Schultes, C. M.; Reszka, A. P.; Moore, M. J.; Double, J. A.; Neidle, S., The G-quadruplex-interactive molecule BRACO-19 inhibits tumor growth, consistent with telomere targeting and interference with telomerase function. *Cancer research* **2005,** *65* (4), 1489-96.
120. Incles, C. M.; Schultes, C. M.; Kempski, H.; Koehler, H.; Kelland, L. R.; Neidle, S., A G-quadruplex telomere targeting agent produces p16-associated senescence and chromosomal fusions in human prostate cancer cells. *Molecular cancer therapeutics* **2004,** *3* (10), 1201-1206.
121. Gunaratnam, M.; Greciano, O.; Martins, C.; Reszka, A. P.; Schultes, C. M.; Morjani, H.; Riou, J. F.; Neidle, S., Mechanism of acridine-based telomerase inhibition and telomere shortening. *Biochemical pharmacology* **2007,** *74* (5), 679-89.
122. Campbell, N. H.; Parkinson, G. N.; Reszka, A. P.; Neidle, S., Structural basis of DNA quadruplex recognition by an acridine drug. *Journal of the American Chemical Society* **2008,** *130* (21), 6722-4.
123. Shin-ya, K.; Wierzba, K.; Matsuo, K.; Ohtani, T.; Yamada, Y.; Furihata, K.; Hayakawa, Y.; Seto, H., Telomestatin, a novel telomerase inhibitor from Streptomyces anulatus. *Journal of the American Chemical Society* **2001,** *123* (6), 1262-3.
124. Kim, M. Y.; Vankayalapati, H.; Shin-Ya, K.; Wierzba, K.; Hurley, L. H., Telomestatin, a potent telomerase inhibitor that interacts quite specifically with the human telomeric intramolecular g-quadruplex. *Journal of the American Chemical Society* **2002,** *124* (10), 2098-9.
125. Gomez, D.; Aouali, N.; Renaud, A.; Douarre, C.; Shin-Ya, K.; Tazi, J.; Martinez, S.; Trentesaux, C.; Morjani, H.; Riou, J. F., Resistance to senescence induction and telomere shortening by a G-quadruplex ligand inhibitor of telomerase. *Cancer research* **2003,** *63* (19), 6149-53.
126. Gomez, D.; Paterski, R.; Lemarteleur, T.; Shin-Ya, K.; Mergny, J. L.; Riou, J. F., Interaction of telomestatin with the telomeric single-strand overhang. *The Journal of biological chemistry* **2004,** *279* (40), 41487-94.

127. Gomez, D.; O'Donohue, M. F.; Wenner, T.; Douarre, C.; Macadre, J.; Koebel, P.; Giraud-Panis, M. J.; Kaplan, H.; Kolkes, A.; Shin-ya, K.; Riou, J. F., The G-quadruplex ligand telomestatin inhibits POT1 binding to telomeric sequences in vitro and induces GFP-POT1 dissociation from telomeres in human cells. *Cancer research* **2006,** *66* (14), 6908-12.
128. Tauchi, T.; Shin-Ya, K.; Sashida, G.; Sumi, M.; Nakajima, A.; Shimamoto, T.; Ohyashiki, J. H.; Ohyashiki, K., Activity of a novel G-quadruplex-interactive telomerase inhibitor, telomestatin (SOT-095), against human leukemia cells: involvement of ATM-dependent DNA damage response pathways. *Oncogene* **2003,** *22* (34), 5338-47.
129. Tauchi, T.; Shin-ya, K.; Sashida, G.; Sumi, M.; Okabe, S.; Ohyashiki, J. H.; Ohyashiki, K., Telomerase inhibition with a novel G-quadruplex-interactive agent, telomestatin: in vitro and in vivo studies in acute leukemia. *Oncogene* **2006,** *25* (42), 5719-25.
130. Temime-Smaali, N.; Guittat, L.; Sidibe, A.; Shin-ya, K.; Trentesaux, C.; Riou, J. F., The G-quadruplex ligand telomestatin impairs binding of topoisomerase IIIalpha to G-quadruplex-forming oligonucleotides and uncaps telomeres in ALT cells. *PloS one* **2009,** *4* (9), e6919.
131. Linder, J.; Garner, T. P.; Williams, H. E.; Searle, M. S.; Moody, C. J., Telomestatin: formal total synthesis and cation-mediated interaction of its seco-derivatives with G-quadruplexes. *Journal of the American Chemical Society* **2011,** *133* (4), 1044-51.
132. Tera, M.; Sohtome, Y.; Ishizuka, H.; Doi, T.; Takagi, M.; Shin-ya, K.; Nagasawa, K. Design and synthesis of telomestatin derivatives and their inhibitory activity of telomerase. Heterocycles 2006, 69, 505–514.
133. Fedoroff, O. Y.; Salazar, M.; Han, H.; Chemeris, V. V.; Kerwin, S. M.; Hurley, L. H., NMR-Based model of a telomerase-inhibiting compound bound to G-quadruplex DNA. *Biochemistry* **1998,** *37* (36), 12367-74.
134. Rangan, A.; Fedoroff, O. Y.; Hurley, L. H., Induction of duplex to G-quadruplex transition in the c-myc promoter region by a small molecule. *The Journal of biological chemistry* **2001,** *276* (7), 4640-6.
135. Rossetti, L.; Franceschin, M.; Bianco, A.; Ortaggi, G.; Savino, M., Perylene diimides with different side chains are selective in inducing different G-quadruplex DNA structures and in inhibiting telomerase. *Bioorganic & medicinal chemistry letters* **2002,** *12* (18), 2527-33.
136. Franceschin, M.; Lombardo, C. M.; Pascucci, E.; D'Ambrosio, D.; Micheli, E.; Bianco, A.; Ortaggi, G.; Savino, M., The number and distances of positive charges of polyamine side chains in a series of perylene diimides significantly influence their ability to induce G-quadruplex structures and inhibit human telomerase. *Bioorganic & medicinal chemistry* **2008,** *16* (5), 2292-304.
137. Franceschin, M.; Pascucci, E.; Alvino, A.; D'Ambrosio, D.; Bianco, A.; Ortaggi, G.; Savino, M., New highly hydrosoluble and not self-aggregated perylene derivatives with three and four polar side-chains as G-quadruplex telomere targeting agents and telomerase inhibitors. *Bioorganic & medicinal chemistry letters* **2007,** *17* (9), 2515-22.
138. Franceschin, M.; Alvino, A.; Ortaggi, G.; Bianco, A., New hydrosoluble perylene and coronene derivatives. *Tetrahedron Letters* **2004,** *45* (49), 9015-9020.
139. Micheli, E.; Lombardo, C. M.; D'Ambrosio, D.; Franceschin, M.; Neidle, S.; Savino, M., Selective G-quadruplex ligands: the significant role of side chain charge density in a series of perylene derivatives. *Bioorganic & medicinal chemistry letters* **2009,** *19* (14), 3903-8.
140. Cuenca, F.; Greciano, O.; Gunaratnam, M.; Haider, S.; Munnur, D.; Nanjunda, R.; Wilson, W. D.; Neidle, S., Tri- and tetra-substituted naphthalene diimides as potent G-quadruplex ligands. *Bioorganic & medicinal chemistry letters* **2008,** *18* (5), 1668-73.
141. Parkinson, G. N.; Cuenca, F.; Neidle, S., Topology conservation and loop flexibility in quadruplex-drug recognition: crystal structures of inter- and intramolecular telomeric DNA quadruplex-drug complexes. *Journal of molecular biology* **2008,** *381* (5), 1145-56.
142. Gunaratnam, M.; Swank, S.; Haider, S. M.; Galesa, K.; Reszka, A. P.; Beltran, M.; Cuenca, F.; Fletcher, J. A.; Neidle, S., Targeting human gastrointestinal stromal tumor cells with a quadruplex-binding small molecule. *Journal of medicinal chemistry* **2009,** *52* (12), 3774-83.
143. Hampel, S. M.; Sidibe, A.; Gunaratnam, M.; Riou, J. F.; Neidle, S., Tetrasubstituted naphthalene diimide ligands with selectivity for telomeric G-quadruplexes and cancer cells. *Bioorganic & medicinal chemistry letters* **2010,** *20* (22), 6459-63.

144. Collie, G. W.; Promontorio, R.; Hampel, S. M.; Micco, M.; Neidle, S.; Parkinson, G. N., Structural Basis for Telomeric G-Quadruplex Targeting by Naphthalene Diimide Ligands. *Journal of the American Chemical Society* **2012**.
145. Paz, E. A.; Garcia-Huidobro, J.; Ignatenkos, N. A., Polyamines in cancer. *Advances in clinical chemistry* **2011,** *54*, 45-70.
146. Bardocz, S.; Duguid, T. J.; Brown, D. S.; Grant, G.; Pusztai, A.; White, A.; Ralph, A., The importance of dietary polyamines in cell regeneration and growth. *The British journal of nutrition* **1995,** *73* (6), 819-28.
147. Cohen, S.S. A Guide to the Polyamines. Oxford Univ. Press, New York, 1998
148. Milovic, V., Polyamines in the gut lumen: bioavailability and biodistribution. *European journal of gastroenterology & hepatology* **2001,** *13* (9), 1021-5.
149. Wallace, H. M.; Fraser, A. V., Polyamine analogues as anticancer drugs. *Biochemical Society transactions* **2003,** *31* (2), 393-6.
150. Thomas, T.; Thomas, T. J., Polyamines in cell growth and cell death: molecular mechanisms and therapeutic applications. *Cellular and molecular life sciences : CMLS* **2001,** *58* (2), 244-58.
151. Gerner, E. W.; Meyskens, F. L., Jr., Polyamines and cancer: old molecules, new understanding. *Nature reviews. Cancer* **2004,** *4* (10), 781-92.
152. Wang, Y.; Murray-Stewart, T.; Devereux, W.; Hacker, A.; Frydman, B.; Woster, P. M.; Casero, R. A., Jr., Properties of purified recombinant human polyamine oxidase, PAOh1/SMO. *Biochemical and biophysical research communications* **2003,** *304* (4), 605-11.
153. Pendeville, H.; Carpino, N.; Marine, J. C.; Takahashi, Y.; Muller, M.; Martial, J. A.; Cleveland, J. L., The ornithine decarboxylase gene is essential for cell survival during early murine development. *Molecular and cellular biology* **2001,** *21* (19), 6549-58.
154. Pegg, A. E., Mammalian polyamine metabolism and function. *IUBMB life* **2009,** *61* (9), 880-94.
155. Lee, J.; Michael, A. J.; Martynowski, D.; Goldsmith, E. J.; Phillips, M. A., Phylogenetic diversity and the structural basis of substrate specificity in the beta/alpha-barrel fold basic amino acid decarboxylases. *The Journal of biological chemistry* **2007,** *282* (37), 27115-25.
156. Casero, R. A., Jr.; Marton, L. J., Targeting polyamine metabolism and function in cancer and other hyperproliferative diseases. *Nature reviews. Drug discovery* **2007,** *6* (5), 373-90.
157. Pegg, A. E., Regulation of ornithine decarboxylase. *The Journal of biological chemistry* **2006,** *281* (21), 14529-32.
158. Nilsson, J. A.; Maclean, K. H.; Keller, U. B.; Pendeville, H.; Baudino, T. A.; Cleveland, J. L., Mnt loss triggers Myc transcription targets, proliferation, apoptosis, and transformation. *Molecular and cellular biology* **2004,** *24* (4), 1560-9.
159. Hermeking, H., The MYC oncogene as a cancer drug target. *Current cancer drug targets* **2003,** *3* (3), 163-75.
160. Ignatenko, N. A.; Zhang, H.; Watts, G. S.; Skovan, B. A.; Stringer, D. E.; Gerner, E. W., The chemopreventive agent alpha-difluoromethylornithine blocks Ki-ras-dependent tumor formation and specific gene expression in Caco-2 cells. *Molecular carcinogenesis* **2004,** *39* (4), 221-33.
161. Hillary, R. A.; Pegg, A. E., Decarboxylases involved in polyamine biosynthesis and their inactivation by nitric oxide. *Biochimica et biophysica acta* **2003,** *1647* (1-2), 161-6.
162. Casero, R. A.; Pegg, A. E., Polyamine catabolism and disease. *The Biochemical journal* **2009,** *421* (3), 323-38.
163. Taylor, M. T.; Lawson, K. R.; Ignatenko, N. A.; Marek, S. E.; Stringer, D. E.; Skovan, B. A.; Gerner, E. W., Sulindac sulfone inhibits K-ras-dependent cyclooxygenase-2 expression in human colon cancer cells. *Cancer research* **2000,** *60* (23), 6607-10.
164. Ignatenko, N. A.; Babbar, N.; Mehta, D.; Casero, R. A., Jr.; Gerner, E. W., Suppression of polyamine catabolism by activated Ki-ras in human colon cancer cells. *Molecular carcinogenesis* **2004,** *39* (2), 91-102.
165. Wallace, H. M.; Fraser, A. V.; Hughes, A., A perspective of polyamine metabolism. *The Biochemical journal* **2003,** *376* (Pt 1), 1-14.
166. Pestell, R. G.; Albanese, C.; Reutens, A. T.; Segall, J. E.; Lee, R. J.; Arnold, A., The cyclins and cyclin-dependent kinase inhibitors in hormonal regulation of proliferation and differentiation. *Endocrine reviews* **1999,** *20* (4), 501-34.

167. Tsihlias, J.; Kapusta, L.; Slingerland, J., The prognostic significance of altered cyclin-dependent kinase inhibitors in human cancer. *Annual review of medicine* **1999,** *50*, 401-23.
168. Thomas, T.; Thomas, T. J., Regulation of cyclin B1 by estradiol and polyamines in MCF-7 breast cancer cells. *Cancer research* **1994,** *54* (4), 1077-84.
169. Tabor, C. W.; Tabor, H., Polyamines. *Annual review of biochemistry* **1984,** *53*, 749-90.
170. Thomas, T.; Thomas, T. J., Estradiol control of ornithine decarboxylase mRNA, enzyme activity, and polyamine levels in MCF-7 breast cancer cells: therapeutic implications. *Breast cancer research and treatment* **1994,** *29* (2), 189-201.
171. Wilcken, N. R.; Prall, O. W.; Musgrove, E. A.; Sutherland, R. L., Inducible overexpression of cyclin D1 in breast cancer cells reverses the growth-inhibitory effects of antiestrogens. *Clinical cancer research : an official journal of the American Association for Cancer Research* **1997,** *3* (6), 849-54.
172. Watts, C. K.; Sweeney, K. J.; Warlters, A.; Musgrove, E. A.; Sutherland, R. L., Antiestrogen regulation of cell cycle progression and cyclin D1 gene expression in MCF-7 human breast cancer cells. *Breast cancer research and treatment* **1994,** *31* (1), 95-105.
173. Schipper, R. G.; Penning, L. C.; Verhofstad, A. A., Involvement of polyamines in apoptosis. Facts and controversies: effectors or protectors? *Seminars in cancer biology* **2000,** *10* (1), 55-68.
174. Nitta, T.; Igarashi, K.; Yamamoto, N., Polyamine depletion induces apoptosis through mitochondria-mediated pathway. *Experimental cell research* **2002,** *276* (1), 120-8.
175. Vaux, D. L.; Strasser, A., The molecular biology of apoptosis. *Proceedings of the National Academy of Sciences of the United States of America* **1996,** *93* (6), 2239-44.
176. www.sgul.ac.uk/depts/immunology/~dash/apoptosis/mito.htm
177. Thornberry, N. A.; Lazebnik, Y., Caspases: enemies within. *Science* **1998,** *281* (5381), 1312-6.
178. Strasser, A.; Cory, S.; Adams, J. M., Deciphering the rules of programmed cell death to improve therapy of cancer and other diseases. *The EMBO journal* **2011,** *30* (18), 3667-83.
179. Boatright, K. M.; Renatus, M.; Scott, F. L.; Sperandio, S.; Shin, H.; Pedersen, I. M.; Ricci, J. E.; Edris, W. A.; Sutherlin, D. P.; Green, D. R.; Salvesen, G. S., A unified model for apical caspase activation. *Molecular cell* **2003,** *11* (2), 529-41.
180. Johnson, D. E., Noncaspase proteases in apoptosis. *Leukemia : official journal of the Leukemia Society of America, Leukemia Research Fund, U.K* **2000,** *14* (9), 1695-703.
181. Olsson, M.; Zhivotovsky, B., Caspases and cancer. *Cell death and differentiation* **2011,** *18* (9), 1441-9.
182. Wang, J.Y.; Casero, R.A.Jr, Polyamine Cell Signaling. Physiology, pharmacology, and cancer research. Humana Press.
183. Thomas, T.; Gunnia, U. B.; Yurkow, E. J.; Seibold, J. R.; Thomas, T. J., Inhibition of calcium signalling in murine splenocytes by polyamines: differential effects on CD4 and CD8 T-cells. *The Biochemical journal* **1993,** *291 (Pt 2)*, 375-81.
184. Desiderio, M. A.; Grassilli, E.; Bellesia, E.; Salomoni, P.; Franceschi, C., Involvement of ornithine decarboxylase and polyamines in glucocorticoid-induced apoptosis of rat thymocytes. *Cell growth & differentiation : the molecular biology journal of the American Association for Cancer Research* **1995,** *6* (5), 505-13.
185. Bello-Fernandez, C.; Packham, G.; Cleveland, J. L., The ornithine decarboxylase gene is a transcriptional target of c-Myc. *Proceedings of the National Academy of Sciences of the United States of America* **1993,** *90* (16), 7804-8.
186. Packham, G.; Cleveland, J. L., Ornithine decarboxylase is a mediator of c-Myc-induced apoptosis. *Molecular and cellular biology* **1994,** *14* (9), 5741-7.
187. Kingsnorth, A. N.; Wallace, H. M., Elevation of monoacetylated polyamines in human breast cancers. *European journal of cancer & clinical oncology* **1985,** *21* (9), 1057-62.
188. Wallace, H. M.; Duthie, J.; Evans, D. M.; Lamond, S.; Nicoll, K. M.; Heys, S. D., Alterations in polyamine catabolic enzymes in human breast cancer tissue. *Clinical cancer research : an official journal of the American Association for Cancer Research* **2000,** *6* (9), 3657-61.
189. Parchment, R. E.; Pierce, G. B., Polyamine oxidation, programmed cell death, and regulation of melanoma in the murine embryonic limb. *Cancer research* **1989,** *49* (23), 6680-6.

190. Ha, H. C.; Woster, P. M.; Yager, J. D.; Casero, R. A., Jr., The role of polyamine catabolism in polyamine analogue-induced programmed cell death. *Proceedings of the National Academy of Sciences of the United States of America* **1997,** *94* (21), 11557-62.
191. Chopra, S.; Wallace, H. M., Induction of spermidine/spermine N1-acetyltransferase in human cancer cells in response to increased production of reactive oxygen species. *Biochemical pharmacology* **1998,** *55* (7), 1119-23.
192. Poulin, R.; Coward, J. K.; Lakanen, J. R.; Pegg, A. E., Enhancement of the spermidine uptake system and lethal effects of spermidine overaccumulation in ornithine decarboxylase-overproducing L1210 cells under hyposmotic stress. *The Journal of biological chemistry* **1993,** *268* (7), 4690-8.
193. Poulin, R.; Pelletier, G.; Pegg, A. E., Induction of apoptosis by excessive polyamine accumulation in ornithine decarboxylase-overproducing L1210 cells. *The Biochemical journal* **1995,** *311 (Pt 3)*, 723-7.
194. Alhonen, L.; Parkkinen, J. J.; Keinanen, T.; Sinervirta, R.; Herzig, K. H.; Janne, J., Activation of polyamine catabolism in transgenic rats induces acute pancreatitis. *Proceedings of the National Academy of Sciences of the United States of America* **2000,** *97* (15), 8290-5.
195. Shah, N.; Thomas, T.; Shirahata, A.; Sigal, L. H.; Thomas, T. J., Activation of nuclear factor kappaB by polyamines in breast cancer cells. *Biochemistry* **1999,** *38* (45), 14763-74.
196. Thomas, T.; Shah, N.; Klinge, C. M.; Faaland, C. A.; Adihkarakunnathu, S.; Gallo, M. A.; Thomas, T. J., Polyamine biosynthesis inhibitors alter protein-protein interactions involving estrogen receptor in MCF-7 breast cancer cells. *Journal of molecular endocrinology* **1999,** *22* (2), 131-9.
197. Stefanelli, C.; Stanic, I.; Zini, M.; Bonavita, F.; Flamigni, F.; Zambonin, L.; Landi, L.; Pignatti, C.; Guarnieri, C.; Caldarera, C. M., Polyamines directly induce release of cytochrome c from heart mitochondria. *The Biochemical journal* **2000,** *347 Pt 3*, 875-80.
198. Stefanelli, C.; Bonavita, F.; Stanic, I.; Mignani, M.; Facchini, A.; Pignatti, C.; Flamigni, F.; Caldarera, C. M., Spermine causes caspase activation in leukaemia cells. *FEBS letters* **1998,** *437* (3), 233-6.
199. Stefanelli, C.; Bonavita, F.; Stanic, I.; Pignatti, C.; Flamigni, F.; Guarnieri, C.; Caldarera, C. M., Spermine triggers the activation of caspase-3 in a cell-free model of apoptosis. *FEBS letters* **1999,** *451* (2), 95-8.
200. Suzuki, K.; Matsubara, H., Recent advances in p53 research and cancer treatment. *Journal of biomedicine & biotechnology* **2011,** *2011*, 978312.
201. Miyashita, T.; Krajewski, S.; Krajewska, M.; Wang, H. G.; Lin, H. K.; Liebermann, D. A.; Hoffman, B.; Reed, J. C., Tumor suppressor p53 is a regulator of bcl-2 and bax gene expression in vitro and in vivo. *Oncogene* **1994,** *9* (6), 1799-805.
202. Miyashita, T.; Reed, J. C., Tumor suppressor p53 is a direct transcriptional activator of the human bax gene. *Cell* **1995,** *80* (2), 293-9.
203. Barkett, M.; Gilmore, T. D., Control of apoptosis by Rel/NF-kappaB transcription factors. *Oncogene* **1999,** *18* (49), 6910-24.
204. Karin, M.; Ben-Neriah, Y., Phosphorylation meets ubiquitination: the control of NF-[kappa]B activity. *Annual review of immunology* **2000,** *18*, 621-63.
205. Qin, Z. H.; Wang, Y.; Nakai, M.; Chase, T. N., Nuclear factor-kappa B contributes to excitotoxin-induced apoptosis in rat striatum. *Molecular pharmacology* **1998,** *53* (1), 33-42.
206. Beg, A. A.; Baltimore, D., An essential role for NF-kappaB in preventing TNF-alpha-induced cell death. *Science* **1996,** *274* (5288), 782-4.
207. Baeuerle, P. A.; Baltimore, D., NF-kappa B: ten years after. *Cell* **1996,** *87* (1), 13-20.
208. Li, L.; Rao, J. N.; Bass, B. L.; Wang, J. Y., NF-kappaB activation and susceptibility to apoptosis after polyamine depletion in intestinal epithelial cells. *American journal of physiology. Gastrointestinal and liver physiology* **2001,** *280* (5), G992-G1004.
209. Pfeffer, L. M.; Yang, C. H.; Murti, A.; McCormack, S. A.; Viar, M. J.; Ray, R. M.; Johnson, L. R., Polyamine depletion induces rapid NF-kappa B activation in IEC-6 cells. *The Journal of biological chemistry* **2001,** *276* (49), 45909-13.
210. Shah, N.; Thomas, T. J.; Lewis, J. S.; Klinge, C. M.; Shirahata, A.; Gelinas, C.; Thomas, T., Regulation of estrogenic and nuclear factor kappa B functions by polyamines and their role in polyamine analog-induced apoptosis of breast cancer cells. *Oncogene* **2001,** *20* (14), 1715-29.

211. Musso, M.; Thomas, T.; Shirahata, A.; Sigal, L. H.; Van Dyke, M. W.; Thomas, T. J., Effects of chain length modification and bis(ethyl) substitution of spermine analogs on purine-purine-pyrimidine triplex DNA stabilization, aggregation, and conformational transitions. *Biochemistry* **1997,** *36* (6), 1441-9.
212. Bloomfield, V. A., DNA condensation by multivalent cations. *Biopolymers* **1997,** *44* (3), 269-82.
213. Egli, M.; Tereshko, V.; Teplova, M.; Minasov, G.; Joachimiak, A.; Sanishvili, R.; Weeks, C. M.; Miller, R.; Maier, M. A.; An, H.; Dan Cook, P.; Manoharan, M., X-ray crystallographic analysis of the hydration of A- and B-form DNA at atomic resolution. *Biopolymers* **1998,** *48* (4), 234-52.
214. Ohishi, H.; Terasoma, N.; Nakanishi, I.; van der Marel, G.; van Boom, J. H.; Rich, A.; Wang, A. H.; Hakoshima, T.; Tomita, K., Interaction between left-handed Z-DNA and polyamine - 3. The crystal structure of the d(CG)3 and thermospermine complex. *FEBS letters* **1996,** *398* (2-3), 291-6.
215. Ouameur, A. A.; Tajmir-Riahi, H. A., Structural analysis of DNA interactions with biogenic polyamines and cobalt(III)hexamine studied by Fourier transform infrared and capillary electrophoresis. *The Journal of biological chemistry* **2004,** *279* (40), 42041-54.
216. Ruiz-Chica, J.; Medina, M. A.; Sanchez-Jimenez, F.; Ramirez, F. J., Fourier transform Raman study of the structural specificities on the interaction between DNA and biogenic polyamines. *Biophysical journal* **2001,** *80* (1), 443-54.
217. Schmid, N.; Behr, J. P., Location of spermine and other polyamines on DNA as revealed by photoaffinity cleavage with polyaminobenzenediazonium salts. *Biochemistry* **1991,** *30* (17), 4357-61.
218. Rich, A.; Nordheim, A.; Wang, A. H., The chemistry and biology of left-handed Z-DNA. *Annual review of biochemistry* **1984,** *53*, 791-846.
219. Egli, M.; Williams, L. D.; Gao, Q.; Rich, A., Structure of the pure-spermine form of Z-DNA (magnesium free) at 1-A resolution. *Biochemistry* **1991,** *30* (48), 11388-402.
220. Feuerstein, B. G.; Pattabiraman, N.; Marton, L. J., Spermine-DNA interactions: a theoretical study. *Proceedings of the National Academy of Sciences of the United States of America* **1986,** *83* (16), 5948-52.
221. Feuerstein, B. G.; Pattabiraman, N.; Marton, L. J., Molecular dynamics of spermine-DNA interactions: sequence specificity and DNA bending for a simple ligand. *Nucleic acids research* **1989,** *17* (17), 6883-92.
222. Maruyama, A.; Katoh, M.; Ishihara, T.; Akaike, T., Comb-type polycations effectively stabilize DNA triplex. *Bioconjugate chemistry* **1997,** *8* (1), 3-6.
223. Pastre, D.; Pietrement, O.; Landousy, F.; Hamon, L.; Sorel, I.; David, M. O.; Delain, E.; Zozime, A.; Le Cam, E., A new approach to DNA bending by polyamines and its implication in DNA condensation. *European biophysics journal : EBJ* **2006,** *35* (3), 214-23.
224. Keniry, M. A., A comparison of the association of spermine with duplex and quadruplex DNA by NMR. *FEBS letters* **2003,** *542* (1-3), 153-8.
225. Sun, H.; Xiang, J.; Liu, Y.; Li, L.; Li, Q.; Xu, G.; Tang, Y., A stabilizing and denaturing dual-effect for natural polyamines interacting with G-quadruplexes depending on concentration. *Biochimie* **2011,** *93* (8), 1351-6.
226. Melchiorre, C., Polymethylene tetraamines: a novel class of cardioselective M2-antagonists. *Medicinal research reviews* **1990,** *10* (3), 327-49.
227. Melchiorre, C., Polymethylene tetramines: a new generation of selective muscarinic antagonists. *Trends in pharmacological sciences* **1988,** *9* (6), 216-20.
228. Melchiorre, C.; Bolognesi, M. L.; Minarini, A.; Rosini, M.; Tumiatti, V., Polyamines in drug discovery: from the universal template approach to the multitarget-directed ligand design strategy. *Journal of medicinal chemistry* **2010,** *53* (16), 5906-14.
229. Minarini, A.; Milelli, A.; Tumiatti, V.; Rosini, M.; Bolognesi, M. L.; Melchiorre, C., Synthetic polyamines: an overview of their multiple biological activities. *Amino acids* **2010,** *38* (2), 383-92.
230. Abeloff, M. D.; Slavik, M.; Luk, G. D.; Griffin, C. A.; Hermann, J.; Blanc, O.; Sjoerdsma, A.; Baylin, S. B., Phase I trial and pharmacokinetic studies of alpha-difluoromethylornithine--an inhibitor of polyamine biosynthesis. *Journal of clinical oncology : official journal of the American Society of Clinical Oncology* **1984,** *2* (2), 124-30.

231. Meyskens, F. L.; Kingsley, E. M.; Glattke, T.; Loescher, L.; Booth, A., A phase II study of alpha-difluoromethylornithine (DFMO) for the treatment of metastatic melanoma. *Investigational new drugs* **1986,** *4* (3), 257-62.
232. Abeloff, M. D.; Rosen, S. T.; Luk, G. D.; Baylin, S. B.; Zeltzman, M.; Sjoerdsma, A., Phase II trials of alpha-difluoromethylornithine, an inhibitor of polyamine synthesis, in advanced small cell lung cancer and colon cancer. *Cancer treatment reports* **1986,** *70* (7), 843-5.
233. Herr, H. W.; Warrel, R. P.; Burchenal, J. H., Phase I trial of alpha-difluoromethyl ornithine (DFMO) and methylglyoxal bis (guanylhydrazone) (MGBG) in patients with advanced prostatic cancer. *Urology* **1986,** *28* (6), 508-11.
234. Meyskens, F. L., Jr.; Gerner, E. W., Development of difluoromethylornithine (DFMO) as a chemoprevention agent. *Clinical cancer research : an official journal of the American Association for Cancer Research* **1999,** *5* (5), 945-51.
235. Raul, F.; Gosse, F.; Osswald, A. B.; Bouhadjar, M.; Foltzer-Jourdainne, C.; Marescaux, J.; Soler, L., Follow-up of tumor development in the colons of living rats and implications for chemoprevention trials: assessment of aspirin-difluoromethylornithine combination. *International journal of oncology* **2007,** *31* (1), 89-95.
236. Mihich, E., Current Studies with Methylglyoxal-Bis(Guanylhydrazone). *Cancer research* **1963,** *23*, 1375-89.
237. Williams-Ashman, H. G.; Schenone, A., Methyl glyoxal bis(guanylhydrazone) as a potent inhibitor of mammalian and yeast S-adenosylmethionine decarboxylases. *Biochemical and biophysical research communications* **1972,** *46* (1), 288-95.
238. Pleshkewych, A.; Kramer, D. L.; Kelly, E.; Porter, C. W., Independence of drug action on mitochondria and polyamines in L1210 leukemia cells treated with methylglyoxal-bis(guanylhydrazone). *Cancer research* **1980,** *40* (12), 4533-40.
239. Seiler, N., Thirty years of polyamine-related approaches to cancer therapy. Retrospect and prospect. Part 2. Structural analogues and derivatives. *Current drug targets* **2003,** *4* (7), 565-85.
240. Regenass, U.; Mett, H.; Stanek, J.; Mueller, M.; Kramer, D.; Porter, C. W., CGP 48664, a new S-adenosylmethionine decarboxylase inhibitor with broad spectrum antiproliferative and antitumor activity. *Cancer research* **1994,** *54* (12), 3210-7.
241. Siu, L. L.; Rowinsky, E. K.; Hammond, L. A.; Weiss, G. R.; Hidalgo, M.; Clark, G. M.; Moczygemba, J.; Choi, L.; Linnartz, R.; Barbet, N. C.; Sklenar, I. T.; Capdeville, R.; Gan, G.; Porter, C. W.; Von Hoff, D. D.; Eckhardt, S. G., A phase I and pharmacokinetic study of SAM486A, a novel polyamine biosynthesis inhibitor, administered on a daily-times-five every-three-week schedule in patients with Advanced solid malignancies. *Clinical cancer research : an official journal of the American Association for Cancer Research* **2002,** *8* (7), 2157-66.
242. Pless, M.; Belhadj, K.; Menssen, H. D.; Kern, W.; Coiffier, B.; Wolf, J.; Herrmann, R.; Thiel, E.; Bootle, D.; Sklenar, I.; Muller, C.; Choi, L.; Porter, C.; Capdeville, R., Clinical efficacy, tolerability, and safety of SAM486A, a novel polyamine biosynthesis inhibitor, in patients with relapsed or refractory non-Hodgkin's lymphoma: results from a phase II multicenter study. *Clinical cancer research : an official journal of the American Association for Cancer Research* **2004,** *10* (4), 1299-305.
243. Millward, M. J.; Joshua, A.; Kefford, R.; Aamdal, S.; Thomson, D.; Hersey, P.; Toner, G.; Lynch, K., Multi-centre Phase II trial of the polyamine synthesis inhibitor SAM486A (CGP48664) in patients with metastatic melanoma. *Investigational new drugs* **2005,** *23* (3), 253-6.
244. Tang, K. C.; Pegg, A. E.; Coward, J. K., Specific and potent inhibition of spermidine synthase by the transition-state analog, S-adenosyl-3-thio-1,8-diaminooctane. *Biochemical and biophysical research communications* **1980,** *96* (3), 1371-7.
245. Pegg, A. E.; Tang, K. C.; Coward, J. K., Effects of S-adenosyl-1,8-diamino-3-thiooctane on polyamine metabolism. *Biochemistry* **1982,** *21* (20), 5082-9.
246. Casero, R. A., Jr.; Woster, P. M., Recent advances in the development of polyamine analogues as antitumor agents. *Journal of medicinal chemistry* **2009,** *52* (15), 4551-73.
247. Edwards, M. L.; Prakash, N. J.; Stemerick, D. M.; Sunkara, S. P.; Bitonti, A. J.; Davis, G. F.; Dumont, J. A.; Bey, P., Polyamine analogues with antitumor activity. *Journal of medicinal chemistry* **1990,** *33* (5), 1369-75.
248. Edwards, M. L.; Snyder, R. D.; Stemerick, D. M., Synthesis and DNA-binding properties of polyamine analogues. *Journal of medicinal chemistry* **1991,** *34* (8), 2414-20.

249. Casero, R. A., Jr.; Woster, P. M., Terminally alkylated polyamine analogues as chemotherapeutic agents. *Journal of medicinal chemistry* **2001,** *44* (1), 1-26.
250. Porter, C. W.; Ganis, B.; Libby, P. R.; Bergeron, R. J., Correlations between polyamine analogue-induced increases in spermidine/spermine N1-acetyltransferase activity, polyamine pool depletion, and growth inhibition in human melanoma cell lines. *Cancer research* **1991,** *51* (14), 3715-20.
251. Porter, C. W.; Berger, F. G.; Pegg, A. E.; Ganis, B.; Bergeron, R. J., Regulation of ornithine decarboxylase activity by spermidine and the spermidine analogue N1N8-bis(ethyl)spermidine. *The Biochemical journal* **1987,** *242* (2), 433-40.
252. Bergeron, C. J.; Basu, H. S.; Marton, L. J.; Deen, D. F.; Pellarin, M.; Feuerstein, B. G., Two polyamine analogs (BE-4-4-4 and BE-4-4-4-4) directly affect growth, survival, and cell cycle progression in two human brain tumor cell lines. *Cancer chemotherapy and pharmacology* **1995,** *36* (5), 411-7.
253. Wolff, A. C.; Armstrong, D. K.; Fetting, J. H.; Carducci, M. K.; Riley, C. D.; Bender, J. F.; Casero, R. A., Jr.; Davidson, N. E., A Phase II study of the polyamine analog N1,N11-diethylnorspermine (DENSpm) daily for five days every 21 days in patients with previously treated metastatic breast cancer. *Clinical cancer research : an official journal of the American Association for Cancer Research* **2003,** *9* (16 Pt 1), 5922-8.
254. Hahm, H. A.; Ettinger, D. S.; Bowling, K.; Hoker, B.; Chen, T. L.; Zabelina, Y.; Casero, R. A., Jr., Phase I study of N(1),N(11)-diethylnorspermine in patients with non-small cell lung cancer. *Clinical cancer research : an official journal of the American Association for Cancer Research* **2002,** *8* (3), 684-90.
255. Streiff, R. R.; Bender, J. F., Phase 1 study of N1-N11-diethylnorspermine (DENSPM) administered TID for 6 days in patients with advanced malignancies. *Investigational new drugs* **2001,** *19* (1), 29-39.
256. Hector, S.; Tummala, R.; Kisiel, N. D.; Diegelman, P.; Vujcic, S.; Clark, K.; Fakih, M.; Kramer, D. L.; Porter, C. W.; Pendyala, L., Polyamine catabolism in colorectal cancer cells following treatment with oxaliplatin, 5-fluorouracil and N1, N11 diethylnorspermine. *Cancer chemotherapy and pharmacology* **2008,** *62* (3), 517-27.
257. Bergeron, R. J.; Muller, R.; Huang, G.; McManis, J. S.; Algee, S. E.; Yao, H.; Weimar, W. R.; Wiegand, J., Synthesis and evaluation of hydroxylated polyamine analogues as antiproliferatives. *Journal of medicinal chemistry* **2001,** *44* (15), 2451-9.
258. Bergeron, R. J.; Yao, G. W.; Yao, H.; Weimar, W. R.; Sninsky, C. A.; Raisler, B.; Feng, Y.; Wu, Q.; Gao, F., Metabolically programmed polyamine analogue antidiarrheals. *Journal of medicinal chemistry* **1996,** *39* (13), 2461-71.
259. Reddy, V. K.; Valasinas, A.; Sarkar, A.; Basu, H. S.; Marton, L. J.; Frydman, B., Conformationally restricted analogues of 1N,12N-bisethylspermine: synthesis and growth inhibitory effects on human tumor cell lines. *Journal of medicinal chemistry* **1998,** *41* (24), 4723-32.
260. Frydman, B.; Porter, C. W.; Maxuitenko, Y.; Sarkar, A.; Bhattacharya, S.; Valasinas, A.; Reddy, V. K.; Kisiel, N.; Marton, L. J.; Basu, H. S., A novel polyamine analog (SL-11093) inhibits growth of human prostate tumor xenografts in nude mice. *Cancer chemotherapy and pharmacology* **2003,** *51* (6), 488-92.
261. Carew, J. S.; Nawrocki, S. T.; Reddy, V. K.; Bush, D.; Rehg, J. E.; Goodwin, A.; Houghton, J. A.; Casero, R. A., Jr.; Marton, L. J.; Cleveland, J. L., The novel polyamine analogue CGC-11093 enhances the antimyeloma activity of bortezomib. *Cancer research* **2008,** *68* (12), 4783-90.
262. Hacker, A.; Marton, L. J.; Sobolewski, M.; Casero, R. A., Jr., In vitro and in vivo effects of the conformationally restricted polyamine analogue CGC-11047 on small cell and non-small cell lung cancer cells. *Cancer chemotherapy and pharmacology* **2008,** *63* (1), 45-53.
263. Valasinas, A.; Sarkar, A.; Reddy, V. K.; Marton, L. J.; Basu, H. S.; Frydman, B., Conformationally restricted analogues of 1N,14N-bisethylhomospermine (BE-4-4-4): synthesis and growth inhibitory effects on human prostate cancer cells. *Journal of medicinal chemistry* **2001,** *44* (3), 390-403.
264. Frydman, B.; Blokhin, A. V.; Brummel, S.; Wilding, G.; Maxuitenko, Y.; Sarkar, A.; Bhattacharya, S.; Church, D.; Reddy, V. K.; Kink, J. A.; Marton, L. J.; Valasinas, A.; Basu, H. S., Cyclopropane-containing polyamine analogues are efficient growth inhibitors of a human prostate tumor xenograft in nude mice. *Journal of medicinal chemistry* **2003,** *46* (21), 4586-600.

265. Valasinas, A.; Reddy, V. K.; Blokhin, A. V.; Basu, H. S.; Bhattacharya, S.; Sarkar, A.; Marton, L. J.; Frydman, B., Long-chain polyamines (oligoamines) exhibit strong cytotoxicities against human prostate cancer cells. *Bioorganic & medicinal chemistry* **2003,** *11* (18), 4121-31.
266. Huang, Y.; Hager, E. R.; Phillips, D. L.; Dunn, V. R.; Hacker, A.; Frydman, B.; Kink, J. A.; Valasinas, A. L.; Reddy, V. K.; Marton, L. J.; Casero, R. A., Jr.; Davidson, N. E., A novel polyamine analog inhibits growth and induces apoptosis in human breast cancer cells. *Clinical cancer research : an official journal of the American Association for Cancer Research* **2003,** *9* (7), 2769-77.
267. Huang, Y.; Keen, J. C.; Pledgie, A.; Marton, L. J.; Zhu, T.; Sukumar, S.; Park, B. H.; Blair, B.; Brenner, K.; Casero, R. A., Jr.; Davidson, N. E., Polyamine analogues down-regulate estrogen receptor alpha expression in human breast cancer cells. *The Journal of biological chemistry* **2006,** *281* (28), 19055-63.
268. Rukunga, G. M.; Waterman, P. G., New macrocyclic spermine (budmunchiamine) alkaloids from Albizia gummifera: with some observations on the structure--activity relationships of the budmunchiamines. *Journal of natural products* **1996,** *59* (9), 850-3.
269. Frydman, B.; Bhattacharya, S.; Sarkar, A.; Drandarov, K.; Chesnov, S.; Guggisberg, A.; Popaj, K.; Sergeyev, S.; Yurdakul, A.; Hesse, M.; Basu, H. S.; Marton, L. J., Macrocyclic polyamines deplete cellular ATP levels and inhibit cell growth in human prostate cancer cells. *Journal of medicinal chemistry* **2004,** *47* (4), 1051-9.
270. Saab, N. H.; West, E. E.; Bieszk, N. C.; Preuss, C. V.; Mank, A. R.; Casero, R. A., Jr.; Woster, P. M., Synthesis and evaluation of unsymmetrically substituted polyamine analogues as modulators of human spermidine/spermine-N1-acetyltransferase (SSAT) and as potential antitumor agents. *Journal of medicinal chemistry* **1993,** *36* (20), 2998-3004.
271. McCloskey, D. E.; Woster, P. M.; Casero, R. A., Jr.; Davidson, N. E., Effects of the polyamine analogues N1-ethyl-N11-((cyclopropyl)methyl)-4,8-diazaundecane and N1-ethylN-11-((cycloheptyl)methyl)-4,8-diazaundecane in human prostate cancer cells. *Clinical cancer research : an official journal of the American Association for Cancer Research* **2000,** *6* (1), 17-23.
272. McCloskey, D. E.; Yang, J.; Woster, P. M.; Davidson, N. E.; Casero, R. A., Jr., Polyamine analogue induction of programmed cell death in human lung tumor cells. *Clinical cancer research : an official journal of the American Association for Cancer Research* **1996,** *2* (3), 441-6.
273. Webb, H. K.; Wu, Z.; Sirisoma, N.; Ha, H. C.; Casero, R. A., Jr.; Woster, P. M., 1-(N-alkylamino)-11-(N-ethylamino)-4,8-diazaundecanes: simple synthetic polyamine analogues that differentially alter tubulin polymerization. *Journal of medicinal chemistry* **1999,** *42* (8), 1415-21.
274. Wang, L.; Price, H. L.; Juusola, J.; Kline, M.; Phanstiel, O. t., Influence of polyamine architecture on the transport and topoisomerase II inhibitory properties of polyamine DNA-intercalator conjugates. *Journal of medicinal chemistry* **2001,** *44* (22), 3682-91.
275. Lee, H. W.; Blasco, M. A.; Gottlieb, G. J.; Horner, J. W., 2nd; Greider, C. W.; DePinho, R. A., Essential role of mouse telomerase in highly proliferative organs. *Nature* **1998,** *392* (6676), 569-74.
276. Counter, C. M.; Hahn, W. C.; Wei, W.; Caddle, S. D.; Beijersbergen, R. L.; Lansdorp, P. M.; Sedivy, J. M.; Weinberg, R. A., Dissociation among in vitro telomerase activity, telomere maintenance, and cellular immortalization. *Proceedings of the National Academy of Sciences of the United States of America* **1998,** *95* (25), 14723-8.
277. Pitts, A. E.; Corey, D. R., Inhibition of human telomerase by 2'-O-methyl-RNA. *Proceedings of the National Academy of Sciences of the United States of America* **1998,** *95* (20), 11549-54.
278. Norton, J. C.; Piatyszek, M. A.; Wright, W. E.; Shay, J. W.; Corey, D. R., Inhibition of human telomerase activity by peptide nucleic acids. *Nature biotechnology* **1996,** *14* (5), 615-9.
279. Yokoyama, Y.; Takahashi, Y.; Shinohara, A.; Lian, Z.; Wan, X.; Niwa, K.; Tamaya, T., Attenuation of telomerase activity by a hammerhead ribozyme targeting the template region of telomerase RNA in endometrial carcinoma cells. *Cancer research* **1998,** *58* (23), 5406-10.
280. Yin, F.; Liu, J.; Peng, X., Triethylene tetraamine: a novel telomerase inhibitor. *Bioorganic & medicinal chemistry letters* **2003,** *13* (22), 3923-6.
281. Yin, F.; Liu, J.; Deng, X.; Wang, J., Effects of triethylene tetraamine on the G-quadruplex structure in the human c-myc promoter. *Journal of biochemistry* **2007,** *141* (5), 669-74.
282. Lixia, G.; Fei, Y.; Jiajia, J.; Jianhui, L., Triethylene tetramine, a novel ligand of G-quadruplex, induces senescence of MCF-7 cells. *Biotechnology letters* **2008,** *30* (1), 47-53.

283. Liu, J.; Guo, L.; Yin, F.; Zheng, X.; Chen, G.; Wang, Y., Characterization and antitumor activity of triethylene tetramine, a novel telomerase inhibitor. *Biomedicine & pharmacotherapy = Biomedecine & pharmacotherapie* **2008,** *62* (7), 480-5.
284. AIRT Working Group I. Tumori in italia, rapporto 2006
285. Dunn, M. W.; Kazer, M. W., Prostate cancer overview. *Seminars in oncology nursing* **2011,** *27* (4), 241-50.
286. Humphrey, P. A., Gleason grading and prognostic factors in carcinoma of the prostate. *Modern pathology : an official journal of the United States and Canadian Academy of Pathology, Inc* **2004,** *17* (3), 292-306.
287. Gleason, D. F., Classification of prostatic carcinomas. *Cancer chemotherapy reports. Part 1* **1966,** *50* (3), 125-8.
288. Mellinger, G. T.; Gleason, D.; Bailar, J., 3rd, The histology and prognosis of prostatic cancer. *The Journal of urology* **1967,** *97* (2), 331-7.
289. Epstein, J. I.; Allsbrook, W. C., Jr.; Amin, M. B.; Egevad, L. L., The 2005 International Society of Urological Pathology (ISUP) Consensus Conference on Gleason Grading of Prostatic Carcinoma. *The American journal of surgical pathology* **2005,** *29* (9), 1228-42.
290. True, L.; Coleman, I.; Hawley, S.; Huang, C. Y.; Gifford, D.; Coleman, R.; Beer, T. M.; Gelmann, E.; Datta, M.; Mostaghel, E.; Knudsen, B.; Lange, P.; Vessella, R.; Lin, D.; Hood, L.; Nelson, P. S., A molecular correlate to the Gleason grading system for prostate adenocarcinoma. *Proceedings of the National Academy of Sciences of the United States of America* **2006,** *103* (29), 10991-6.
291. Tipton, K. F.; Boyce, S.; O'Sullivan, J.; Davey, G. P.; Healy, J., Monoamine oxidases: certainties and uncertainties. *Current medicinal chemistry* **2004,** *11* (15), 1965-82.
292. Shih, J. C.; Chen, K.; Ridd, M. J., Monoamine oxidase: from genes to behavior. *Annual review of neuroscience* **1999,** *22*, 197-217.
293. Westlund, K. N.; Denney, R. M.; Kochersperger, L. M.; Rose, R. M.; Abell, C. W., Distinct monoamine oxidase A and B populations in primate brain. *Science* **1985,** *230* (4722), 181-3.
294. Youdim, M. B.; Edmondson, D.; Tipton, K. F., The therapeutic potential of monoamine oxidase inhibitors. *Nature reviews. Neuroscience* **2006,** *7* (4), 295-309.
295. Edmondson, D. E.; Newton-Vinson, P., The covalent FAD of monoamine oxidase: structural and functional role and mechanism of the flavinylation reaction. *Antioxidants & redox signaling* **2001,** *3* (5), 789-806.
296. Binda, C.; Angelini, R.; Federico, R.; Ascenzi, P.; Mattevi, A., Structural bases for inhibitor binding and catalysis in polyamine oxidase. *Biochemistry* **2001,** *40* (9), 2766-76.
297. Binda, C.; Li, M.; Hubalek, F.; Restelli, N.; Edmondson, D. E.; Mattevi, A., Insights into the mode of inhibition of human mitochondrial monoamine oxidase B from high-resolution crystal structures. *Proceedings of the National Academy of Sciences of the United States of America* **2003,** *100* (17), 9750-5.
298. Silverman, R. B.; Hoffman, S. J., N-(1-Methyl)cyclopropylbenzylamine: a novel inactivator of mitochondrial monoamine oxidase. *Biochemical and biophysical research communications* **1981,** *101* (4), 1396-401.
299. Brown, L. E.; Hamilton, G. A., Some model reactions and a general mechanism for flavoenzyme-catalyzed dehydrogenations. *Journal of the American Chemical Society* **1970,** *92* (24), 7225-7.
300. Miller, J. R.; Edmondson, D. E., Structure-activity relationships in the oxidation of para-substituted benzylamine analogues by recombinant human liver monoamine oxidase A. *Biochemistry* **1999,** *38* (41), 13670-83.
301. Wimbiscus, M.; Kostenko, O.; Malone, D., MAO inhibitors: risks, benefits, and lore. *Cleveland Clinic journal of medicine* **2010,** *77* (12), 859-82.
302. Jia, Z.; Wei, S.; Zhu, Q., Monoamine oxidase inhibitors: benzylidene-prop-2-ynyl-amines analogues. *Biological & pharmaceutical bulletin* **2010,** *33* (4), 725-8.
303. Da Prada, M.; Kettler, R.; Keller, H. H.; Burkard, W. P.; Muggli-Maniglio, D.; Haefely, W. E., Neurochemical profile of moclobemide, a short-acting and reversible inhibitor of monoamine oxidase type A. *The Journal of pharmacology and experimental therapeutics* **1989,** *248* (1), 400-14.
304. Provost, J. C.; Funck-Brentano, C.; Rovei, V.; D'Estanque, J.; Ego, D.; Jaillon, P., Pharmacokinetic and pharmacodynamic interaction between toloxatone, a new reversible monoamine

oxidase-A inhibitor, and oral tyramine in healthy subjects. *Clinical pharmacology and therapeutics* **1992,** *52* (4), 384-93.
305. Medvedev, A. E.; Kirkel, A. A.; Kamyshanskaya, N. S.; Moskvitina, T. A.; Axenova, L. N.; Gorkin, V. Z.; Andreeva, N. I.; Golovina, S. M.; Mashkovsky, M. D., Monoamine oxidase inhibition by novel antidepressant tetrindole. *Biochemical pharmacology* **1994,** *47* (2), 303-8.
306. Anderson, M. C.; Hasan, F.; McCrodden, J. M.; Tipton, K. F., Monoamine oxidase inhibitors and the cheese effect. *Neurochemical research* **1993,** *18* (11), 1145-9.
307. Schalken, J. A.; van Leenders, G., Cellular and molecular biology of the prostate: stem cell biology. *Urology* **2003,** *62* (5 Suppl 1), 11-20.
308. Tokar, E. J.; Ancrile, B. B.; Cunha, G. R.; Webber, M. M., Stem/progenitor and intermediate cell types and the origin of human prostate cancer. *Differentiation; research in biological diversity* **2005,** *73* (9-10), 463-73.
309. van Leenders, G. J.; Schalken, J. A., Epithelial cell differentiation in the human prostate epithelium: implications for the pathogenesis and therapy of prostate cancer. *Critical reviews in oncology/hematology* **2003,** *46 Suppl*, S3-10.
310. Zhao, H.; Nolley, R.; Chen, Z.; Reese, S. W.; Peehl, D. M., Inhibition of monoamine oxidase A promotes secretory differentiation in basal prostatic epithelial cells. *Differentiation; research in biological diversity* **2008,** *76* (7), 820-30.
311. Dizeyi, N.; Bjartell, A.; Nilsson, E.; Hansson, J.; Gadaleanu, V.; Cross, N.; Abrahamsson, P. A., Expression of serotonin receptors and role of serotonin in human prostate cancer tissue and cell lines. *The Prostate* **2004,** *59* (3), 328-36.
312. Palm, D.; Lang, K.; Niggemann, B.; Drell, T. L. t.; Masur, K.; Zaenker, K. S.; Entschladen, F., The norepinephrine-driven metastasis development of PC-3 human prostate cancer cells in BALB/c nude mice is inhibited by beta-blockers. *International journal of cancer. Journal international du cancer* **2006,** *118* (11), 2744-9.
313. Zhao, H.; Flamand, V.; Peehl, D. M., Anti-oncogenic and pro-differentiation effects of clorgyline, a monoamine oxidase A inhibitor, on high grade prostate cancer cells. *BMC medical genomics* **2009,** *2*, 55.
314. Li, C. F.; MacDonald, J. R.; Wei, R. Y.; Ray, J.; Lau, K.; Kandel, C.; Koffman, R.; Bell, S.; Scherer, S. W.; Alman, B. A., Human sterile alpha motif domain 9, a novel gene identified as down-regulated in aggressive fibromatosis, is absent in the mouse. *BMC genomics* **2007,** *8*, 92.
315. Berger, R.; Febbo, P. G.; Majumder, P. K.; Zhao, J. J.; Mukherjee, S.; Signoretti, S.; Campbell, K. T.; Sellers, W. R.; Roberts, T. M.; Loda, M.; Golub, T. R.; Hahn, W. C., Androgen-induced differentiation and tumorigenicity of human prostate epithelial cells. *Cancer research* **2004,** *64* (24), 8867-75.
316. Yu, J.; Rhodes, D. R.; Tomlins, S. A.; Cao, X.; Chen, G.; Mehra, R.; Wang, X.; Ghosh, D.; Shah, R. B.; Varambally, S.; Pienta, K. J.; Chinnaiyan, A. M., A polycomb repression signature in metastatic prostate cancer predicts cancer outcome. *Cancer research* **2007,** *67* (22), 10657-63.
317. Nojima, T.; Ohtsuka, K.; Nagamatsu, T.; Takenaka, S., Bis-naphthalene diimide exhibiting an effective bis-threading intercalating ability. *Nucleic Acids Res Suppl* **2003,** (3), 123-4.
318. Gianolio, D. A.; McLaughlin, L. W., Tethered naphthalene diimide intercalators enhance DNA triplex stability. *Bioorganic & medicinal chemistry* **2001,** *9* (9), 2329-34.
319. Balasubramanian, S.; Neidle, S., G-quadruplex nucleic acids as therapeutic targets. *Current opinion in chemical biology* **2009,** *13* (3), 345-53.
320. Morgan, A. R.; Lee, J. S.; Pulleyblank, D. E.; Murray, N. L.; Evans, D. H., Review: ethidium fluorescence assays. Part 1. Physicochemical studies. *Nucleic acids research* **1979,** *7* (3), 547-69.
321. McConnaughie, A. W.; Jenkins, T. C., Novel acridine-triazenes as prototype combilexins: synthesis, DNA binding, and biological activity. *Journal of medicinal chemistry* **1995,** *38* (18), 3488-501.
322. Berman, H. M.; Westbrook, J.; Feng, Z.; Gilliland, G.; Bhat, T. N.; Weissig, H.; Shindyalov, I. N.; Bourne, P. E., The Protein Data Bank. *Nucleic acids research* **2000,** *28* (1), 235-42.
323. Canals, A.; Purciolas, M.; Aymami, J.; Coll, M., The anticancer agent ellipticine unwinds DNA by intercalative binding in an orientation parallel to base pairs. *Acta crystallographica. Section D, Biological crystallography* **2005,** *61* (Pt 7), 1009-12.
324. Lavrik, I. N.; Golks, A.; Krammer, P. H., Caspases: pharmacological manipulation of cell death. *The Journal of clinical investigation* **2005,** *115* (10), 2665-72.

325. Robertson, J. D.; Orrenius, S.; Zhivotovsky, B., Review: nuclear events in apoptosis. *Journal of structural biology* **2000,** *129* (2-3), 346-58.
326. Balmanno, K.; Cook, S. J., Tumour cell survival signalling by the ERK1/2 pathway. *Cell death and differentiation* **2009,** *16* (3), 368-77.
327. Collie, G. W.; Promontorio, R.; Hampel, S. M.; Micco, M.; Neidle, S.; Parkinson, G. N., Structural basis for telomeric g-quadruplex targeting by naphthalene diimide ligands. *Journal of the American Chemical Society* **2012,** *134* (5), 2723-31.
328. Cuenca, F.; Moore, M. J.; Johnson, K.; Guyen, B.; De Cian, A.; Neidle, S., Design, synthesis and evaluation of 4,5-di-substituted acridone ligands with high G-quadruplex affinity and selectivity, together with low toxicity to normal cells. *Bioorganic & medicinal chemistry letters* **2009,** *19* (17), 5109-13.
329. Gunaratnam, M.; de la Fuente, M.; Hampel, S. M.; Todd, A. K.; Reszka, A. P.; Schatzlein, A.; Neidle, S., Targeting pancreatic cancer with a G-quadruplex ligand. *Bioorganic & medicinal chemistry* **2011,** *19* (23), 7151-7.
330. Chaignon, F.; Falkenstrom, M.; Karlsson, S.; Blart, E.; Odobel, F.; Hammarstrom, L., Very large acceleration of the photoinduced electron transfer in a Ru(bpy)3-naphthalene bisimide dyad bridged on the naphthyl core. *Chem Commun (Camb)* **2007,** (1), 64-6.
331. Kabsch, W., Xds. *Acta crystallographica. Section D, Biological crystallography* **2010,** *66* (Pt 2), 125-32.
332. Kissinger, C. R.; Gehlhaar, D. K.; Smith, B. A.; Bouzida, D., Molecular replacement by evolutionary search. *Acta crystallographica. Section D, Biological crystallography* **2001,** *57* (Pt 10), 1474-9.
333. Vagin, A. A.; Steiner, R. A.; Lebedev, A. A.; Potterton, L.; McNicholas, S.; Long, F.; Murshudov, G. N., REFMAC5 dictionary: organization of prior chemical knowledge and guidelines for its use. *Acta crystallographica. Section D, Biological crystallography* **2004,** *60* (Pt 12 Pt 1), 2184-95.
334. McCoy, A. J.; Grosse-Kunstleve, R. W.; Adams, P. D.; Winn, M. D.; Storoni, L. C.; Read, R. J., Phaser crystallographic software. *Journal of applied crystallography* **2007,** *40* (Pt 4), 658-674.